**Charles University**
**2nd Faculty of Medicine**

and

**Czech Academy of Sciences**
**Institute of Experimental Medicine**

Study programme: Neurosciences

**Mgr. Kristýna Kekulová**

# Natural biomaterials and mesenchymal stem cells in regeneration of spinal cord injury

# Přírodní biomateriály a mesenchymální kmenové buňky v léčbě míšního poranění

PhD thesis

Supervisor: PharmDr. Šárka Kubinová, Ph.D.

Prague, 2018

**Prohlášení:**

Prohlašuji, že jsem závěrečnou práci zpracovala samostatně a že jsem řádně uvedla a citovala všechny použité prameny a literaturu. Současně prohlašuji, že práce nebyla využita k získání jiného nebo stejného titulu.

Souhlasím s trvalým uložením elektronické verze mé práce v databázi systému meziuniverzitního projektu Theses.cz za účelem soustavné kontroly podobnosti kvalifikačních prací.

V Praze, 10. 12. 2018

Mgr. Kristýna Kekulová

**Identifikační záznam:**

KEKULOVÁ, Kristýna. *Přírodní biomateriály a mesenchymální kmenové buňky v léčbě míšního poranění. [Natural biomaterials and mesenchymal stem cells in regeneration of spinal cord injury]*. Praha, 2018. 97 stran, 3 přílohy. Dizertační práce (Ph.D.). Univerzita Karlova, 2. lékařská fakulta, Ústav experimentální medicíny, AV ČR v.v.i. Školitel: Kubinová, Šárka.

**Poděkování:**

Chtěla bych velmi poděkovat své školitelce PharmDr. Šárce Kubinové, Ph.D. za odborné vedení a cenné rady. Dále děkuji všem kolegům za pomoc při experimentech, Mgr. Kristýně Kárové, Ph.D. za kontrolu angličtiny v této práci a můj velký dík patří především kolegyním v kanceláři za příjemné pracovní prostředí. V neposlední řadě bych chtěla velice poděkovat svému manželovi a rodině za všestrannou podporu a pochopení.

## Abstrakt

Poranění míchy je závažné trauma a navzdory intenzivnímu výzkumu stále neexistuje účinná léčba pro pacienty. Cílem této dizertační práce je studium nových možností terapie míšního poranění na zvířecích modelech. Zaměřili jsme se na využití přírodních materiálů, kmenových buněk, genovou terapii a možnost kombinace těchto přístupů.

Byl zkoumán efekt materiálů na bázi extracelulární matrix (ECM) připravených decelularizací prasečí míchy a prasečího močového měchýře na regeneraci tkáně po akutní hemisekci míchy. Dalším testovaným materiálem byl hydrogel na bázi kyseliny hyaluronové modifikovaný RGD adhesivním peptidem aplikovaný do léze po akutní a subakutní míšní hemisekci. Ukázali jsme, že oba typy biomateriálů pozitivně ovlivnily regeneraci míšní tkáně tím, že umožnily přemostění léze a podpořily vrůstání axonů. ECM hydrogely navíc podporovaly vrůstání cév do místa poškození. Kombinace hydrogelů s mesenchymálními kmenovými buňkami izolovanými z lidského pupečníku (hWJ-MSCs) měla synergický efekt, ale vzhledem k tomu, že do hydrogelů bylo možné inkorporovat pouze omezené množství buněk, nebyl tento efekt spojený se zlepšením motorických schopností. Limitací testovaných hydrogelů na bázi ECM je rychlá degradace materiálu, která neumožní plnohodnotnou obnovu poškozené tkáně.

Další část práce je zaměřena na intratekální transplantaci hWJ-MSCs do balónkové kompresní léze. Prokázali jsme, že efekt buněk závisí na použité dávce, přičemž 1,5 milionu transplantovaných hWJ-MSCs v jedné dávce nebo ve třech dávkách po 0,5 milionu je minimální počet hWJ-MSCs, který se projeví zlepšením behaviorálních a histologických parametrů, jako je vrůstání axonů a redukce gliové jizvy. Avšak pouze opakovaná aplikace 1,5 milionu hWJ-MSCs vedla k signifikantnímu zlepšení v náročnějším behaviorálním testu, který vyžaduje koordinaci pohybů.

Jako další možný terapeutický přístup byla zvolena transfekce neurálních buněk. Ukázali jsme, že genová terapie vektory pro α9 integrinovou podjednotku a pro aktivátor integrinů kindlin 1 kombinovaná s implantací biomateriálu modifikovaného specifickým adhezivním peptidem by mohla být dalším možným přístupem, jak podpořit vrůstání axonů do místa poškození.



**Klíčová slova:** míšní poranění, regenerace, extracelulární matrix, kyselina hyaluronová, hydrogel, mesenchymální kmenové buňky, integrinové receptory

## Abstract

Spinal cord injury is a serious trauma and despite intensive research there is still no effective treatment for patients. The aim of this thesis is to study new possibilities of spinal cord injury therapy in animal models. We have focused on the use of natural materials, stem cells, gene therapy and the possibility of combining these approaches.

The effect of extracellular matrix (ECM) based materials prepared by decellularization of porcine spinal cord and porcine urinary bladder on tissue regeneration after acute hemisection of the spinal cord was investigated. Another tested material was a hydrogel based on hyaluronic acid modified with RGD adhesion peptide, which was applied acutely and subacutely into the hemisection lesion. We have shown that both types of biomaterials have positive effect on regeneration of the spinal cord tissue by bridging the lesion and promotion of axonal ingrowth. In addition, ECM hydrogels promote the growth of blood vessels into the lesion site. The combination of hydrogels with mesenchymal stem cells derived from human umbilical cord (hWJ-MSCs) had synergistic effect, but since only a limited number of cells could be incorporated into hydrogels, this effect was not associated with improvement in motor skills. The limitation of ECM hydrogels is their rapid degradation, which will not allow full recovery of damaged tissue.

Another part of this work is focused on intrathecal transplantation of hWJ-MSCs into the balloon-induced compression lesion. We have shown that the effect of cells is dose dependent and that 1.5 million transplanted hWJ-MSCs in one dose or in three doses of 0.5 million is the minimum number of hWJ-MSCs, which leads to improvements in behavioural and histological parameters such as axonal ingrowth and reduction of the glial scar. However, only repeated application of 1.5 million hWJ-MSCs led to significant improvement in more demanding behavioural test that requires coordination of movements.

As another possible therapeutic approach, neural cell transfection was chosen. We have shown that gene therapy using vectors with α9 integrin subunit and the integrin activator kindlin 1 combined with the implantation of a biomaterial modified with specific adhesion peptide could be another possible approach how to promote the growth of axons into the lesion site.



**Key words:** spinal cord injury, regeneration, extracellular matrix, hyaluronic acid, hydrogel, mesenchymal stem cells, integrin receptors

# Table of content

1 List of abbreviations ....4
2 Introduction....7
2.1 Spinal cord injury....9
2.2 Spinal cord injury treatment....11
2.3 Biomaterials....12
2.3.1 ECM derived hydrogels....14
2.3.2 HA based hydrogels....14
2.3.3 Fibrin gel....15
2.3.4 Biomaterials in clinical applications....16
2.4 Stem cell therapy....17
2.4.1 Mesenchymal stem cells....19
2.5 Gene therapy....20
2.6 Combinatory therapies....21
2.7 Experimental models of SCI....22
3 Aims and hypotheses....24
4 Materials and methods....25
4.1 Hydrogel preparation....25
4.1.1 ECM hydrogel preparation....25
4.1.2 HA-PH-RGD hydrogel preparation and crosslinking....25
4.2 Mesenchymal stem cell isolation and culture....26
4.3 *In vitro* cell growth and viability....27
4.4 Dorsal root ganglion neuron culture and transfection....27
4.5 Spinal cord injury animal models....28
4.5.1 Hemisected SCI lesion....28
4.5.2 Balloon-induced compression SCI lesion....29
4.5.3 Hydrogel application into spinal cord hemisection....29
4.5.4 Intrathecal cell transplantation....30
4.6 Behavioural analysis....31
4.6.1 BBB test....31
4.6.2 Rotarod test....31
4.6.3 Beam walk test....31
4.6.4 Analysis of locomotor function using MotoRater....31
4.7 Tissue processing and histology....32
4.7.1 Quantitative analysis of axonal and blood vessels ingrowth and glial scarring .33

4.7.2 Grey and white matter sparing ..... 33
4.8 Gene expression analysis of spinal cord lesions ..... 34
4.9 Statistical evaluation ..... 35
5 Results ..... 36
5.1 Effect of ECM hydrogels derived from porcine spinal cord and urinary bladder on SCI repair (Tukmachev *et al.*, 2016) ..... 36
5.1.1 *In vitro* cell culture on ECM hydrogels ..... 36
5.1.2 Histological evaluation of ECM hydrogels after acute SCI ..... 37
5.1.3 Gene expression analysis induced by injection of ECM hydrogels ..... 42
5.1.4 Summary I ..... 45
5.2 Hydroxyphenyl derivate of hyaluronic acid hydrogel modified with RGD for SCI repair (Zaviskova *et al.*, 2018) ..... 46
5.2.1 *In vitro* cell culture on HA-PH hydrogels ..... 46
5.2.2 Evaluation of HA-PH-RGD hydrogels in acute SCI lesions ..... 47
5.2.3 Histological evaluation of HA-PH-RGD hydrogels in subacute SCI lesion ..... 49
5.2.4 Gene expression analysis in subacute SCI lesions ..... 53
5.2.5 Analysis of locomotor functions in subacute SCI lesions ..... 54
5.2.6 Summary II ..... 56
5.3 Effect of different hWJ-MSCs doses on spinal cord regeneration (Krupa *et al.*, 2018) ..... 57
5.3.1 hWJ-MSCs characterization ..... 57
5.3.2 Behavioural analysis after hWJ-MSCs application ..... 58
5.3.3 Histology and immunohistochemistry after hWJ-MSCs transplantation ..... 60
5.3.4 Gene expression induced by hWJ-MSCs application ..... 63
5.3.5 Summary III ..... 65
5.4 Stimulation of neurite growth by transgenic activation of α9 integrin and kindlin 1 (unpublished results) ..... 66
5.4.1 Summary IV ..... 69
6 Discussion ..... 70
6.1 Different animal models of SCI and experimental settings ..... 70
6.2 Advantages and limitations of natural biomaterials in spinal cord regeneration ..... 72
6.3 Therapeutic potential of hWJ-MSCs for SCI repair ..... 73
6.4 Tissue regeneration after SCI using histology and qPCR ..... 74
6.5 Behavioural outcome after SCI ..... 76
7 Evaluation of study aims ..... 77
8 Conclusion ..... 78

9 Souhrn....79
10 Author’s publications....80
11 References....82

# 1 List of abbreviations

| | |
|---|---|
| AEIDGIEL | Peptide: alanine – glutamic acid – isoleucine – aspartic acid – glycine – isoleucine – glutamic acid – leucine |
| Arg1 | Arginase 1 |
| BBB | Basso, Beattie and Bresnahan test (open field test) |
| BDNF | Brain-derived neurotrophic factor |
| BI | Before injury |
| CAG | Promotor (C – the cytomegalovirus early enhancer element; A – the first exon and the first intron of chicken beta-actin gene; G – the splice acceptor of the rabbit beta-globin gene) |
| Casp3 | Caspase 3 |
| Ccl | Chemokine (C-C motif) |
| CD | Cluster of differentiation |
| Cd163 | Gene for cluster of differentiation 163 |
| Cd86 | Gene for cluster of differentiation 86 |
| cDNA | Complementary deoxyribonucleic acid |
| ChABC | Chondroitinase ABC |
| CNS | Central nervous system |
| CSPG | Chondroitin sulfate proteoglycan |
| CTCF | Corrected total cell fluorescence |
| DAPI | 4,6-diamidino-2-phenylindole |
| DRG | Dorsal root ganglion |
| ECM | Extracellular matrix |
| ED1 | Anti-CD68 antibody |
| F | Fibrinogen |
| Fgf2 | Fibroblast growth factor 2 |
| Gap43 | Growth associated protein 43 |
| Gapdh | Glyceraldehyde 3-phosphate dehydrogenase |
| GFAP | Glial fibrillary acidic protein |
| GFP | Green fluorescent protein |
| $H_2O_2$ | Hydrogen peroxide |
| HA | Hyaluronic acid |
| HA-CHO | Hyaluronan polyaldehyde |

| | |
|---|---|
| HA-PH | Hydroxyphenyl derivate of hyaluronic acid |
| HA-PH-RGD | Hydroxyphenyl derivate of hyaluronic acid modified with the integrin binding peptide arginine – glycine – aspartic acid |
| HA-PH-RGD/F | HA-PH-RGD combined with fibrinogen |
| HCl | Hydrochloric acid |
| HLA | Human leukocyte antigen |
| HRP | Horseradish peroxidase |
| hWJ-MSCs | Human Wharton's jelly-derived mesenchymal stem cells |
| IKVAV | Peptide: isoleucine – lysine – valine – alanine – valine |
| Il | Interleukin |
| iPSCs | Induced pluripotent stem cells |
| Irf5 | Interferon regulatory factor 5 |
| IS | Immunosuppression |
| MHC | Major histocompatibility complex |
| Mrc1 | Macrophage mannose receptor 1 |
| mRNA | Messenger ribonucleic acid |
| MSCs | Mesenchymal stem cells |
| MTCO2 | Mitochondrially encoded cytochrome C oxidase 2 |
| NaCl | Sodium chloride |
| NaOH | Sodium hydroxide |
| Ncan | Neurocan |
| NF-160 | Neurofilament marker |
| NGF | Nerve growth factor |
| Nos2 | Nitric oxide synthase 2 |
| NSCs | Neural stem cells |
| NT-3 | Neurotrophin-3 |
| OSP | Oligodendrocyte specific protein |
| PBS | Phosphate-buffered saline |
| Ptgs2 | Prostaglandin-endoperoxide synthase 2 |
| Ptprz1 | Phosphacan 1 |
| qPCR | Quantitative real-time polymerase chain reaction |
| RECA | Anti-endothelial cell antibody |
| RGD | Peptide: arginine – glycine – aspartic acid |
| RNA | Ribonucleic acid |

| | |
|---|---|
| SC-ECM | Extracellular matrix hydrogel derived from porcine spinal cord |
| SCI | Spinal cord injury |
| SCs | Stem cells |
| SEM | Standard error of the mean |
| Sort1 | Sortilin 1 |
| Th | Thoracic vertebra |
| UB-ECM | Extracellular matrix hydrogel derived from porcine urinary bladder |
| Vegfa | Vascular endothelial growth factor A |

# 2 Introduction

The nervous system consists of peripheral and central nervous system (CNS). Both are built up of neurons and glial cells. Neurons are characterized by their ability to respond to stimuli with an electric discharge and fast conduction of the nerve impulse over long distances. The primary functions of glial cells in CNS, which include astrocytes, oligodendrocytes and microglia, are to support and protect neurons.

CNS can be anatomically divided into the brain and the spinal cord. The brain represents the highest control centre of the nervous system. The spinal cord serves as a bidirectional connection between the brain and peripheral nerves. It enables transmission of motor signals to body and sensory signals to the brain. Moreover, the spinal cord is also able to produce spinal reflexes.

The spinal cord contains a central region with gray matter surrounded by white matter and is covered with pia mater, arachnoid and dura mater. The gray matter, which consists of dorsal and ventral horns, is formed from different neuron types and glial cells. Motor neurons reside in the ventral horns and their axons leave the spinal cord via ventral roots to reach skeletal muscles, smooth muscles and glands. On the other hand, sensory neurons with cell bodies in the dorsal root ganglia (DRG) receive signals from sensory organs in the body and their axons enter the cord via dorsal roots to transmit information to the brain. Furthermore, interneurons ensure correct communication within spinal cord (Figure 1).

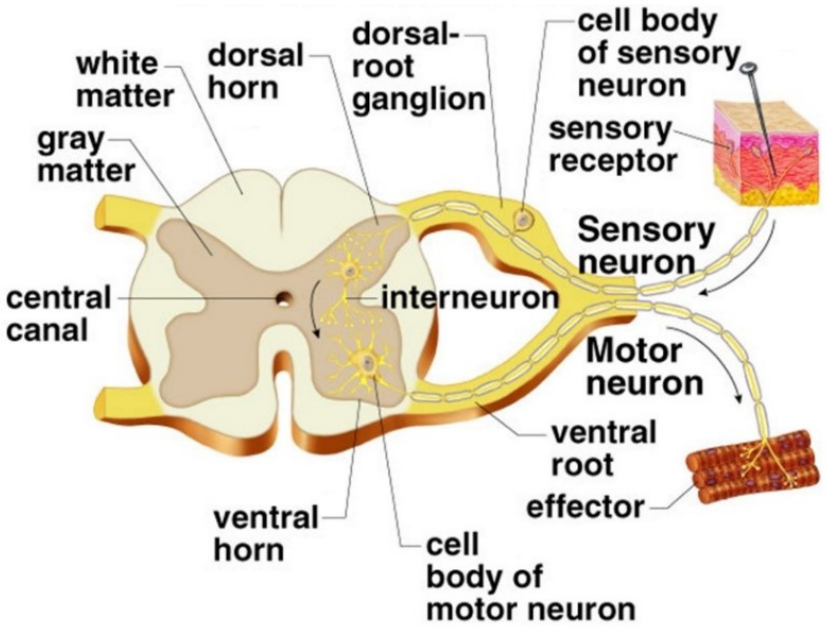


**Figure 1:** Schematic picture of the spinal cord anatomy (https://anatomybody101.com/spinal-cord-cross-section/spinal-cord-cross-section-image7/).

The white matter is mostly composed of groups of myelinated axons, which form ascending and descending tracts (Figure 2). Ascending tracts, which transmit mainly somatosensory information to higher level include posterior columns (fasciculus gracilis and fasciculus cuneatus), spinocerebellar, spinothalamic and spinoreticular tract. Descending tracts enable the brain control of spinal cord neurons and the periphery and can be divided into two major groups according function: pyramidal tract (corticospinal) for voluntary control of the musculature, and extrapyramidal tracts (reticulospinal, tectospinal, vestibulospinal and rubrospinal) for autonomous control of the musculature such as muscle tone, balance and posture. Additionally, propriospinal axons interconnect neurons of different parts of the spinal cord.

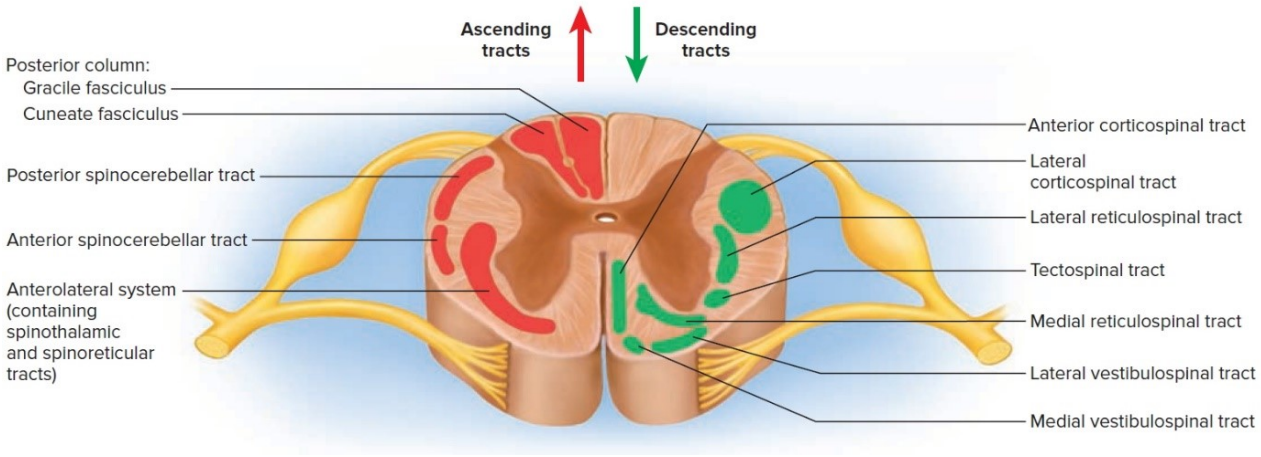


**Figure 2:** Approximated location of ascending and descending tracts in human spinal cord (Silva *et al.*, 2014).

The spinal cord is vertically organised in segments, which are divided into four regions: cervical, thoracic, lumbar and sacral. Humans and rats have similar number of segments with comparable functions. The human spinal cord comprises of 31 spinal nerves: 8 cervical, 12 thoracic, 5 lumbar, 5 sacral and 1 coccygeal. While the spinal cord of the rat comprises 34 spinal nerves: 8 cervical, 13 thoracic, 6 lumbar, 4 sacral and 3 coccygeal. From each segment arise paired spinal nerves form connection of dorsal and ventral roots, one on each side of the spinal cord (Figure 1). Cervical nerves control muscles and glands and receive sensory input from the neck, shoulder, arm and hand. Thoracic nerves are associated with the chest and abdominal walls. Lumbar nerves are connected with the hip and leg. Sacral nerves are linked to the genitals and lower digestive tract and coccygeal nerves supply the skin over the coccyx.

## 2.1 Spinal cord injury

Spinal cord injury (SCI) is a severe trauma affecting 250 – 500 thousand people worldwide every year (according World Health Organization). The leading causes of SCI are motor vehicle crashes, sport related accidents, falls and violence injures, affecting mostly young people. SCI often leads to a permanent loss of sensory and motor functions, which results in decreased quality of life and serious socio-economic consequences (Pego *et al.*, 2012; Raspa *et al.*, 2015). Pathophysiology of SCI is a complex set of phenomena, which together create an inhibitory environment blocking the axonal growth and repair (Delgado *et al.*, 2015; Hulsebosch, 2002; Willerth and Sakiyama-Elbert, 2008).

The SCI is usually caused by a mechanical insult to the spinal cord parenchyma followed by compression of fractured vertebra or disk protruding into the spinal canal (Macaya and Spector, 2012). SCI trauma can be divided into primary and secondary phase. Primary injury happens in the first seconds after the impact or laceration of the spinal cord tissue. The initial mechanical insult tends to damage primarily the central gray matter and blood supply (Dumont *et al.*, 2001).

Processes of the primary phase are further developed in the secondary phase (Figure 3). Secondary injury can be characterized as acute phase, which occurs 2 – 48 hours after primary injury, subacute phase in the following two weeks, and chronic phase starting several weeks after SCI. Secondary injury leads to additional cell death, scarring and loss of function. Detrimental biochemical changes include excessive calcium influx, which leads to glutamate excitotoxicity, lipid peroxidation, nitrous oxide excess and apoptosis of neurons, oligodendrocytes, microglia, and astrocytes (Oliveri *et al.*, 2014). The death of oligodendrocytes in white matter tracts continues for many weeks after the injury and may contribute to post-injury demyelination (Macaya and Spector, 2012; Silva *et al.*, 2014).

Vascular changes, including hemorrhage, breakdown of a blood-brain barrier and infiltration of inflammatory cells, leads to edema, necrosis and ischemia. Neutrophils and monocytes infiltrate the lesion over the course of hours to days. In later stages, monocytes differentiate into macrophages and resident microglia also become activated. Similarly, supportive astrocytes at the lesion periphery begin to hypertrophy and proliferate into a reactive phenotype (Donnelly and Popovich, 2008; Silva *et al.*, 2014).

The glial scar formed around the injury acts as a physical as well as biochemical barrier, preventing axons to grow through it. The scar is formed predominantly by reactive astrocytes, but also by microglia/macrophages and potent neurite growth-inhibiting substances such as

chondroitin sulphate proteoglycans (CSPGs), tenascin-C, myelin-associated glycoprotein, myelin oligodendrocyte glycoprotein, and neurite outgrowth inhibitor Nogo (Oliveri *et al.*, 2014). The CSPGs including aggrecan, brevican, neurocan, NG2, phosphacan, and versican, are proteoglycans consisting of a protein core and a chondroitin sulfate side chain. They act as guidance cues for developing growth cones during development, but on the contrary, in the adult CNS they inhibit axon growth after SCI (Silva *et al.*, 2014). Glycoprotein tenascin-C is also expressed mainly during CNS development and it is re-expressed following CNS injury. Tenascin-C can promote regeneration but also its inhibition because it has the ability to both support and restrict neurite outgrowth depending on tenascin-C splice variant. Nevertheless, one of the reasons for poor regeneration of adult CNS might be the lack of a receptor for tenascin-C (Andrews *et al.*, 2009; Chen *et al.*, 2010).

Chronic phase occurring months and years after the injury comprises of events such as white matter demyelination, Wallerian degeneration, gray matter disintegration, cavity formation, connective tissue deposition and reactive astrogliosis that stabilizes glial scar (Figure 3). Additionally, Schwann cells and their associated axons from the peripheral nervous system infiltrate the lesion. This ingrowth potentially serves as an impediment to neurite outgrowth and may cause pain, spasticity and other abnormal physical responses (Norenberg *et al.*, 2004).

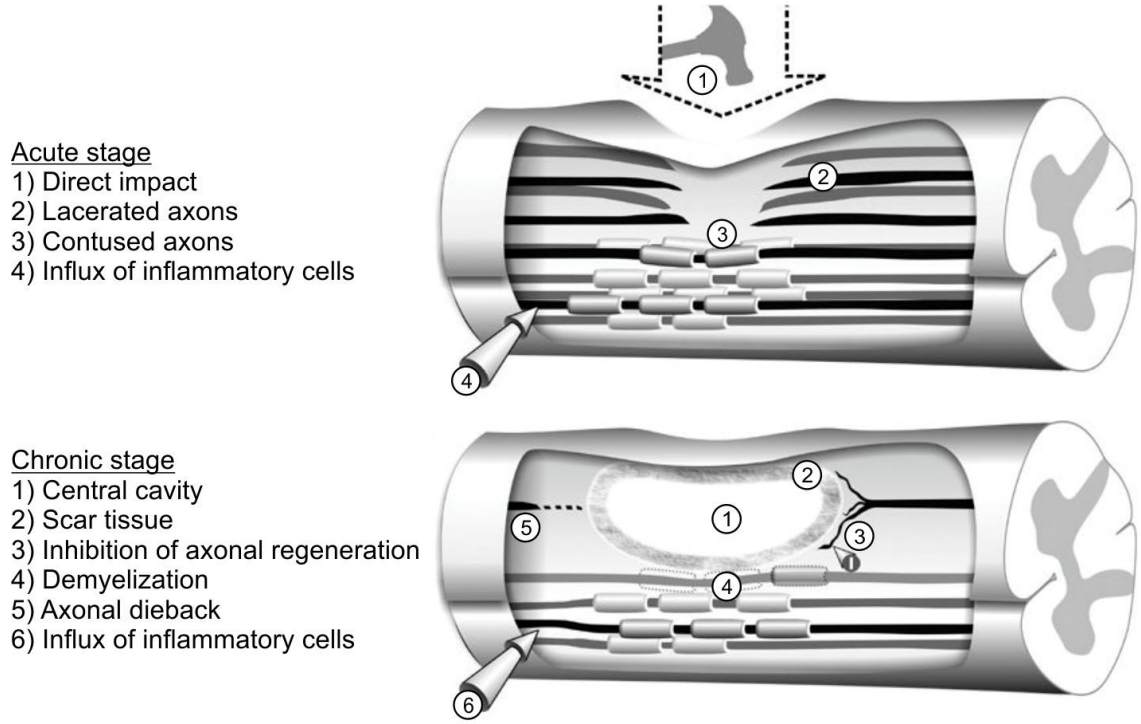


**Figure 3:** Schematic representation of the pathophysiological processes in the injured spinal cord in acute and chronic stages (Ronsyn *et al.*, 2008).

## 2.2 Spinal cord injury treatment

Currently, there is no effective therapy for SCI, which could successfully recover the lost functions. Existing interventions attempt to minimize secondary injury and protect neural tissue, which survived the mechanical injury. Standard therapy of acute SCI consists of surgical decompression of the injured segments, stabilization of the patient and, in some cases, the administration of methylprednisolon to neutralize acute inflammation. Chronic SCI treatment focuses on pain relief, rehabilitation, neural prostheses, decreasing spasticity and the prevention of side effects (Baptiste and Fehlings, 2007; Macaya and Spector, 2012).

Several research groups worldwide are focused on the experimental treatment of SCI. These include neuroprotection, activation of intrinsic neuronal regeneration capacity, removal of inhibition, regulation of gliosis and scar formation, reducing excitotoxicity and inflammatory response, replacing lost neurons and glia or providing cellular bridges for axon growth. Combinations of these therapies may reveal synergistic effects and represent a promising therapeutic approach in SCI treatment (Figure 4). The aim of tissue engineering is development of biomaterials, which could fill the cavity formed after SCI, provide permissive environment, and serve as structural support for axonal regrowth and angiogenesis (more in 2.3). Alternatively, cell therapy using various stem cells types (e.g. mesenchymal stem cells) or glial cells (e.g. olfactory ensheathing cells), which then secrete growth factors and modulate immune response in the site of injury, have been shown to have beneficial effects (more in 2.4) (Kubinova and Sykova, 2012; Raspa *et al.*, 2015). The experimental treatment of SCI in recent years also includes gene therapy, which has great regeneration potential due to long-term local delivery of therapeutic molecules into the injury site (more in 2.5) (Uchida *et al.*, 2014).

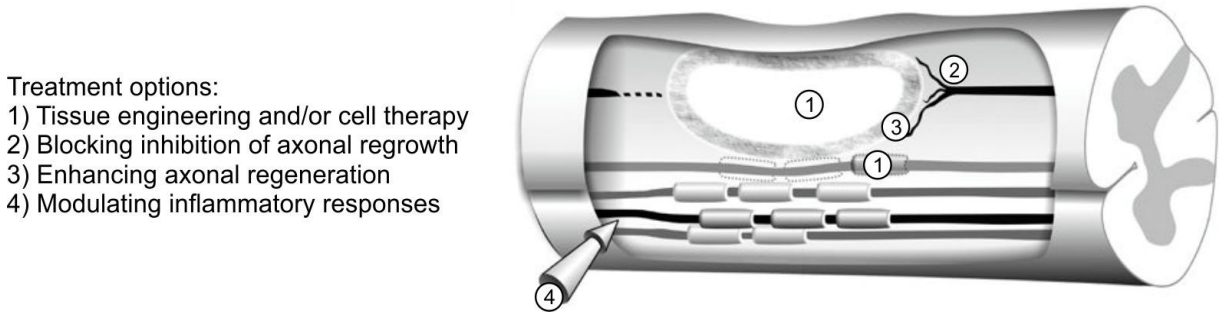


**Figure 4:** Schematic representation of different treatment options in SCI (Ronsyn *et al.*, 2008).

Molecular therapies usually focus on the modulation of inflammatory response, administration of growth-stimulating factors and/or blocking the inhibitory nature of the injured adult spinal cord tissue. Axonal growth can be stimulated for example by application of nerve

growth factor (NGF), brain-derived neurotrophic factor (BDNF) or neurotrophin-3 (NT-3). Moreover, ingrowth of blood vessels can be enhanced with vascular endothelial growth factor (Silva *et al.*, 2014). The inhibitory environment after SCI is caused mainly by CSPGs, components of the glial scar. This inhibition can be overcome by chondroitinase ABC (ChABC), which degrades CSPGs. Other obstacles in tissue regeneration after SCI are myelin-associated inhibitors such as Nogo. Therefore, a molecular therapy may use blocking antibodies against Nogo receptors (Young, 2014).

For axonal growth it is also necessary that growth cones interact with local extracellular matrix (ECM), which is mediated by integrin receptors. Integrin expression is at high levels in embryonal and early postnatal development, but is limited in adult CNS. Moreover, after SCI, the inhibitory molecules CSPGs and Nogo further inactivate integrin function. It has been shown that forced integrin activation by their intracellular activators kindlin and talin can overcome this inhibition (Eva and Fawcett, 2014; Lemons and Condic, 2008). Higher integrin expression also correlated with better neuronal regeneration (Condic, 2001; Cheah *et al.*, 2016).

## 2.3 Biomaterials

Cavity formation and the surrounding inhibitory glial scar are the main obstacles in axon regeneration after SCI. A convenient treatment is the implantation of a biomaterial, which can fill the tissue gap and serve as a bridge for axonal growth across the lesion cavity (Hejcl *et al.*, 2008a). Biomaterials that are suitable for SCI repair should fulfil several criteria:

- Biocompatibility (no toxicity, without any adverse effects).
- Similar physical and mechanical properties as the spinal cord tissue.
- Cell adhesive surface that allows attachment of both endogenous and transplanted cells.
- Porous structure allowing cell infiltration, axonal and blood vessels ingrowth.
- Controlled degradability in a physiological environment with matched material degradation and tissue regeneration rates (Kubinova and Sykova, 2012; Raspa *et al.*, 2015).

Many synthetic and natural biomaterials have been developed to treat SCI. These materials can be implanted in solid form or injected as liquid, which polymerizes *in situ* (Hejcl *et al.*, 2008a; Kubinova and Sykova, 2012; Pego *et al.*, 2012). Injectable scaffolds enable the filling of small defects like the cavities formed after SCI. Therefore, they can eliminate void spaces and create an integrative implant-tissue interface to restore the continuity of the tissue

(Macaya and Spector, 2012). On the other hand, solid implantable materials can be prepared with oriented pores or guiding tubular channels that can direct regenerating axons (Friedman *et al.*, 2002).

The most convenient materials for SCI tissue engineering are hydrogels. Hydrogels are three-dimensional networks composed of crosslink hydrophilic polymers, which contain a large proportion of water (up to 98 %), therefore allowing metabolite exchange (El-Sherbiny and Yacoub, 2013) and their mechanical properties can be set to match the neural tissue. Moreover, the adhesion properties of hydrogels can be enhanced by various functionalizations, such as integrin specific peptide sequences (for example RGD, IKVAV) or by using functional groups with a positive or negative charges (Hejcl *et al.*, 2008a).

Synthetic hydrogels can be custom made in a reproducible manner. However, they are unable to fully recapitulate the complexity of organization and bioactivity present in natural materials (Macaya and Spector, 2012). Non-degradable synthetic hydrogels include biomaterials based on poly(2-hydroxyethyl methacrylate) (Hejcl *et al.*, 2008b; Kubinova *et al.*, 2013), poly(N-(2-hydroxypropyl)-methacrylamide) (Woerly *et al.*, 2001) or polyethylene glycol (Borgens and Shi, 2000). The disadvantage is their persistence in the lesion site, which blocks full tissue reconstruction (Kubinova and Sykova, 2012). Synthetic biodegradable polymers used for neural applications generally consist of aliphatic polyesters, such as poly(lactic acid) (Hurtado *et al.*, 2011), poly(caprolactone) (Hwang *et al.*, 2011) or copolymer poly(lactic-co-glycolic acid) (Chen *et al.*, 2011; Kang *et al.*, 2011). Degradable biomaterials serve as a temporary filling of the cavity, which is gradually replaced by an anatomically appropriate and functional tissue. However, degradation products of these materials can potentially cause an inflammatory reaction (Kubinova and Sykova, 2012).

Natural-based materials used for CNS tissue repair include single ECM-molecules, such as collagen, fibronectin, hyaluronic acid (HA), and other naturally occurring polysaccharides (alginate, agarose, chitosan, gellan gum) or their combinations (Macaya and Spector, 2012; Madigan *et al.*, 2009). Another promising technique of how produce a natural scaffold that resembles structural and biochemical cues of the native tissue is tissue decellularization, in which the ECM is obtained by cell removal from the source tissue (Crapo *et al.*, 2012; Koci *et al.*, 2017). Advantages of natural biomaterials are their biocompatibility, biodegradability and support of cell adhesion. On the other hand, a disadvantage can be their variability and potential immunogenicity (Pego *et al.*, 2012).

### *2.3.1 ECM derived hydrogels*

Biological scaffolds composed of native ECM represent structures very similar to those of the uninjured host tissue with biological properties promoting cell adhesion and proliferation, three-dimensional structure, and biodegradability (Crapo *et al.*, 2012). Additionally, the degradation of ECM evokes the recruitment of endogenous stem and progenitor cells and modulates the innate immune response. After the removal of cellular antigens, ECM scaffolds are considered biocompatible and non-immunogenic even in allogeneic and xenogeneic settings (Badylak and Gilbert, 2008; Reing *et al.*, 2009).

ECM hydrogels can be prepared by the decellularization of variety of tissues, such as brain, spinal cord (Medberry *et al.*, 2013), heart valves (Kasimir *et al.*, 2003), blood vessels (Dahl *et al.*, 2003), urinary bladder (Meng *et al.*, 2015), liver (Lin *et al.*, 2004), ligaments (Woods and Gratzer, 2005), skin (Chen *et al.*, 2004), muscle (Zhang *et al.*, 2011) or umbilical cord (Koci *et al.*, 2017). Currently, ECM scaffolds are being widely used for various tissue reconstructions, including urinary tract (Wood *et al.*, 2005), myocardium (Ota *et al.*, 2008), lung (O'Neill *et al.*, 2013), skeletal muscles (Agrawal *et al.*, 2009), tendon (Zantop *et al.*, 2006), peripheral nerves (Karabekmez *et al.*, 2009), dura mater (Bejjani *et al.*, 2007) and spinal cord (Koci *et al.*, 2017). A number of ECM scaffolds derived from a range of source species and tissues have also been approved by the FDA and are commercially available for clinical use (Badylak, 2014).

Badylak *et al.* developed tissue specific injectable ECM hydrogels prepared by the decellularization of porcine brain, spinal cord and urinary bladder. All types of ECM hydrogels were found to be cytocompatible and increased the number of mouse neuroblastoma cells extending neurites *in vitro*, but only brain ECM increased the neurite length suggesting a possible tissue-specific effect. According to these results, ECM hydrogels derived from CNS might be advantageous in providing support for CNS repair also *in vivo* (Medberry *et al.*, 2013). In our group, we evaluated CNS ECM derived from porcine spinal cord (SC-ECM) and non-CNS ECM hydrogels derived from porcine urinary bladder (UB-ECM) (results in 5.1) and human umbilical cord in neural tissue repair (Koci *et al.*, 2017).

### *2.3.2 HA based hydrogels*

HA is an important structural component of ECM and it is widely used due to its biocompatibility, biodegradability, and non-immunogenicity as a biomaterial in clinical settings. Among its structural functions, HA also acts as a signalling molecule via specific HA

receptors, which actively modulates tissue regeneration (Knopf-Marques *et al.*, 2016; Litwiniuk *et al.*, 2016).

In neural tissue engineering, HA-based materials have been studied alone, *in vitro* as substrates for neural stem cell cultures (Seidlits *et al.*, 2010), as well as *in vivo* as carriers for cell delivery to improve cell retention and integration (Li *et al.*, 2017a; Liang *et al.*, 2013; Mothe *et al.*, 2013). Injectable HA-derived hydrogels were also developed for localized intrathecal delivery of bioactive molecules into SCI (Fuhrmann *et al.*, 2015; Gupta *et al.*, 2006).

Native HA does not form a gel nor does it support cell adhesion. Therefore, it is necessary to chemically modify the functional groups of HA and adjust its chemical, physical or biological properties according to the specific demands of a particular application. With regard to the gel formation, various HA derivatives can be stabilized by crosslinking, such as the dihydrazide crosslink of HA polyaldehyde, thiol-en click crosslinking of norbornene-HA derivative, initiated by UV light, copper catalyzed 1,3-dipolar cycloaddition reaction, or UV initiated crosslinking of methacrylated HA (Knopf-Marques *et al.*, 2016). To enable cell adhesion, the functionalization of HA-based materials has been achieved using a variety of techniques, such as the incorporation of poly-L-lysine (Wei *et al.*, 2010), laminin (Hou *et al.*, 2005), fibronectin (Seidlits *et al.*, 2011), fibrinogen (Snyder *et al.*, 2014), blending with methylcellulose (Caicco *et al.*, 2013), or modifying HA with integrin ligands derived from ECM, such as arginine-glycine-aspartic acid (RGD) sequence (Cui *et al.*, 2006).

One of such promising HA-based materials capable to form covalently cross-linked hydrogel with the required mechanical properties, is the hydroxyphenyl derivate of HA (HA-PH) (Darr and Calabro, 2009; Wolfova *et al.*, 2013). The cross-linking reaction of this HA-PH derivate can be triggered by the enzyme horseradish peroxidase (HRP) and hydrogen peroxide ($H_2O_2$) *in situ* under physiological conditions and without a negative effect on encapsulated cells during cross-linking reaction and gel forming (Kučera *et al.*, 2015). The potential of HA-PH hydrogel for SCI treatment was tested in this work for the first time (results in 5.2).

### *2.3.3 Fibrin gel*

A plasma derived polymer fibrin is being used as fibrin glue in many biomedical applications. Fibrin is a desirable biomaterial for nerve regeneration, based on its role in wound repair and tissue reconstruction. It also has inherent cell-binding sites (Madigan *et al.*, 2009). Fibrin scaffolds are formed from monomers following fibrinogen cleavage by thrombin and can be additionally crosslinked with factor XIIIa. Advantage of crosslinking with factor XIIIa

is also possibility to modified fibrin gel using bi-domain peptide with factor XIIIa substrate in one domain and bioactive peptide in another domain (Schense and Hubbell, 1999).

In neural tissue engineering, fibrin has been used as a matrix to fill nerve guidance tubes implanted following sciatic nerve injury, and was shown to promote axonal regeneration and cell migration (Lee *et al.*, 2003). Fibrin scaffolds have also been used in acute studies of complete spinal cord transection and were found to elicit increased neural fiber sprouting (Taylor *et al.*, 2006). Moreover, a study implanting fibrin polymer scaffolds into a dorsal hemisection model demonstrated delayed astrocytosis and improved neuron fiber extension (Johnson *et al.*, 2010). Fibrin scaffolds can also be used for stem cell transplantation and growth factor delivery (McCreedy *et al.*, 2014). In this work, we studied fibrin gel crosslinked with factor XIIIa and modified with integrin specific adhesion peptide as potential material for SCI treatment (preliminary results in 5.4).

### *2.3.4 Biomaterials in clinical applications*

Despite the intensive research in animal SCI models, no biomaterial has been introduced in human clinical practice yet. However, Table 1 shows, that some materials have already been studied in clinical trials (phase 1-3). A collagen scaffold, NeuroRegen, combined with human umbilical cord mesenchymal stem cells (MSCs) was used in a study of eight patients with chronic complete SCI. No adverse events were observed during one year of follow-up and primary efficacy outcomes, including better sensation level and increased finger activity, were observed in some patients (Zhao *et al.*, 2017). The Neuro-Spinal Scaffold is composed of two biocompatible and bioresorbable polymers, poly(lactic-co-glycolic acid) and poly-L-lysine. The 6-month follow-up of a nonrandomized human clinical trial evaluating the impact of implanting this scaffold reported an improvement of recovery (Guest *et al.*, 2018).

**Table 1**: Clinical trials for SCI using biomaterials.

| ClinicalTrials.gov Identifier | Title | Intervention | State | Phase |
|---|---|---|---|---|
| NCT02510365 | Functional Neural Regeneration Collagen Scaffold Transplantation in Acute Spinal Cord Injury Patients | Functional collagen scaffold | China | 1 |
| NCT02352077 | NeuroRegen Scaffold™ With Stem Cells for Chronic Spinal Cord Injury Repair | NeuroRegen scaffold with bone marrow mononuclear cells or MSCs transplantation | China | 1 |
| NCT02688062 | NeuroRegen Scaffold™ With Bone Marrow Mononuclear Cells Transplantation vs. Intradural Decompression and Adhesiolysis in SCI | NeuroRegen Scaffold with bone marrow mononuclear cells transplantation | China | 1 |
| NCT02688049 | NeuroRegen Scaffold™ Combined With Stem Cells for Chronic Spinal Cord Injury Repair | NeuroRegen scaffold/MSCs transplantation | China | 1 |
| | | NeuroRegen scaffold/neural stem cells transplantation | | 2 |
| NCT02138110 | The INSPIRE Study: Probable Benefit of the Neuro-Spinal Scaffold for Treatment of AIS A Thoracic Acute Spinal Cord Injury | Neuro-Spinal Scaffold | USA | 3 |

## 2.4 Stem cell therapy

Stem cells (SCs) are undifferentiated cells, which are capable of self-renewal and differentiation into other cell types. SCs normally function in a quiescent or slow cycling state, dividing only to maintain the SCs pool. When tissue regeneration is needed, they undergo the process of asymmetrical cell division, which results in two cell types: self-renewing SCs and cells beginning differentiation into the cell type that is needed. Pluripotent SCs differentiate into cells of all three embryonic lineages. Multipotent SCs can develop into multiple specialized cells in a specific tissue and unipotent cells differentiate only into one cell type (Dulak *et al.*, 2015).

There are three major types of SCs: embryonic, fetal and adult SCs. Embryonic SCs are pluripotent and are obtained from the inner cell mass of the blastocyst. Their disadvantages are the ethical concerns and high risk of tumorigenesis, which can be eliminated by pre-differentiation of embryonic SCs *in vitro* into neural precursors or oligodendroglia progenitors (Wu *et al.*, 2007a). Fetal SCs can be isolated from fetal blood and bone marrow as well as from other fetal tissues (O'Donoghue and Fisk, 2004). Adult SCs, which exist in the postnatal

organism, are either multipotent or unipotent. They include a wide range of cells, for example hematopoietic SCs, mesenchymal stem cells (MSCs), intestinal SCs, and neural stem cells (NSCs) (Dulak *et al.*, 2015). Moreover, induced pluripotent stem cells (iPSCs) are formed by reprograming fully differentiated somatic cells (e.g. fibroblasts) back to an embryonic-like state (Takahashi and Yamanaka, 2006).

For human clinical trials it is necessary to consider cell compatibility with the host tissue. Therefore, MSCs and iPSCs are very convenient due to possible autologous application when cells are derived from the patients' own tissue (Pego *et al.*, 2012). Other important criterion for selection of the right cell type is their effect on SCI regeneration. Neural precursors derived from embryonic SCs, fetal SCs, iPSCs or NSCs have the capacity to become neurons or glial cells after transplantation into the CNS and therefore are able to replace the missing or lost cells (Figure 5). However, only limited number of these cells is able to survive in the lesion and fully differentiate (Pego *et al.*, 2012). Oligodendrocyte progenitor cells generated from embryonic SCs or iPSCs have been shown to differentiate into oligodendrocytes and promote remyelination after transplantation into the demyelinated mouse spinal cord (Nistor *et al.*, 2005). Along with SCs, olfactory ensheathing cells and Schwann cells also support remyelination of injured axons (Pego *et al.*, 2012; Raspa *et al.*, 2015).

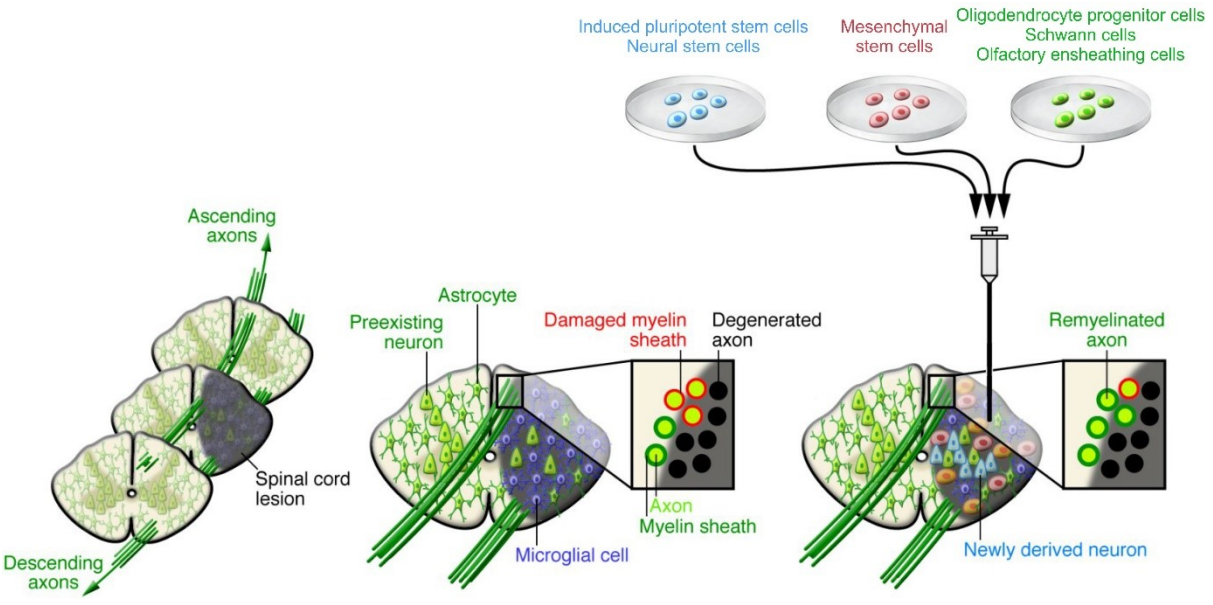


**Figure 5:** Schematic representation of stem cell therapy of SCI using different cell types (Lindvall and Kokaia, 2010).

### *2.4.1 Mesenchymal stem cells*

MSCs are stromal cells capable of self-renewal and differentiation into osteogenic, chondrogenic and adipogenic lineages. MSCs are primary located in bone marrow. However, they can also be easily isolated from adipose tissue, umbilical cord blood, dental pulp, skin, liver or Wharton's jelly. The use of MSCs lacks ethical controversy and allows for autologous transplantation with minimal immunoreactivity (Oliveri *et al.*, 2014; Raspa *et al.*, 2015).

MSCs have been shown to address and modulate many of the detrimental effects associated with acute and chronic damage in the traumatised spinal cord. Therapeutic effect of transplanted MSCs is mainly of paracrine nature, because these cells secrete a number of neurotrophic factors, anti-inflammatory cytokines and anti-apoptotic proteins (Pego *et al.*, 2012; Sykova *et al.*, 2006; Wright *et al.*, 2011). They protect neurons from glutamate excitotoxicity (Voulgari-Kokota *et al.*, 2012), reduce levels of stress-associated proteins, pro-inflammatory cytokines and reactive oxygen species (Zhou *et al.*, 2009). MSCs support revascularisation (Hou *et al.*, 2014), polarisation of classically activated pro-inflammatory M1 into alternatively activated pro-reparatory M2 macrophage phenotype (Giunti *et al.*, 2012). Additionally, MSCs have been shown to enhance NSCs oligodendrogenic differentiation and remyelinisation (Steffenhagen *et al.*, 2012). MSCs also reduce cavity formation and reactive astrocyte proliferation and gliosis (Voulgari-Kokota *et al.*, 2012) and stimulate neurite outgrowth in the presence of CSPGs, myelin associated glycoprotein and Nogo-A (Wright *et al.*, 2007).

Many studies show positive effects of MSCs transplantation on spinal cord regeneration (Hejcl *et al.*, 2010; Urdzikova *et al.*, 2006; Urdzikova *et al.*, 2014) and their safety has already been verified in a number of clinical trials, including studies in SCI (Pal *et al.*, 2009; Sykova *et al.*, 2006; Yoon *et al.*, 2007). The effects of MSCs on SCI repair were found after direct injection into the spinal cord lesion, as well as after intrathecal (Ohta *et al.*, 2004) and intravenous delivery (Urdzikova *et al.*, 2006). Several studies showed that rats grafted with human bone marrow MSCs intrathecally had reduced inflammatory response and apoptosis along with a rearranged glial scar leading to improved functional recovery after SCI (Cheng *et al.*, 2012; Oliveri *et al.*, 2014; Urdzikova *et al.*, 2014). Moreover, positive effect of MSCs on motor function can be enhanced by their repeated application (Cizkova *et al.*, 2011).

Apart from bone marrow and adipose tissue, Wharton's jelly derived mesenchymal stem cells (hWJ-MSCs) represent an easily accessible source without ethical concerns. Compared to adult MSCs isolated from bone marrow or adipose tissue, WJ-MSCs are more primitive, have greater *ex vivo* expansion capabilities (Amable *et al.*, 2014), lower immunogenicity due to lower

levels of MHC-I and absence of MHC-II expression (Zhou *et al.*, 2011) and they have been proven to be non-tumorigenic (Kim *et al.*, 2013).

hWJ-MSCs can be induced to differentiate *in vitro* into cartilage, bone, adipose tissue (Karahuseyinoglu *et al.*, 2007), skeletal muscle (Conconi *et al.*, 2006), cardiomyocytes (Wang *et al.*, 2004), endothelium (Wu *et al.*, 2007b) and neural cells (Fu *et al.*, 2006; Mitchell *et al.*, 2003). Therapeutic benefit of hWJ-MSCs in SCI alone (Cheng *et al.*, 2014; Liu *et al.*, 2013) as well as in combination with a biomaterial (Li *et al.*, 2017b; Zhao *et al.*, 2017) has been shown in several experimental and clinical studies. In this study, we explore whether the positive influence of hWJ-MSCs on SCI repair can be enhanced with a higher cell dose and/or their repeated application (results in 5.3).

## 2.5 Gene therapy

Gene therapy is characterized by the delivery of exogenous nucleic acids or gene products using various means including viruses and plasmids into cells. This modern method receives widespread attention in recent years as substantial progress has been made with improved tools for vector design. With gene therapy it may be possible to replace defective genes with functional ones, eliminate malfunctioning genes or introduce new genes to change cell phenotype that may help restore lost function (Franz *et al.*, 2012; Mantilla, 2017).

Viral vectors prepared especially from adeno-associated viruses and lentiviruses are currently the most widely used in CNS application. Genes involved in viral replication must be modified to ensure safety in clinical use. At the same time, the gene of interest is inserted into the viral vector. This construct can be then used for genetic modification of transplanted cells *in vitro* or directly *in vivo* in CNS tissue (Uchida *et al.*, 2014).

Genetic modification of cells can drive them to produce trophic factors, which promote tissue regeneration. This may overcome the problem of fast degradation of neurotrophic factors after their direct application into the injury site. For example, MSCs, NSCs, Schwann cell and fibroblast were modified to secrete higher amount of BDNF or NT-3 (Uchida *et al.*, 2014).

Therapeutic strategies are also focused on restoration of the intrinsic regenerative state of injured neurons. Viral transfer of BDNF gene was successful at promoting a regenerative response in rubrospinal neurons following acute cervical SCI (Kwon *et al.*, 2007). Expression of α9 integrin enabled neurite outgrowth from adult DRG neurons on tenascin-C *in vitro* (Andrews *et al.*, 2009). Similarly, overexpression of integrin activator kindlin 1 in cultured neurons increased axon growth on an inhibitory aggrecan substrate (Tan *et al.*, 2012). Finally,

sensory axons forced to express α9 integrin and kindlin 1 together displayed increased ability to regenerate after dorsal root crush and thus allowing restoration of sensory functions (Cheah *et al.*, 2016). In our laboratory, we have used this knowledge and developed a biomaterial modified with α9 specific adhesion peptide derived from tenascin-C, which will be transplanted into SCI together with viral mediated activation of α9 integrin and kindlin 1 (preliminary results in 5.4).

## 2.6 Combinatory therapies

SCI displays a very complex pathophysiology, therefore a combination of various therapeutic approaches is considered as the most effective strategy to complete recovery of motor and sensory functions. Figure 6 shows that several features of SCI pathophysiology can be treated using suitable cells compatible with neural tissue; three-dimensional scaffold mimicking the natural ECM; signalling molecules such as proteins, enzymes and growth factors targeting dysfunctional cellular processes; or enzymatic degradation of glial scar using ChABC (El-Sherbiny and Yacoub, 2013).

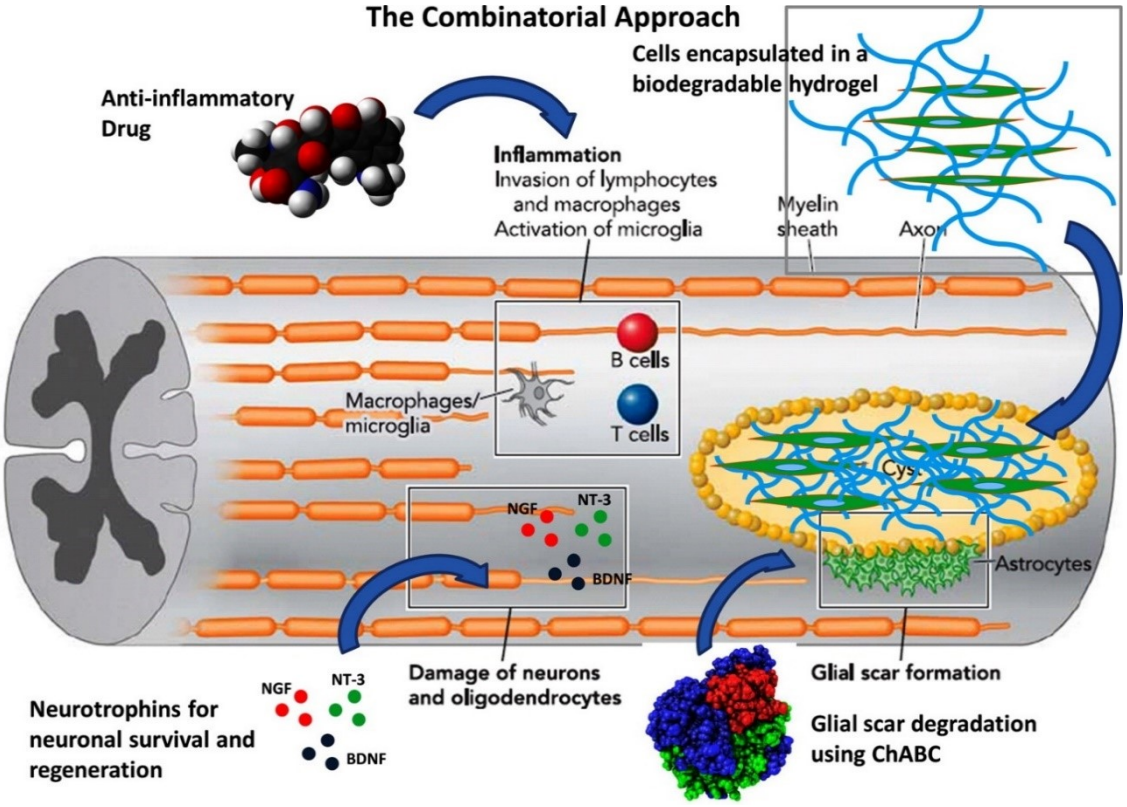


**Figure 6:** Schematic representation of potential combinatory therapy for SCI repair. The SCI pathophysiology can by treated using biomaterials, cells, anti-inflammatory drugs, neurotrophins (NGF: nerve growth factor, BDNF: brain-derived neurotrophic factor, NT-3: neurotrophin-3), and chondroitinase ABC (ChABC) (Silva *et al.*, 2014).

Various therapeutic strategies can be combined to achieve their synergistic effects. Biomaterials serve as a carrier for cells, enzymes and/or growth factors. Injectable materials are especially appropriate, because in their liquid state they can be mixed with cells and other therapeutics prior to delivery into the spinal cord defect (Macaya and Spector, 2012). Another way to improve the potential of biomaterials is to combine them with neurotrophic factors like BDNF, NT-3 and NGF. The addition of growth factors may provide a spatial cue for regenerating axons to prevent dieback and induce growth into the scaffold (McCreedy and Sakiyama-Elbert, 2012).

## 2.7 Experimental models of SCI

Many animal species have been used in SCI modelling including mice, rats, rabbits, cats, dogs, and primates. However, rats are the most commonly used animal to model SCI, because they are relatively inexpensive, readily available and have demonstrated similar functional, electrophysiological and morphological outcomes when compared to humans following SCI (Metz *et al.*, 2000). Based on the character of injury, SCI models can be classified as sharp or blunt.

Sharp injury models, such as transection or hemisection (Figure 7 A-C) are produced by complete or partial cut in one spinal cord segment. They are used especially for scaffold evaluation and studying axonal regeneration, but they poorly represent a typical human injury. A full transection results in a complete separation between caudal and rostral segments. An advantage of spinal cord transection model is its easy reproducibility, however, it causes a very severe injury and animals need intensive postoperative care. In a hemisection model, only half of spinal cord segments (lateral or dorsal) is removed, which leads to a milder animal impairment. Lateral hemisection leads to a loss of motor and sensory functions in the ipsilateral part of the body. While dorsal hemisection affects sensory function on both ipsilateral and contralateral side without considerable locomotor problems (Cheriyan *et al.*, 2014).

Blunt injury models, compression or contusion, are more clinically relevant and useful for studying acute pathophysiological processes. However, spared axons around the lesion can complicate evaluation of regeneration (Kwon *et al.*, 2004). In a compression model, prolonged pressure is applied on the spinal cord, which leads to cavity formation (Figure 7 D). A balloon-induced compression lesion involves the insertion of a catheter with a small inflatable balloon at its end into the epidural or subdural space. The balloon is then inflated with a fixed volume of saline leading to a compression of the spinal cord for a specified amount of time (Vanicky *et*

*al.*, 2001). Contusion injury models are produced by a controlled and short strike using a sharp impactor (Cheriyan *et al.*, 2014).

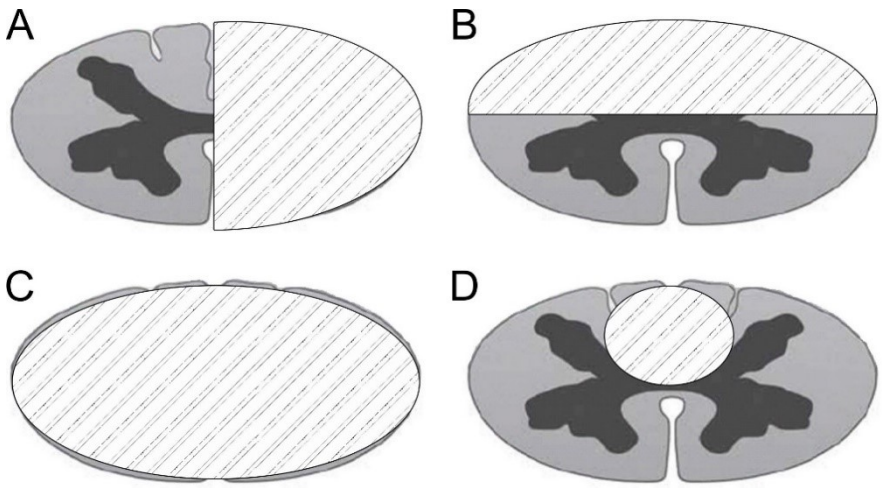


**Figure 7**: Experimental models of SCI. (A) Lateral hemisection, (B) dorsal hemisection, (C) transection, and (D) compression or contusion injury. The white dashed area on transverse sections indicates (A-C) a cut or (D) a damaged part of the spinal cord.

SCI models can also be classified according to the period between injury and treatment as acute, subacute and chronic. Acute intervention occurs immediately after injury. However, a delayed treatment in the subacute or chronic phase is more clinically relevant.

# 3 Aims and hypotheses

The general aim of this work was to study new possibilities of SCI treatment using biomaterials, stem cell and gene therapy in rat experimental models.

**Hypothesis 1:** Injectable natural biomaterials are suitable for SCI repair and help create permissive environment for tissue regeneration. Combination of biomaterials with hWJ-MSCs enhances effects of the treatment.

*Aim 1:* Evaluation of neuroregenerative potential of ECM hydrogels derived from porcine urinary bladder and porcine spinal cord alone or in combination with hWJ-MSCs in acute SCI.

*Aim 2:* Evaluation of neuroregenerative potential of HA hydrogel alone or in combination with hWJ-MSCs in acute and subacute models of SCI.

**Hypothesis 2:** Repeated intrathecal transplantation of hWJ-MSCs into SCI have beneficial and dose dependent effects on tissue repair and functional recovery after SCI.

*Aim 3:* Evaluation of therapeutic effects of single and repeated intrathecal transplantation of low (0.5 million) and high (1.5 million) dose of hWJ-MSCs after SCI.

**Hypothesis 3:** Transfection of adult DRG neurons with α9 integrin subunit and/or integrin activator kindlin 1 stimulates neurite outgrowth and has the potential to overcome the effect of the inhibitory environment which occurs after SCI.

*Aim 4:* Transfection of adult DRG neurons with kindlin 1 and evaluation of neurite growth in inhibitory environment induced by aggrecan *in vitro*.

*Aim 5:* Transfection of adult DRG neurons with α9 integrin subunit and evaluation of neurite growth on biomaterial modified with the α9 specific peptide (AEIDGIEL) derived from tenascin-C *in vitro*.

# 4 Materials and methods

## 4.1 Hydrogel preparation

### *4.1.1 ECM hydrogel preparation*

Porcine urinary bladders and spinal cords were obtained from an abattoir (Český Brod, Czech Republic). Spinal cord tissue was agitated at 200 rpm unless otherwise stated in the following decellularization baths: deionized water (16 h at 4 °C; 60 rpm), 0.02% trypsin/0.05% EDTA (60 min at 37 °C; 60 rpm; Invitrogen, USA), 3.0% Triton X-100 (60 min; Sigma-Aldrich, USA), 1.0 M sucrose (15 min; Fisher Scientific, USA), water (15 min), 4.0% deoxycholate (60 min; Sigma), 0.1% peracetic acid (Rochester Midland, USA) in 4.0% ethanol (120 min), phosphate-buffered saline (PBS) (15 min), deionized water (twice for 15 min each rinse), and PBS (15 min).

ECM from urinary bladder was prepared after connective tissue was removed from the serosal surface of the bladder. The tunica serosa, tunica submucosa, and a majority of the tunica muscularis mucosa were mechanically delaminated, which left the basement membrane and tunica propria intact. Luminal urothelial cells were dissociated from the basement membrane by soaking the UB-ECM in deionized water. The UB-ECM was then agitated in 0.1% peracetic acid in 4.0% ethanol (120 min; 300 rpm) followed by a series of PBS and deionized water rinses and lyophilization.

For hydrogel preparation, ECM samples were solubilized with 1.0 mg/ml pepsin in 0.01N HCl (Sigma-Aldrich, USA) at a concentration of 10 mg/ml and stirred at room temperature for 48 hours to form a pre-gel solution (pH ~ 2). The pepsin-HCl ECM solution was neutralized to pH 7.4 with 0.1N NaOH, isotonically balanced with 10x PBS, and diluted with 1x PBS to the concentration of 8 mg/ml. To form a hydrogel, the neutralized pre-gel was placed in 37°C for 45 min (Medberry *et al.*, 2013).

### *4.1.2 HA-PH-RGD hydrogel preparation and crosslinking*

HPA-K-AHA-GRGD oligopeptide sequence was synthesized by solid phase synthesis using Fmoc-SPPS protocol (Amblard *et al.*, 2006). The RGD sequence was further conjugated with hyaluronan polyaldehyde (HA-CHO; DS = 10 %; Mw = 400 kDa; purchased from Contipro a. s.) via reductive amination (Huerta-Angeles *et al.*, 2012; Šedová *et al.*, 2013). HA-CHO (1.00 g, 2.50 mmol dimers of HA) was dissolved in 100 ml of demineralized water. Then, HPA-K-Ahx-GRGD (0.25 mmol) was added to the reaction mixture and the mixture was further stirred for 1 hour at room temperature. Subsequently, a solution of picoline-borane complex

(0.625 mmol) in 10 ml of 50% propan-2-ol was added to the mixture. The reaction mixture was stirred for another 12 hours at room temperature. The final product was obtained after precipitation by propan-2-ol. The degree of substitution of HPA-K-Ahx-GRGD of such hydroxyphenyl derivate of hyaluronic acid modified with RGD (HA-PH-RGD) was 2.5%.

The HA-PH-RGD (20 mg/ml) was dissolved in 0.9 % NaCl and stirred for a period of at least 6 hours at room temperature to gain homogenous solutions. The crosslinking of HA-PH-RGD solution and hydrogel formation was initiated by the addition of 0.04 U/ml HPR (Sigma-Aldrich, USA) and 0.165 mM $H_2O_2$ (Merck, Germany) to the HA-PH-RGD solution. Fibrinogen (1 mg/ml) was added into HA-PH-RGD solution to form HA-PH-RGD/F. Cylindric teflon moulds with a volume of 0.4 ml were used for gel forming and maturation.

## 4.2 Mesenchymal stem cell isolation and culture

Human umbilical cord samples were collected from healthy full-term neonates after spontaneous delivery at the Department of Obsterics and Gynecology, University Hospital of Pilsen, Czech Republic. The samples were obtained upon written informed consent from mothers using the guidelines approved by the Institutional Ethics Committee. The proximal part of the umbilical cord close to the placenta (10-15 cm) was cut and immersed in sterile PBS (IKEM, Czech Republic) with antibiotic-antimycotic solution (Sigma-Aldrich, USA). Samples were transferred to the laboratory on ice to be processed within 24 hours of partum. After washing in PBS and betadine (EGIS Pharmaceuticals PLC, Hungary) and the removal of blood vessels and amniotic membrane, the remaining tissue (Wharton's jelly) was chopped into small pieces (1-2 $mm^3$). The pieces were transferred to culture dishes (Nunc; Schoeller, Czech Republic) containing the alpha-minimum essential medium (East Port, Czech Republic) supplemented with 5% platelet lysate (IKEM, Czech Republic) and gentamicin 10 mg/ml (Sandoz, Czech Republic), and cultivated at 37°C in a humidified atmosphere containing 5% $CO_2$. On day 10, the explants were removed from culture dishes, and the remaining adherent cells were cultured until 90% confluence and passaged using 0.05% Trypsin/EDTA (Life Technologies, USA). After passaging, cells were seeded into culture flasks (Nunc) at a density of 5 x $10^3$ cells/$cm^2$. The medium was changed twice a week.

The hWJ-MSCs from passage three were used for both *in vitro* and *in vivo* studies. The mesenchymal stem cell phenotype was characterized using fluorescence-activated cell sorting (FACS) analysis of surface marker profiles (FACSAria; Becton Dickinson, USA). The following antibodies against human antigens CD14, CD34, CD45, CD73, CD90, (Exbio, Czech

Republic), CD105 (BioLegend, USA), HLA ABC, and HLA-DR (Pharmingen, USA) were tested. Data analysis was performed using BD FASCDiVa software. hWJ-MSCs were differentiated into adipocytes, osteoblasts and chondrocytes to show their multilineage potential, which was confirmed by specific staining.

### 4.3 *In vitro* cell growth and viability

*In vitro* cell growth on the surface of ECM hydrogels was characterized using hWJ-MSCs cultures. Cell viability was determined after 1, 3, 7 and 14 days in culture using WST-1 reagent (Roche, Germany). Cells were cultured in 96-well plates (5000 cells/per well) coated with ECM hydrogels (90 µl/well) prior to cell seeding. Similarly, proliferation of hWJ-MSCs in the presence of HA-PH-RGD or HA-PH-RGD/F was determined after 3 hours, 1 day and 3 days in culture using WST-1 reagent (Roche, Germany). The hWJ-MSCs were mixed with HA-PH-RGD/F hydrogel to form 3D culture (20 µl, 8 x $10^4$ cells) in 1 ml of medium in a 24-well plate. The same volume of hydrogel without cells served as a background. At the measured time points, WST-1 reagent was added to each well and the plates were incubated for 2 hours at 37°C. The absorbance was measured using a Tecan Spectra ELISA plate reader (Tecan Trading AG, Switzerland) at 450 nm with a reference reading at 620 nm.

The hWJ-MSCs proliferation on HA-PH or HA-PH-RGD hydrogels alone or in combination with fibrinogen (1 mg/ml; Sigma-Aldrich, USA) was also evaluated using CellTiter-Glo reagent (Promega, USA). Hydrogels were formed into hydrogel film to cover the 24-well culture plate. The culture wells were seeded by 1.5 x $10^5$ of hWJ-MSCs per well. Luminescence was measured after 3, 7 or 12 days of cultivation.

The morphology of hWJ-MSCs grown in 2D or 3D hydrogels cultures was examined by fluorescent staining for actin filaments. After fixation in 4% paraformaldehyde in 0.1M PBS for 10-15 min, the cells were stained with Alexa-Fluor 568 phalloidin (1:400, Molecular Probes, USA), and the nuclei were visualized by using 4,6-diamidino-2-phenylindole (DAPI) fluorescent dye (1:1000, Invitrogen, UK).

### 4.4 Dorsal root ganglion neuron culture and transfection

DRG were dissected from adult male Wistar rats (3 months). The neurons were dissociated with 0.2% collagenase from Clostridium histolyticum and 0.1% trypsin and then centrifuged through 15% bovine serum albumin (all from Sigma-Aldrich, USA). The cells were

transfected with Neon transfection kit (Thermo Fisher Scientific, USA). For each reaction, 1 µg of plasmid (CAG-α9-V5, CAG-kindlin1-GFP or CAG-GFP) was used to transfect $10^5$ cells at 1200 V, 20 ms, and two pulses (Cheah *et al.*, 2016).

The glass cover slips were coated with poly-D-lysine (20 µg/ml) over night and then with laminin (1 µg/ml), aggrecan (25 µg/ml), MAPTRIX-M-VAEIDGIEL peptide (5-20 µg/ml, all from Sigma-Aldrich). Fibrin gel was made by mixing fibrinogen solution (fibrinogen 7.5 mg/ml, TG-aprotinin 10 ug/ml and TG-AEIDGIEL 1-2 mg/ml in Hepes buffer) and enzyme solution (thrombin 2 U/ml, $CaCl_2$ 2 mM, factor XIIIa 5 U/ml in Hepes buffer) in 1:1 ratio and incubated in 37°C for 1 hour. All chemicals were from Sigma, except TG-aprotinin, TG-AEIDGIEL and factor XIIIa kindly provided by Hubbell Lab, The University of Chicago, USA.

After electroporation, DRG were cultivated in DMEM (Thermo Fisher Scientific, USA) supplemented with fetal bovine serum (10%; Thermo Fisher Scientific, USA) and NGF (10 ng/ml; Sigma-Aldrich, USA) over night. Next day, the medium was changed and supplemented additionally with penicillin–streptomycin–fungizone (1%; Lonza, Switzerland) and mitomycin C (0.25 µg/ml; Sigma-Aldrich, USA).

Cells were fixed after 1, 2 or 3 days with 4% paraformaldehyde in PBS and stained with chicken anti-GFP, mouse anti-V5 and secondary antibody goat anti-chicken Alexa Fluor® 488, and goat anti-mouse Alexa Fluor® 488 (all from Thermo Fisher Scientific, USA). For quantitative analysis, length of the longest neurite of each cell was measured using ImageJ (National Institutes of Health, USA).

## 4.5 Spinal cord injury animal models

Adult male Wistar rats (250 - 300 g, Velaz, Czech Republic) were used as an experimental model. All experiments were performed in accordance with the European Communities Council Directive of 22$^{nd}$ of September 2010 (2010/63/EU) regarding the use of animals in research and were approved by the Ethics Committee of the Institute of Experimental Medicine, Academy of Sciences of the Czech Republic in Prague. After surgery procedure, all animals were housed two rats in a cage with food and water *ad libitum.*

### *4.5.1 Hemisected SCI lesion*

The surgery was performed under adequate pentobarbital anesthesia (60 mg/kg). The animals received local injections of mesocain (0.3 ml at the surgery site) additionally to general anaesthesia, as well as gentamicin (0.05 ml, intramuscularly, Lek Pharmaceutical, Slovenia)

and atropine (0.2 ml, atropine solution 1:5, BB Pharma, Czech Republic) injections. A laminectomy at the level of the 8$^{th}$ thoracic vertebra (Th8) was performed, the dura was incised with micro-scissors. The right half of one spinal cord segment (2 mm long) was dissected to generate a hemisection cavity. The dura mater was sutured with 10/0 monofil unresorbable thread (B Braun, Aesculap, Germany). The muscles and skin were sutured with 4/0 monofil unresorbable thread (4/0 Chirmax, Czech Republic).

### *4.5.2 Balloon-induced compression SCI lesion*

The animals were anesthetized with Isoflurane (Forane; Abbott Laboratories, UK), analgesia was induced by intramuscular injection of carprofen (Rimadyl, Cymedica, 4 mg/kg) and surgical prophylaxis was maintained by intramuscular injection gentamicin (5 mg/kg; Lek Pharmaceutical, Slovenia). After the skin incision, the paravertebral muscles were separated at the level of Th7 – Th12 and laminectomy of Th10 was performed. A sterile 2-french Fogarty catheter was carefully inserted into the epidural space until the centre of the balloon rested on the level of Th8. The balloon was rapidly inflated with 15 µl saline and kept for 5 minutes. During this procedure, 3 % isoflurane in air was administered at a flow rate of 0.3 l/minute, and the animal's body temperature was kept at 37 °C with a heating pad. After 5 minutes the catheter was rapidly deflated and removed, and separated muscles and incised skin were sutured by single non-absorbable stitches. The lesioned animals were assisted in feeding and urination until they had recovered sufficiently to perform these functions on their own. The animals received gentamicin (5 mg/kg) for 7 days to prevent postoperative infections.

### *4.5.3 Hydrogel application into spinal cord hemisection*

The neutralized and isotonically balanced liquid pre-gel solution of SC-ECM and UB-ECM hydrogels (8 mg/ml) were acutely injected into the spinal cord defect by an Omnican Insulin syringe for U-100 Insulin (B.Braun, Germany) and allowed to gelate *in situ*, followed by histological and gene expression analysis after 2, 4 and 8 weeks after the implantation (n = 5 per group, per time point). In the animal group treated with SC-ECM hydrogel seeded with hWJ-MSCs (n = 4) the hydrogels were mixed with cells prior to their implantation into the hemisection cavity. This animal group received daily cyclosporin A (10 mg/kg, intraperitoneally; Sandimmun; Novartis, Switzerland), azathioprine (2 mg/kg, perorally; Imuran, Aspen Europe GmbH, Germany) and methylprednisolon (2 mg/kg, intramuscularly; Solu-Medrol, Pfizer, Belgium).

In the animals with acute application of HA-PH-RGD hydrogel (n = 3, in each time point and group), the cavity was filled with hydrogel immediately after the hemisection was performed. Two methods of hydrogel application were used. First, HA-PH-RGD solution (20 mg/ml) was mixed with crosslinking components (HRP, $H_2O_2$) to form a gel in the teflon mould. The adjusted hydrogel volume was then implanted into the lesion to fill the hemisection cavity. In the second approach, approximately 5 µl of HA-PH-RGD hydrogel solution mixed with crosslinking agents was immediately injected by Omnican Insulin syringe for U-100 Insulin (B. Braun, Germany) into the lesion cavity, where the complete *in situ* gelation occurred. The control lesion was filled with saline.

Animals with a subacute lesion underwent hemisection one week before hydrogel injection. The liquid pre-gel solution of HA-PH-RGD hydrogel (n = 6), HA-PH-RGD/F (n=6) and HA-PH-RGD/F combined with hWJ-MSCs (3 million cells/0.5 ml, ~ 3 x $10^4$ transplanted cells in 5 µl of the hydrogel) (n = 7), was mixed with crosslinking agents and immediately injected into the hemisection cavity by Omnican Insulin syringe for U-100 Insulin to form gel *in situ*. The hemisection defect was filled with saline in the control SCI group (n = 8). From 5 days after the hemisection induction, all animal groups with a subacute hydrogel injection and controls received a daily injection of three immunosuppressants as described above.

### *4.5.4 Intrathecal cell transplantation*

Transplantation of hWJ-MSCs was performed on the 7$^{th}$, 14$^{th}$ and 21$^{st}$ day after the balloon-induced compression lesion. Table 2 shows four groups with single or repeated transplantation of different amount of cells and control group with saline. No differences between simple and repetitive application of the saline were found, so the results were pooled together as a single control. Treatment was given intrathecally by a lumbar puncture between lumbar vertebrae L3 and L4 or L4 and L5 through a 25 G needle under the short-time general anaesthesia (isofurane). After injection the needle was rested *in situ* for 30 seconds to prevent backflow of the content. The day before the transplantation, all animals received cyclosporine A (10 mg/kg; Novartis, Switzerland) which continued daily until the end of the experiment.

**Table 2**: Names of experimental groups with number of animals in each group.

| | | Single dose - 7$^{th}$ day after SCI | 3 doses - 7$^{th}$, 14$^{th}$ and 21$^{st}$ day after SCI |
|---|---|---|---|
| Dose | 0.5 million of hWJ-MSCs in 50 µl saline | 0.5M (n = 12) | 3x 0.5M (n = 8) |
| | 1.5 million of hWJ-MSCs in 50 µl saline | 1.5M (n = 9) | 3x 1.5M (n = 7) |
| | 50 µl saline | Saline (n = 11) | |

## 4.6 Behavioural analysis

### *4.6.1 BBB test*

The BBB open field test, originally described by Basso, Beattie and Bresnahan (Basso *et al.*, 1995), was used to assess basic locomotor functions (the joint movement, weight support, forelimb-hindlimb coordination, paw placement and stability of the body). The rats were placed on the floor surrounded by boundaries making a rectangular shape once a week. Results were evaluated in the range of 0-21 points (0 indicated complete lack of motor capability and 21 movements as a healthy rat).

### *4.6.2 Rotarod test*

Rotarod unit machine (Ugo Basile, Italy) was used to test advanced ability to balance on a rotating rod and the latency to fall off the rod was measured. Each animal was taught this task before surgery. Animals were placed on a rotating rod at a fixed speed of 10 rpm before surgery and 5 rpm after surgery and were left to walk for maximally 60 seconds. There were four trials per day within 5 consecutive days starting 3 week after SCI.

### *4.6.3 Beam walk test*

The beam walk test measured the ability to cross a 1m long narrow beam with a flat surface. Rats were placed on one side of the beam and on the other side was placed an escape box. The latency (maximum 60 seconds) to traverse the beam were measured and recorded by a video tracking system (TSE-Systems Inc., Germany). Performance of locomotor coordination was evaluated twice per day for 3 consecutive days starting 3 weeks after SCI using 0-7 point scale modified from Goldstein (Goldstein, 1997) (0 indicate inability to stand on the beam, 7 use and coordination of both legs).

### *4.6.4 Analysis of locomotor function using MotoRater*

To investigate the effect of the hydrogel treatment on the gait of the rat, locomotor functions were quantitatively evaluated using MotoRater 303030 and TSE Motion 8.5.11 software (TSE-systems, Germany). Animals were pretested before injury and their iliac crests, hips and knees were point-marked with a tattoo machine. The analysis was based on video recordings captured with a high-speed colour camera (CamRecord CL600x2, 1280 x 1024 pixel, Stemmer Imaging, Germany). In each day of recording, iliac crests, hips, knees, ankles, metatarsophalangeal joints of the 5$^{th}$ toe, and paws were additionally marked with a black marker. Parameters which displayed differences when compared to the healthy control animals

were determined as described previously (Zorner *et al.*, 2010). Minimal and maximal angles in the hip and knee ankle were calculated between three neighbouring points. Protraction and retraction were determined as the maximal and minimal distance of iliac crest and metatarsophalangeal joint on the x-axis. All parameters were determined from the side view of the right (defected) leg using TSE Motion 8.5.11 software, and compared to the parameters obtained for the healthy animals.

### 4.7 Tissue processing and histology

At the end of experiment, the animals were deeply anesthetized with an intraperitoneal injection of overdose 10% chloral hydrate (Sigma-Aldrich, USA) and intracardially perfused with PBS and then 4% paraformaldehyde in 0.1 M PBS. The spinal cord was left in the bone for one week in 4% paraformaldehyde in 0.1 M PBS. In experiments with hemisection, a 3cm long segments of the spinal cord containing the lesioned site were dissected out, transferred to sucrose and frozen. Then, a series of 40 μm thick longitudinal sections were collected. After balloon-induced compression lesion, the spinal cords were dissected and removed from the spinal column and embedded in paraffin wax. Serial cross-sections 5 μm thick were obtained by microtome within a 2cm long segment around the centre of the lesion. Each sample of the spinal cord was cut at 1mm intervals. A total number of fifteen cross-sections, including the centre of the lesion, were analysed.

Hematoxylin-eosin, Luxol-fast blue and Cresyl violet staining were performed using a standard protocols. Immunohistological staining was used to visualize neuronal filaments, blood vessels, glial scar, macrophages, oligodendrocytes, and human cells. Non-specific immunohistological staining was avoided by the application of blocking goat or donkey serum (1:10; Sigma-Aldrich, USA) depending on the secondary antibody host organism. Triton X-100 (0.1% in 0.1M PBS; Sigma-Aldrich, USA) was used for the permeabilization of cell membranes. Samples were stained with antibodies against neurofilaments 160 kDa (NF-160, 1:200), glial fibrillary acidic protein (GFAP, conjugated with Cy3, 1:800; all from Sigma-Aldrich, USA); growth associated protein 43 (GAP43, 1:100), M2 macrophages (CD206, 1:250; all from Santa Cruz, USA); endothelial cell (RECA-1, 1:500), microglia/macrophages (ED1, 1:150), oligodendrocytes (OSP, 1:1000), human mitochondria (MTCO2, 1:250; all from Abcam, UK); and human nucleus (HuNu, 1:40, Merck-Millipore, Germany). Donkey anti-mouse IgG AlexaFluor® 488, donkey anti-goat IgG AlexaFluor® 594, donkey anti-goat IgG Alexa Fluor® 488, goat anti-mouse IgG Alexa Fluor® 488, goat anti-mouse IgG Alexa Fluor®

594 (all 1:400; Life Technologies, USA), and goat anti-mouse IgM Cy3 (1:200; Merck-Millipore, Germany) were used as secondary antibodies. The nuclei were visualized by using DAPI fluorescent dye (1:1000; Invitrogen, UK).

Fluorescent micrographs were taken using fluorescence microscopes Observer D1 and Axioskop 2 with AxioVision 4.8.2 software (Zeiss, Germany), LEICA DMI6000B (Leica, Germany) with TissueFAXS software (TissueGnostics GmbH, Austria) and a laser scanning confocal microscope LSM 5 DUO (Zeiss, Germany).

### *4.7.1 Quantitative analysis of axonal and blood vessels ingrowth and glial scarring*

For analysis of axonal and blood vessels ingrowth, three images across the lesion (cranial side, central and caudal side) from three longitudinal sections for each animal were taken using a 20x objective. The relative area of the axons (NF-160 staining) and blood vessels (RECA staining) within the images was analysed using ImageJ software (National Institutes of Health, USA). Quantification analysis expressed the percentage of NF-160 or RECA positive area from a total lesion area.

The newly sprouted axons were visualized immunohistochemically using GAP43 staining. The acquired images taken by a 20x objective were analysed and the number of GAP43-positive fibers per section was manually counted.

To evaluate glial scarring after hemisection, three mosaic images of GFAP staining for each animal was taken using a 20x objective. Integrated density and mean grey value of three areas around the lesion (cranial side, central and caudal side) and background (uninjured part of spinal cord) was measured by ImageJ software. Results were expressed as the corrected total cell fluorescence (CTCF), while CTCF = Integrated Density – (Area x Mean grey value of background) (McCloy *et al.*, 2014).

To determine the extent of the glial scar after balloon-induced compression lesion images from fifteen cross-sections were taken using a 20x objective. The acquired images were analysed using ImageJ software. GFAP positive area around the central cavity together with the number of protoplasmic astrocytes was measured on each section.

### *4.7.2 Grey and white matter sparing*

For visualizing white and grey matter of the spinal cord, Luxol fast blue and Cresyl violet staining were used. Acquired images taken by a 5x objective were analysed for the total area of spared grey and white matter by ImageJ software.

### 4.8 Gene expression analysis of spinal cord lesions

Changes in the mRNA expression of genes related to M1 macrophages (*Irf5, Cd86, Nos2*), M2 macrophages (*Mrc1, Cd163, Arg1*), axonal growth (*Gap43*), angiogenesis (*Vegfa*), growth factors (*Fgf2, Sort1*), apoptosis (*Casp3*), inflammation (*Ccl3, Ccl5, Ptgs2, Il2, Il6, Il12b*), astrogliosis (*Gfap*) and glial scar related CSPGs (*Ncan, Ptprz1, Cspg4*) were determined by quantitative real-time PCR (qPCR). RNA was isolated from paraformaldehyde-fixed frozen tissue sections in experiments with hemisection SCI model, and from paraffin cross sections in study with balloon-induced compression lesion. The High Pure RNA Paraffin Kit (Roche, Germany) was used and RNA amounts were quantified using NanoPhotometer® P 330 (Implen, Germany). The isolated RNA was reverse transcribed into complementary DNA (cDNA) using the Transcriptor Universal cDNA Master (Roche, Germany) and T100$^{TM}$ Thermal Cycler (Bio-Rad, USA). The qPCR reactions were performed using cDNA solution, FastStart Universal Probe Master (Roche, Germany) and TagMan® Gene Expression Assays (Table 3; Thermo Fisher Scientific, USA). The qPCR was carried out in a final volume of 10 µl containing 20 - 25 ng of extracted RNA. Amplification was performed on the real-time PCR cycler (StepOnePlus$^{TM}$, Life Technologies, USA). All amplifications were run under the same cycling conditions: 2 min at 50°C, 10 min at 95°C, followed by 40 cycles of 15 s at 95°C and 1 min at 60°C. All samples were run in duplicate and water was included in each array as negative control; with *Gapdh* as a reference gene. Results were expressed as log2-fold changes of ΔΔCt values relative to control spinal cord lesions treated with saline or unlesioned spinal cord.

**Table 3:** List of used TagMan® Gene Expression Assays

| **Gene** | **Catalog number** |
|---|---|
| Arginase 1 (*Arg1*) | Rn00566603_m1 |
| Caspase 3 (*Casp3*) | Rn00563902_m1 |
| Cluster of differentiation 163 (*Cd163*) | Rn01492519_m1 |
| Cluster of differentiation 86 (*Cd86*) | Rn00571654_m1 |
| Fibroblast growth factor 2 (*Fgf2*) | Rn00570809_m1 |
| Glial fibrillary acidic protein (*Gfap*) | Rn00566603_m1 |
| Glyceraldehyde 3-phosphate dehydrogenase (*Gapdh*) | Rn01775763_g1 |
| Growth associated protein 43 (*Gap43*) | Rn01474579_m1 |
| Chemokine (C-C motif) ligand 3 (*Ccl3*) | Rn01464736_g1 |
| Chemokine (C-C motif) ligand 5 (*Ccl5*) | Rn00579590_m1 |
| Inducible nitric oxide synthase 2 (*Nos2*) | Rn00561646_m1 |
| Interferon regulatory factor 5 (*Irf5*) | Rn01500522_m1 |
| Interleukin 12b (*Il12b*) | Rn00575112_m1 |
| Interleukin 2 (*Il2*) | Rn00587673_m1 |
| Interleukin 6 (*Il6*) | Rn01410330_m1 |
| Macrophage mannose receptor 1 (*Mrc1*) | Rn01487342_m1 |
| Neurocan (*Ncan*) | Rn00581331_m1 |
| Chondroitin sulfate proteoglycan 4 (*Cspg4*) | Rn00578849_m1 |
| Phosphacan (*Ptprz1*) | Rn00689852_m1 |
| Prostaglandin-endoperoxide synthase 2 (*Ptgs2*) | Rn01483828_m1 |
| Sortilin 1 (*Sort1*) | Rn01521847_m1 |
| Vascular endothelial growth factor A (*Vegfa*) | Rn01511601_m1 |

## 4.9 Statistical evaluation

The statistical significance of the differences in histological and gene expression analysis between the groups was assessed using either one-way ANOVA, or two-way ANOVA in the case of a second factor (time, concentration). Differences between the groups in behavioural tests and in areal measuring of the grey/white matter sparing and GFAP positive area of glial scar was measured with two-way repeated measurement ANOVA. Student-Newman-Keuls or Holm-Sidak *post hoc* pair-to-pair test was used (SigmaPlot V13; Systat Software Inc., USA). Differences were considered statistically significant if $p < 0.05$. All data in graphs are expressed as mean ± standard error of the mean (SEM).

# 5 Results

## 5.1 Effect of ECM hydrogels derived from porcine spinal cord and urinary bladder on SCI repair (Tukmachev *et al.*, 2016)

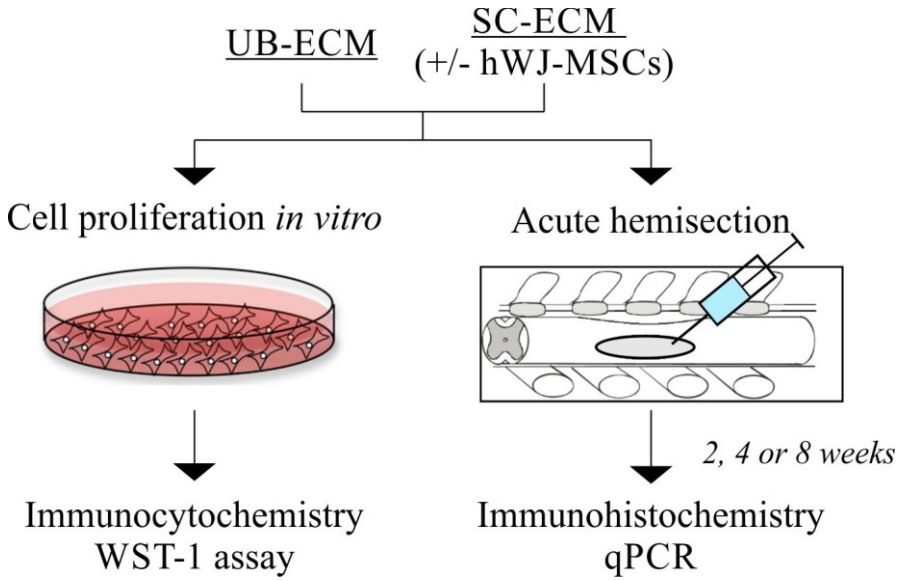


**Figure 8:** Schematic representation of experimental design.

### *5.1.1 In vitro cell culture on ECM hydrogels*

The solubilized ECM matrix self-assemble from the pre-gel form into a hydrogel at 37ºC and physiological pH. The biocompatibility and bioadhesive properties of ECM hydrogels were confirmed *in vitro* using hWJ-MSCs in the 2D and 3D cell cultures. After seeding on the ECM hydrogels, cells spread and proliferated on both SC-ECM and UB-ECM. Cell proliferation was determined using WST-1 assay after 1, 3, 7 and 14 days in culture (Figure 9 A). Both ECM hydrogels showed comparable ability to support *in vitro* cell proliferation, which did not significantly differ from the control cell proliferation on tissue culture plastic. Cell viability increased until day 7 of culture, then after reaching confluency it decreased on both hydrogel types as well as on tissue culture plastic. When seeded in 3D culture (0.5 million cells per 0.2 ml), hWJ-MSCs extended their lamelipodia within the hydrogels and formed a 3D network apparent after 4 and 24 hours (Figure 9 D-G).

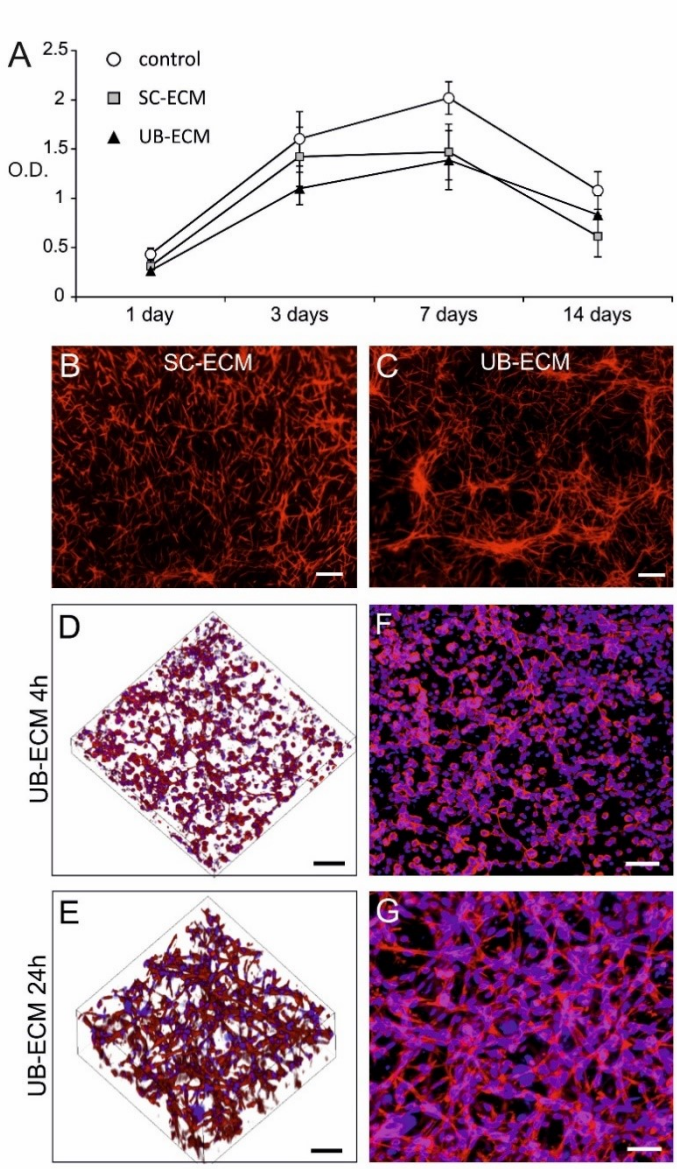


**Figure 9:** (A) Proliferation of hWJ-MSCs on ECM hydrogels using WST-1 assay. 2D cell culture on (B) SC-ECM and (C) UB-ECM hydrogel at 3 days. 3D cell cultures in UB-ECM (D, F) at 4 h and (E, G) 24 h. Cells were stained for phalloidin (red) and cell nuclei (DAPI, blue). Scale bar: (B, C) 100 µm, (D-G) 50 µm.

### *5.1.2 Histological evaluation of ECM hydrogels after acute SCI*

UB-ECM and SC-ECM hydrogels were injected into the spinal cord hemisection and histologically evaluated 2, 4 and 8 weeks later by analysing axonal ingrowth, vascularization and infiltration of astrocytes, macrophages, and oligodendrocytes within the injury site.

Hematoxylin-eosin staining of longitudinal spinal cord sections demonstrated that both hydrogel types were detectable in the lesion area in 2$^{nd}$ week after implantation, they were biocompatible with the surrounding host tissue and filled the lesion cavity with no signs of any

adverse effects (Figure 10 A, B). In 4th week after the injury, several small cysts developed due to the rapid graft degradation (Figure 10 D, E) and in 8th week the progression of cyst formation continued (Figure 10 G, H). Nevertheless, the newly formed tissue interconnected with the host tissue and bridged the lesion centre. In contrast to the tissue remodelling process observed in the lesion after hydrogel injection, large pseudocysts were formed in the control sham-treated lesion (Figure 10 C, F, I).

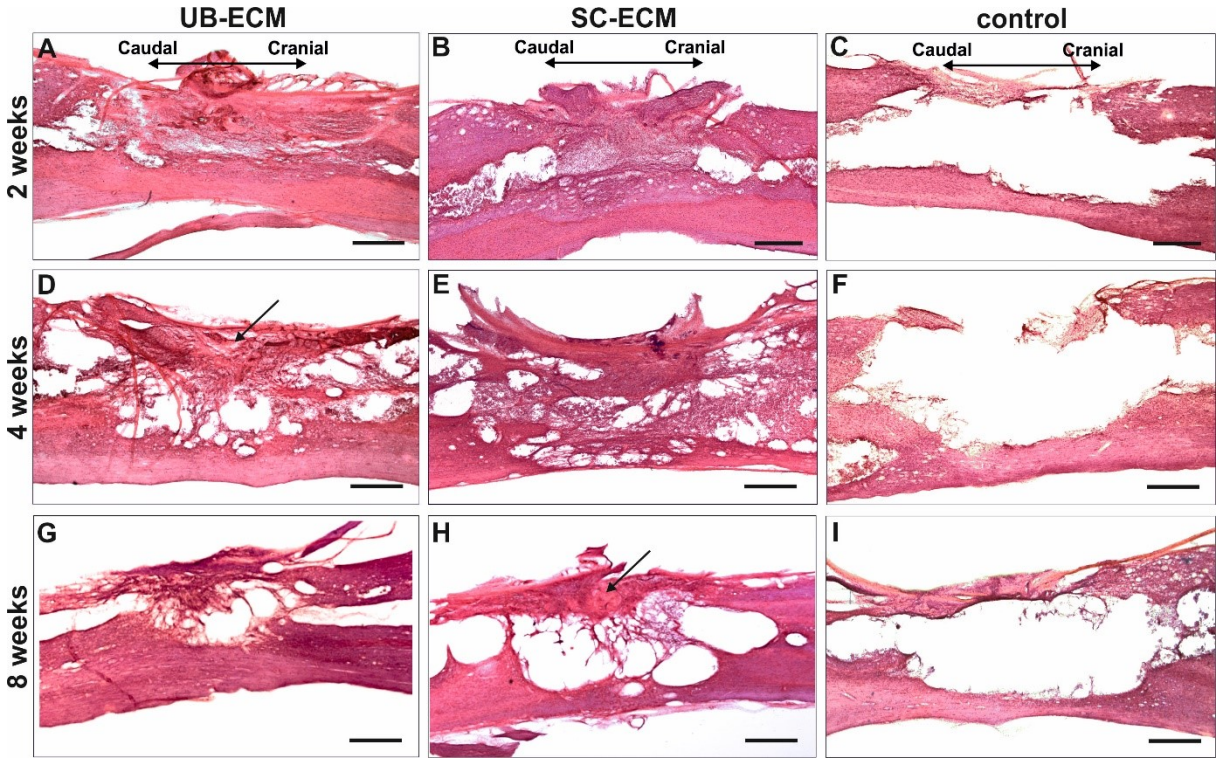


**Figure 10:** Hematoxylin-eosin staining of the longitudinal sections of the spinal cord lesion (A-C) 2 weeks, (D-F) 4 weeks and (F-I) 8 weeks after injection of (A, D, G) UB-ECM hydrogel; (B, E, H) SC-ECM hydrogel or (C, F, I) sham-operated control lesion. Scale bar: 500 µm.

To evaluate axonal ingrowth into the hydrogels, a neurofilaments marker (NF-160) was used (Figure 11 A, B, D, E). Robust ingrowth of NF-160 positive fibres into the ECM hydrogel treated lesion was observed from both caudal and cranial site of the lesion and the dense infiltration of neurofilaments was also found in the centre of the lesion. Quantitative analysis was expressed as percentage value of NF-160 positive area relative to the lesion area. The ingrowth of neurofilaments reached maximum levels at 2nd week in both hydrogel groups and did not further increase in later time points. No differences in the NF-160 area were found between UB-ECM and SC-ECM hydrogels in any of the time points (Figure 11 G). Astrocytes,

evaluated by immunofluorescent staining of GFAP, did not migrate inside the lesion and only a few astrocytic processes grew into the graft from the lesion edge (Figure 11 C, F).

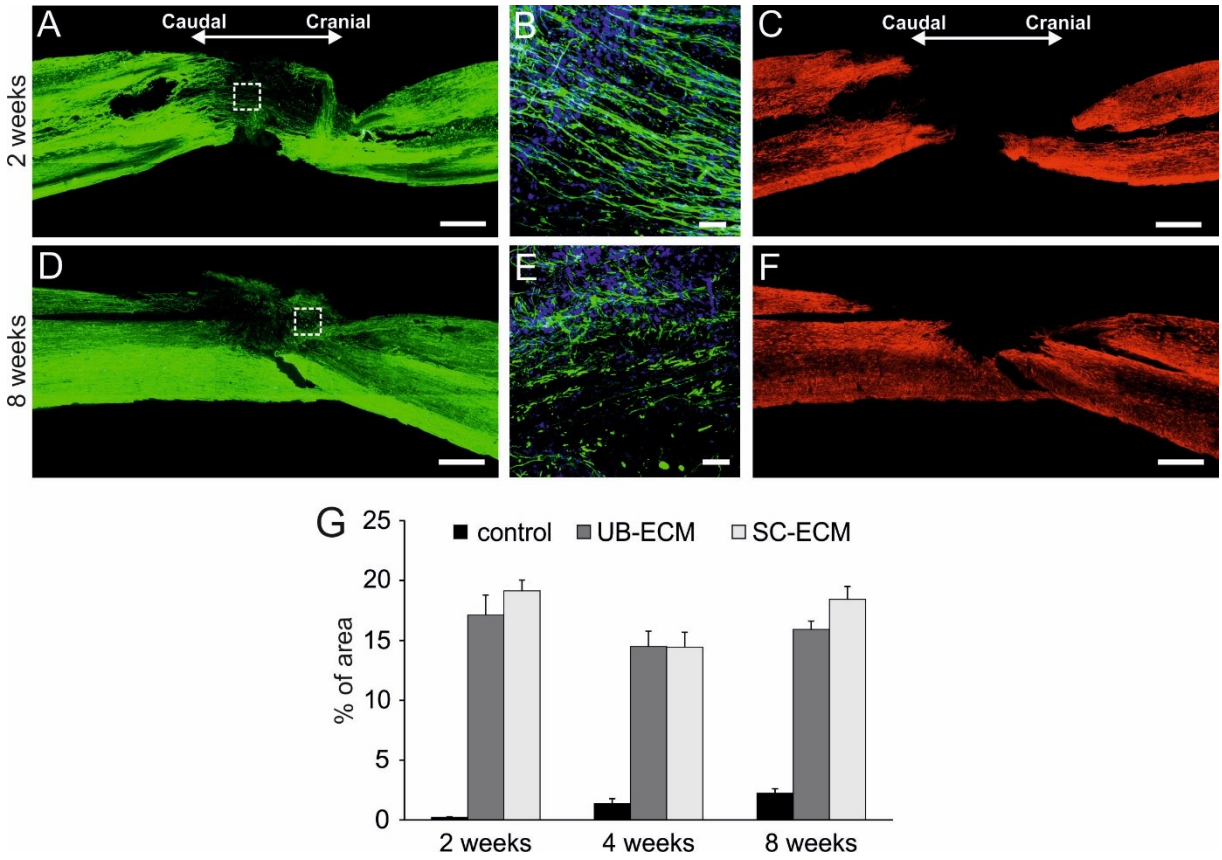


**Figure 11:** Longitudinal sections of the spinal cord lesion (A-C) at 2 weeks and (D-F) at 8 weeks after injection of SC-ECM hydrogel. Immunofluorescent staining of (A, B, D, E) neurofilaments (NF-160, green), (C, F) astrocytes (GFAP, red) and (B, E) cell nuclei (DAPI, blue). Dashed squares in (A, D) represent the area magnified on the right (B, E). (G) The effect of ECM hydrogels on the ingrowth of neurofilaments. A significantly higher neurofilament ingrowth was found in both ECM hydrogel groups when compared to the control lesion in all time points. Scale bar: (A, C, D, F) 500 µm, (B, E) 50 µm.

Regarding vascularization, higher number of blood vessels (RECA staining) grew into the hydrogel treated lesions compared to controls in all time points (Figure 12 A-D). The relative area of blood vessels gradually increased in time, but no statistical differences in blood vessel density were found between the UB-ECM and SC-ECM hydrogels at any of the time points (Figure 12 E).

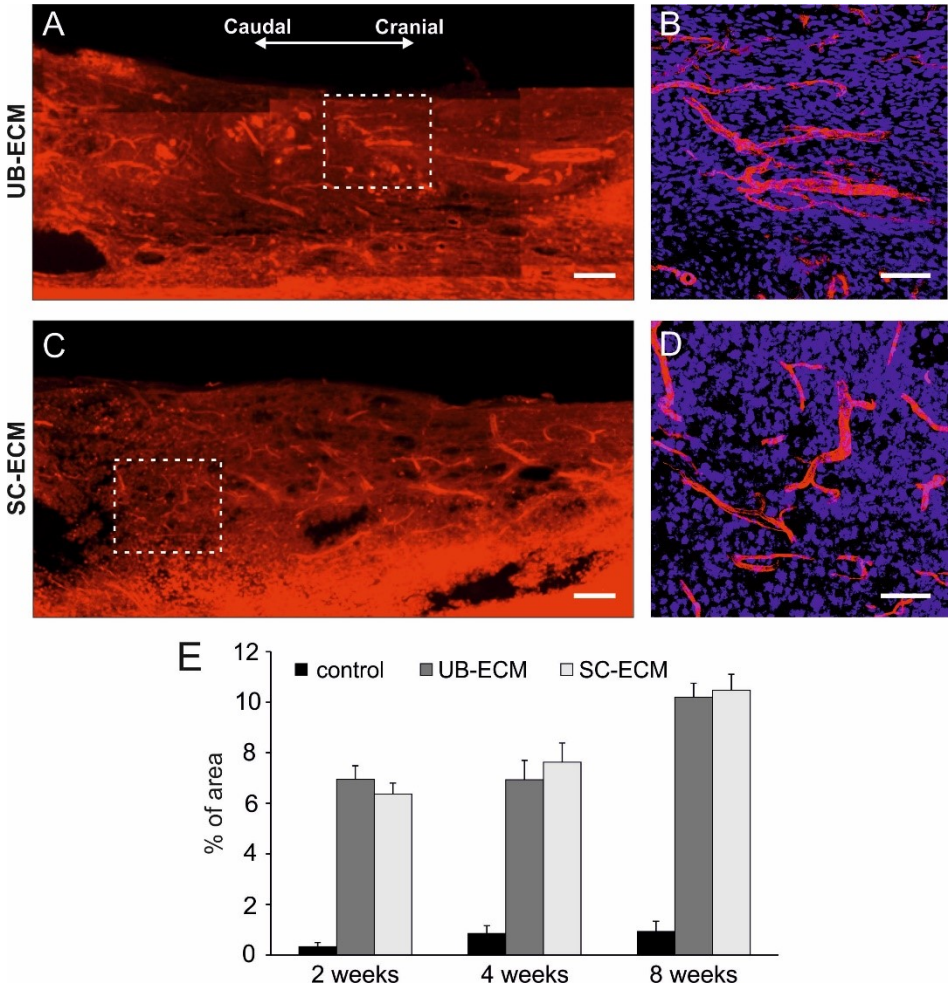


**Figure 12:** Longitudinal sections of the spinal cord lesion at 2 weeks after injection of (A, B) UB-ECM and (C, D) SC-ECM hydrogels. Immunofluorescent staining for blood vessels (RECA, red) and (B, D) cell nuclei (DAPI, blue). Dashed squares in (A, C) represent the area magnified on the right (B, D). (E) The effect of ECM hydrogels on the vascularization. A significantly higher ingrowth of blood vessels was found in both ECM hydrogel groups when compared to the control lesion in all time points. Scale bar: (A, C) 500 µm, (B, D) 50 µm.

The host tissue inflammatory response was characterized by robust infiltration of macrophages throughout the entire lesion area (Figure 13 A, B), which populated the hydrogels at all time points and persisted in the lesion site also after the hydrogel degradation. As is apparent from the staining for M1 and M2 macrophage phenotype in Figure 13 C, macrophages in neural tissue were predominantly of pro-inflammatory M1 phenotype (CD86 staining) while anti-inflammatory M2 phenotype macrophages (CD206 staining) were mostly present within the hydrogel. Infiltration of oligodendrocytes (OSP staining, Figure 13 D) within the lesion area showed that myelination occurred in some regenerating axons. Newly sprouted axonal fibers were detected using GAP43 staining (Figure 13 E).

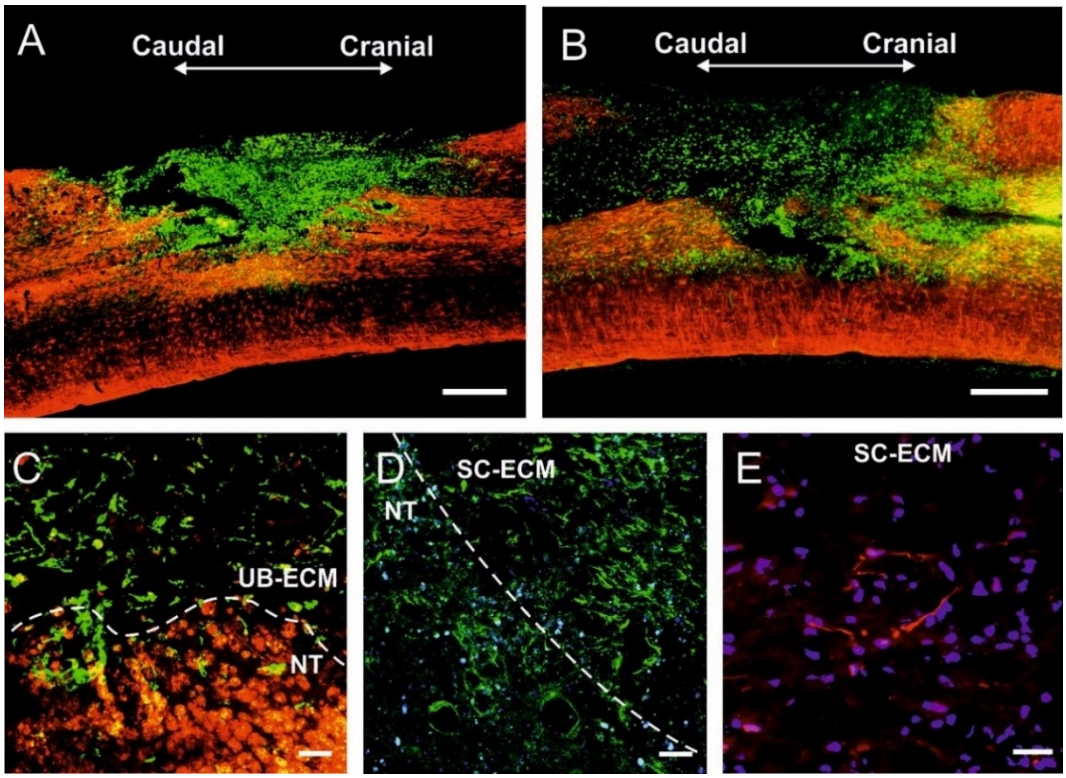


**Figure 13:** Immunofluorescent staining of (A, B) macrophages (ED1, green) and astrocytes (GFAP, red) in (A) UB-ECM at 2 weeks and (B) SC-ECM seeded with hWJ-MSCs at 4 weeks. Confocal micrographs of the staining for (C) M1 macrophages (CD86, red) and M2 macrophages (CD206, green) in UB-ECM hydrogel at 2 weeks; (D) oligodendrocytes (OSP, green) and cell nuclei (DAPI, blue) in SC-ECM at 4 weeks; (E) neuronal growth cones (GAP43, red) and cell nuclei (DAPI, blue) in SC-ECM at 4 weeks. The dotted line in (C, D) describes the border between ECM hydrogel and neural tissue (NT). Scale bar: (A, B) 500 µm, (C, D) 50 µm, (E) 25 µm.

To evaluate the potential of ECM hydrogels as cell carriers, the SC-ECM hydrogel was mixed with hWJ-MSCs (0.5 million cells per 0.2 ml), and the cell-hydrogel constructs were implanted into the hemisection cavity. Dense grafts were integrated with endogenous tissue while cysts developed at the graft-tissue interface 4 weeks after the injection (Figure 14 A). Only few surviving cells, positive for marker of human mitochondria (MTCO2), were detected in the lesion (Figure 14 B). Increased relative area of NF-160 positive fibres was found in groups of animals that received immunosuppression. However, transplanted cells did not further increase the ingrowth of NF-160 positive fibres or blood vessels (Figure 14 F).

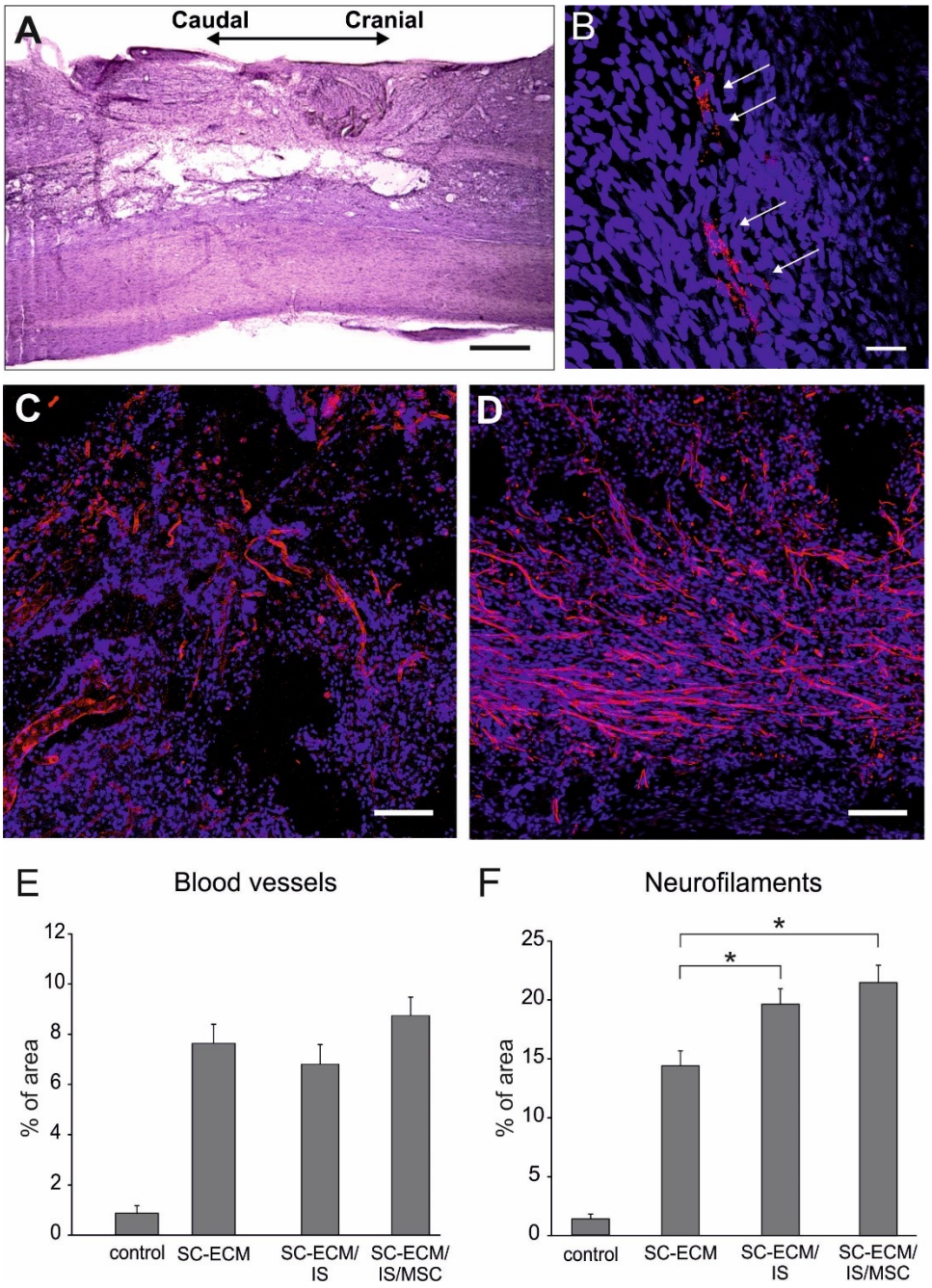


**Figure 14:** Longitudinal section of the spinal cord lesion after implantation of SC-ECM seeded with hWJ-MSCs at 4 weeks. (A) Hematoxylin-eosin staining. Confocal micrographs of staining of (B) human mitochondria (MTCO2, red); (C) blood vessels (RECA, red); (D) neurofilaments (NF-160, red) and (B - D) cell nuclei (DAPI, blue). Effect of the SC-ECM hydrogel seeded with hWJ-MSCs on the ingrowth of (E) blood vessels and (F) neurofilaments. (IS) animal groups that received immunosuppression. * $p < 0.05$. Scale bar: (A) 500 µm, (B-D) 50 µm.

### *5.1.3 Gene expression analysis induced by injection of ECM hydrogels*

Changes in the mRNA expression of genes related to growth factors (*Sort1, Fgf2*), axonal sprouting (*Gap43*), astrogliosis (*Gfap*), angiogenesis (*Vegfa*), M1 macrophages (*Irf5, Cd86, Nos2*), M2 macrophages (*Mrc1, Cd163, Arg1*), inflammation (*Ptgs2, Ccl3, Ccl5, Il2, Il6, Il12b*),

and apoptosis (*Casp3*) were determined at 2, 4 and 8 weeks after hydrogel injection and compared to the control SCI lesion (Figure 15, Table 4).

Two weeks after the injury, the treatment with both UB-ECM and SC-ECM significantly downregulated expression of *Fgf2, Gap43, Ccl5, Irf5, Cd163*, while *Gfap* and *Sort1* was decreased only in UB-ECM group. Effect of hydrogels disappeared 4 weeks after the injury. Nevertheless, immunosuppression alone decreased *Casp3, Gfap, Cd86, Sort1* and increased *Vegfa* and *Ccl3*. Importantly, combination of SC-ECM with hWJ-MSCs significantly increased mRNA levels of *Gap43* and *Vegfa* compared to SC-ECM only. Tissue specific effect of hydrogels was observed at 8 weeks after the injury, when *Fgf2, Casp3, Irf5,* and *Sort1* expressions were upregulated in group with SC-ECM and not UB-ECM. Expression of pro-inflammatory cytokines *Il2, Il6, Il12b* and *Nos2* was undetectable in all groups.

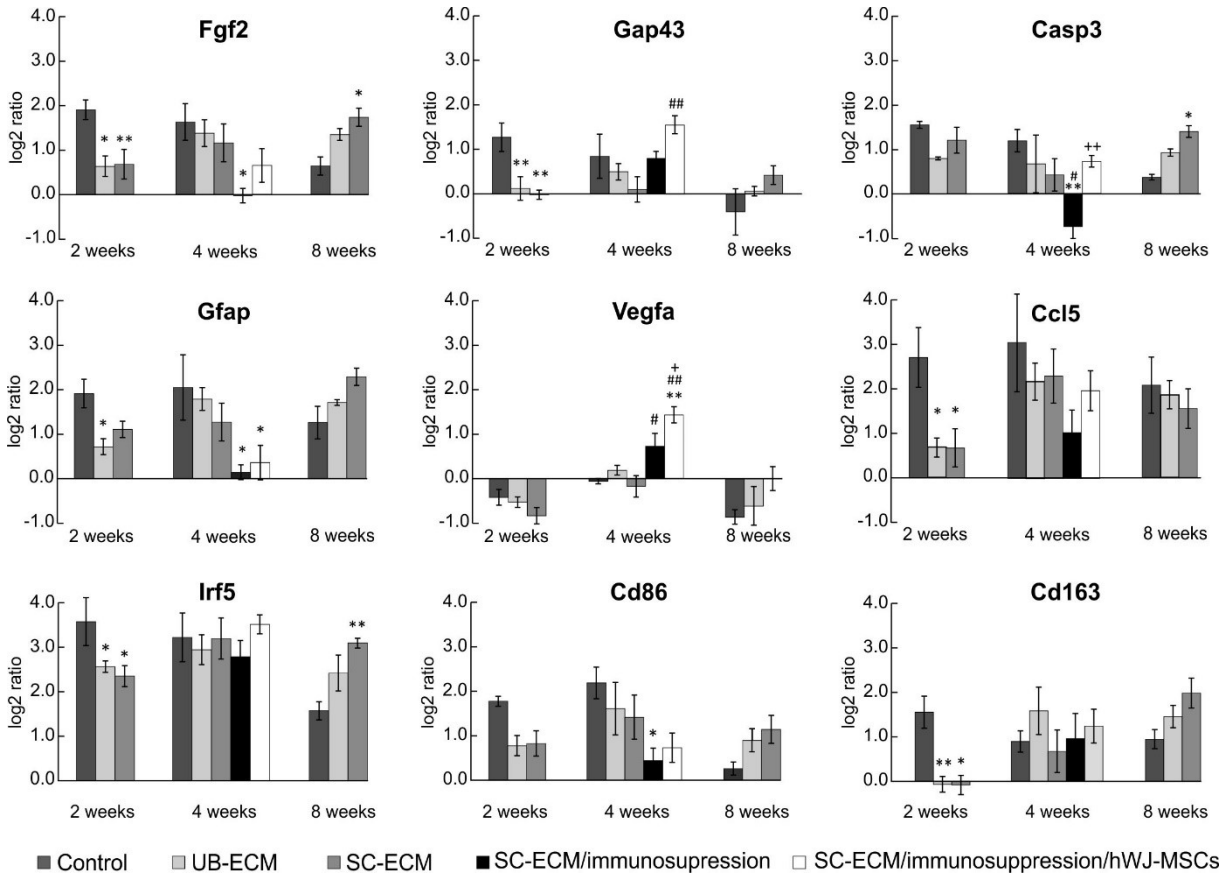


**Figure 15:** Analysis of mRNA gene expression of several genes involved in inflammatory and reparative processes following SCI treated with ECM hydrogels. The graphs show the log2 fold changes in gene expression over intact spinal cord tissue. * $p < 0.05$, ** $p < 0.01$ ΔCt values of ECM hydrogel vs control lesion. # $p < 0.05$, ## $p < 0.01$ ΔCt values of SC-ECM hydrogel with immunosuppression vs SC-ECM. + $p < 0.05$, ++ $p < 0.01$ ΔCt values of SC-ECM hydrogel with immunosuppression and hWJ-MSCs vs empty SC-ECM with immunosuppression.

**Table 4:** Expression of selected genes in the spinal cord lesions treated with ECM hydrogels. The values are expressed as log2 fold changes ± SEM in gene expression relative to intact spinal cord tissue.

| **Sort1** | Control | UB-ECM | SC-ECM | SC-ECM/IS | SC-ECM/IS + hWJ-MSCs |
|---|---|---|---|---|---|
| **2 weeks** | 0.66 ± 0.36 | -0.56 ± 0.21 ** | -0.02 ± 0.33 | | |
| **4 weeks** | 0.83 ± 0.20 | 0.47 ± 0.21 | 0.004 ± 0.39 | -0.56 ± 0.12 * | 0.22 ± 0.28 |
| **8 weeks** | -0.30 ± 0.07 | 0.35 ± 0.21 | 0.81 ± 0.08 * | | |
| | | | | | |
| **Arg1** | Control | UB-ECM | SC-ECM | SC-ECM/IS | SC-ECM/IS + hWJ-MSCs |
| **2 weeks** | 0.62 ± 0.17 | -1.17 ± 0.41 | -1.07 ± 0.35 | | |
| **4 weeks** | 0.18 ± 0.41 | 1.88 ± 0.43 # | -0.06 ± 0.81 | 0.80 ± 0.72 | 1.56 ± 0.57 |
| **8 weeks** | -0.18 ± 0.30 | 1.04 ± 0.41 | 0.21 ± 0.22 | | |
| | | | | | |
| **Ccl3** | Control | UB-ECM | SC-ECM | SC-ECM/IS | SC-ECM/IS + hWJ-MSCs |
| **2 weeks** | 5.01 ± 0.08 | 4.96 ± 0.53 | 5.14 ± 0.57 | | |
| **4 weeks** | 5.69 ± 0.62 | 5.90 ± 0.76 | 5.26 ± 0.60 | 2.89 ± 0.22 *# | 4.05 ± 0.79 |
| **8 weeks** | 3.14 ± 0.56 | 4.16 ± 0.89 | 4.09 ± 0.99 | | |
| | | | | | |
| **Ptgs2** | Control | UB-ECM | SC-ECM | SC-ECM/IS | SC-ECM/IS + hWJ-MSCs |
| **2 weeks** | 2.22 ± 0.58 | 1.48 ± 0.14 | 1.60 ± 0.52 | | |
| **4 weeks** | 2.35 ± 0.83 | 1.51 ± 0.13 | 1.79 ± 0.46 | 0.91 ± 0.33 | 2.31 ± 0.31 |
| **8 weeks** | 1.14 ± 0.59 | 1.64 ± 0.15 | 2.40 ± 0.37 | | |
| | | | | | |
| **Mrc1** | Control | UB-ECM | SC-ECM | SC-ECM/IS | SC-ECM/IS + hWJ-MSCs |
| **2 weeks** | 3.63 ± 0.48 | 2.67 ± 0.26 | 2.50 ± 0.34 | | |
| **4 weeks** | 3.16 ± 0.36 | 3.19 ± 0.64 | 2.63 ± 0.40 | 0.77 ± 0.23 | 1.44 ± 0.12 |
| **8 weeks** | 2.01 ± 0.31 | 2.57 ± 0.10 | 2.59 ± 0.07 | | |

* $p < 0.05$, ** $p < 0.01$ $\Delta$Ct values of ECM hydrogel vs control lesion.
# $p < 0.05$ $\Delta$Ct values of SC-ECM hydrogel with immunosuppression vs SC-ECM.

### *5.1.4 Summary I*

- Both ECM hydrogels bridged the lesion, modulated immune response, stimulated vascularization and axonal growth into the lesion while no significant differences were found between UB-ECM and SC-ECM.

Limitations:

- Degradation of ECM is important for tissue remodelling, but it was found to be too fast to ensure full tissue reconstruction.
- Combination of SC-ECM with hWJ-MSCs did not further promote ingrowth of axons and blood vessels.

## 5.2 Hydroxyphenyl derivate of hyaluronic acid hydrogel modified with RGD for SCI repair (Zaviskova *et al.*, 2018)

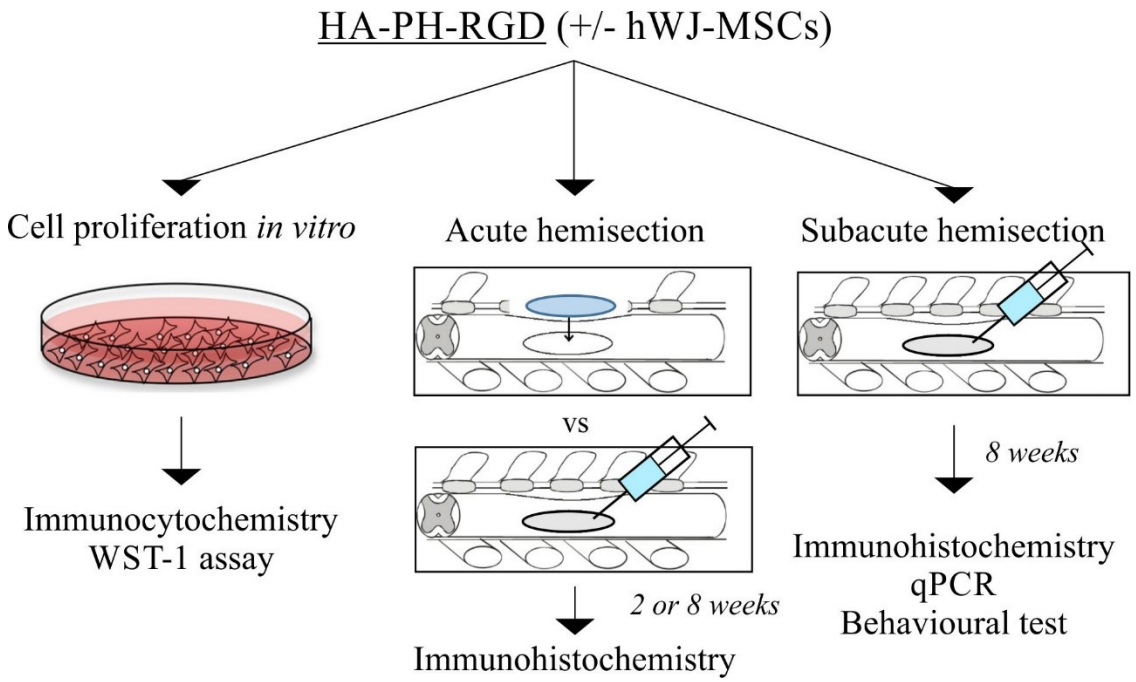


**Figure 16:** Schematic representation of experimental design.

### *5.2.1 In vitro cell culture on HA-PH hydrogels*

The toxicity of crosslinking agents (HRP and $H_2O_2$) was tested by their addition to hWJ-MSCs culture and no cytotoxic effects were observed at concentrations which were used for the hydrogel gelation.

Proliferation of hWJ-MSCs seeded on HA-PH and HA-PH-RGD hydrogels, combined with fibrinogen (F) is shown in Figure 17 A. Low cell proliferation was found in case of the unmodified HA-PH hydrogel, which was increased when using the HA-PH modified with RGD. A remarkable increase in cell proliferation rate was achieved when the HA-PH and HA-PH-RGD hydrogels were combined with F. Therefore, for cell encapsulation 1 mg/ml F was added into the HA-PH-RGD hydrogel. The ability of HA-PH-RGD/F to support cell proliferation in 3D culture was further verified by the WST-1 method at 3 hours, 1 and 3 days after seeding (Figure 17 B). Despite of the enhanced cell proliferation, the morphology of hWJ-MSCs after 1 day in 3D culture was found to be similar in HA-PH-RGD and HA-PH-RGD/F (Figure 17 C, D).

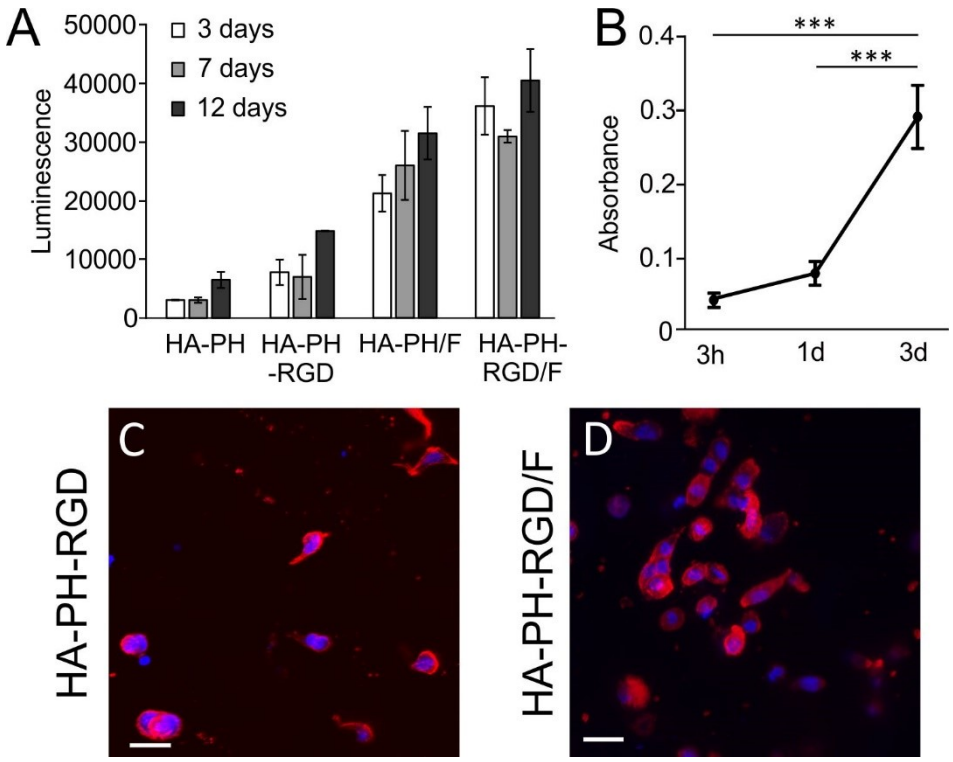


**Figure 17:** (A) Proliferation of hWJ-MSCs in HA-PH hydrogels on different adhesive substrates (RGD peptide, F = fibrinogen) measured by luminescence of ATP. (B) Proliferation of hWJ-MSCs in 3D culture of HA-PH-RGD/F hydrogel measured by WST-1 assay (n = 3). ***p < 0.001. (C, D) The morphology of hWJ-MSCs in 3D culture in (C) HA-PH-RGD and (D) HA-PH-RGD/F hydrogel after 1 day of cultivation stained for phalloidin (red) and DAPI (blue). Scale bar: 25 µm.

### *5.2.2 Evaluation of HA-PH-RGD hydrogels in acute SCI lesions*

Two ways of hydrogel application were compared in the acute SCI lesion; implantation of the *in vitro* crosslinked HA-PH-RGD hydrogel and injection of the HA-PH-RGD together with crosslinking agents to form a hydrogel *in situ*. Both implanted and injected HA-PH-RGD hydrogels filled the lesion cavity and were highly populated with endogenous cells. The dense ingrowth of neurofilaments (Figure 18 A) as well as blood vessels (Figure 18 B) into the hydrogel-treated lesion was observed throughout the whole implant after 2 weeks, and persisted with no considerable increase 8 weeks after application. Quantitative analysis revealed a higher density of neurofilaments (Figure 18 C) and blood vessels (Figure 18 D) in both hydrogel groups compared to the control lesion while no differences were found between the lesion treated with hydrogel implantation or injection at any time point. Figure 18 E, G depicts migrating astrocytes (GFAP staining) and Figure 18 H the newly formed axonal growth cones (GAP43 staining) protruding into the hydrogel treated lesion. The results show that the hydrogel injection into the lesion and its subsequent crosslinking *in situ* is not harmful to the surrounding

tissue and represents a non-invasive and effective way of hydrogel delivery resulting in tissue repair.

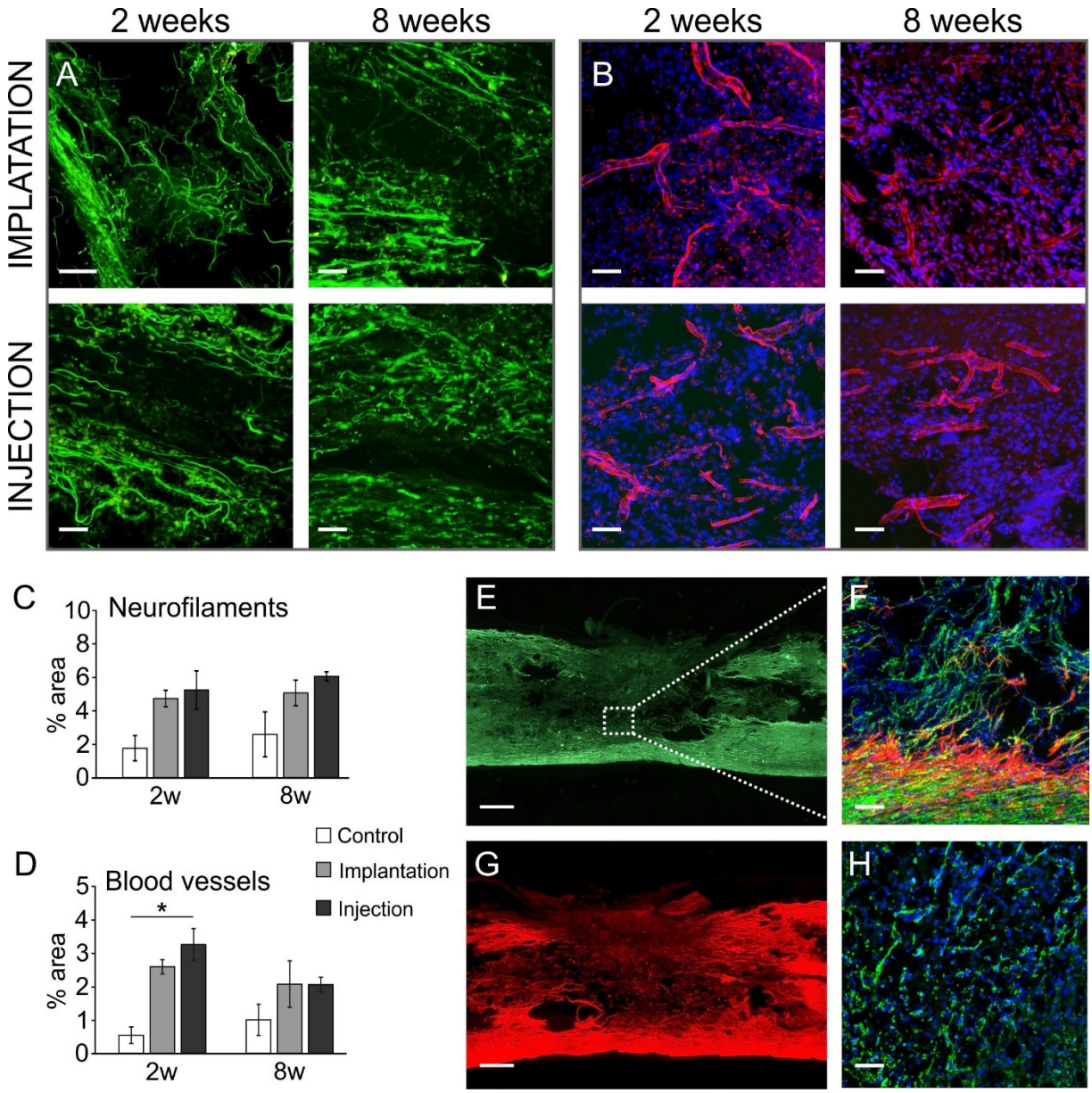


**Figure 18:** Representative images of longitudinal sections of the spinal cord lesion at 2 and 8 weeks after the acute HA-PH-RGD hydrogel injection or implantation into the hemisection cavity: staining of (A) neurofilaments (NF-160, green) and (B) blood vessels (RECA, red; DAPI, blue). Quantitative analysis of the ingrowth of (C) neurofilaments and (D) blood vessels into the lesion area at 2 and 8 weeks after the injection or implantation of HA-PH-RGD hydrogel. The values are expressed as the percentage of (C) NF-160 or (D) RECA positive area of the total lesion area (n = 3). *$p < 0.05$. (E) Immunofluorescent staining for neurofilaments (NF-160); square in (E) is shown under the higher magnification inset in (F); (F) immunofluorescent staining for neurofilaments (NF-160, green), astrocytes (GFAP, red) and cell nuclei (DAPI, blue) and (G) immunofluorescent staining for astrocytes (GFAP) at 2 weeks after HA-PH-RGD injection. (H) Immunofluorescent staining for growth associated protein 43 (GAP43, green) and cell nuclei (DAPI, blue) at 8 weeks after HA-PH-RGD hydrogel implantation. Scale bar: (E, G) 500 µm, (A, B, F, H) 50 µm.

### *5.2.3 Histological evaluation of HA-PH-RGD hydrogels in subacute SCI lesion*

The tissue response of the subacute injection of HA-PH-RGD, HA-PH-RGD/F and HA-PH-RGD/F combined with hWJ-MSCs was evaluated 8 weeks after implantation. As is apparent from Figure 19, both HA-PH-RGD and HA-PH-RGD/F hydrogels significantly improved the density of neurofilaments within the lesion when compared to the control untreated lesion and this effect was further enhanced by the addition of hWJ-MSCs. Because the immunohistochemical results of HA-PH-RGD/F did not significantly differ from the results obtained with HA-PH-RGD, we did not show the immunohistochemistry of this group.

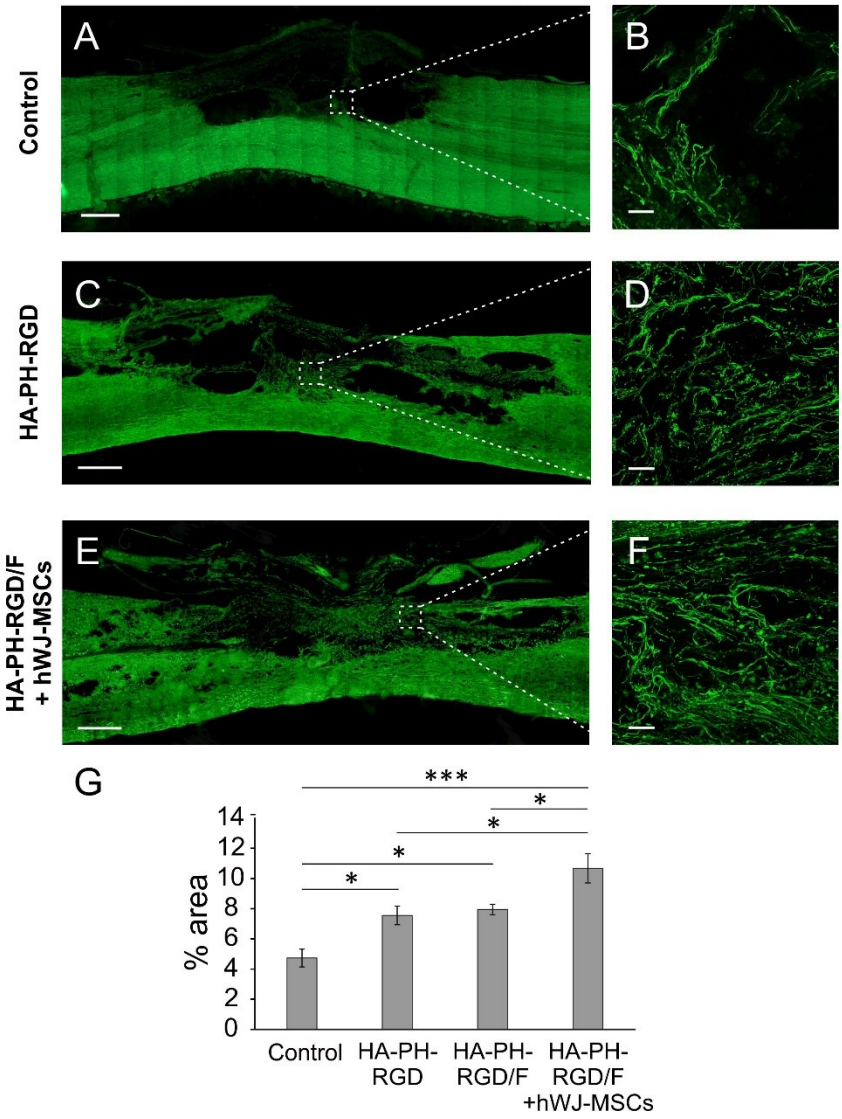


**Figure 19**: Representative images of the longitudinal sections of the spinal cord lesion in (A, B) controls and at 8 weeks after the subacute injection of (C, D) HA-PH-RGD and (E, F) HA-PH-RGD/F hydrogel combined with hWJ-MSCs, stained for neurofilaments (NF-160). Squares (A, C, E) are also shown under higher magnification insets (B, D, F). (G) Quantitative analysis of axonal ingrowth is expressed as the percentage of NF-160 positive area of the total lesion area (n = 6). *p < 0.05, ***p < 0.001. Scale bar: (A, C, E) 500 µm, (B, D, F) 50 µm.

Astrocytes, detected by immunofluorescence staining of GFAP (Figure 20), migrated from the lesion border to the lesion area which was treated by hydrogel suggesting a formation of permissive environment promoting glial cell infiltration (Figure 20 D, F). Quantitative evaluation of the GFAP staining density around the lesion, which should reflect the density of the glial scar, did not reveal significant differences between the control and hydrogel treated groups (Figure 20 G). Blood vessels densely infiltrated the hydrogel treated lesion, however the increase in blood vessel density was not found to be significant when compared to the control lesion (Figure 21).

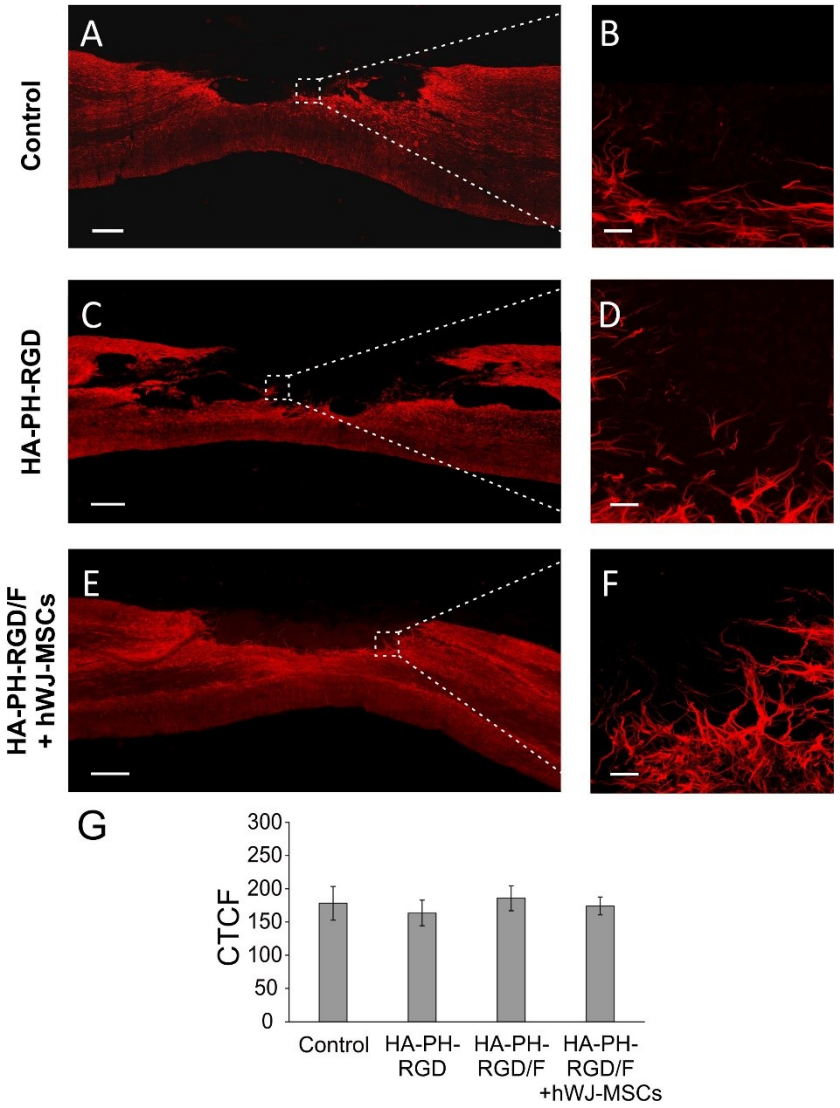


**Figure 20:** Representative images of the longitudinal sections of the spinal cord lesion in (A, B) control and at 8 weeks after subacute injection of (C, D) HA-PH-RGD and (E, F) HA-PH-RGD/F hydrogels combined with hWJ-MSCs stained for astrocytes (GFAP). Squares (A, C, E) are also shown under higher magnification insets (B, D, F). (G) Quantitative analysis of the glial scar density around the lesion was expressed as the corrected total cell fluorescence (CTCF) of GFAP staining (n = 6). Scale bar: (A, C, E) 500 µm, (B, D, F) 50 µm.

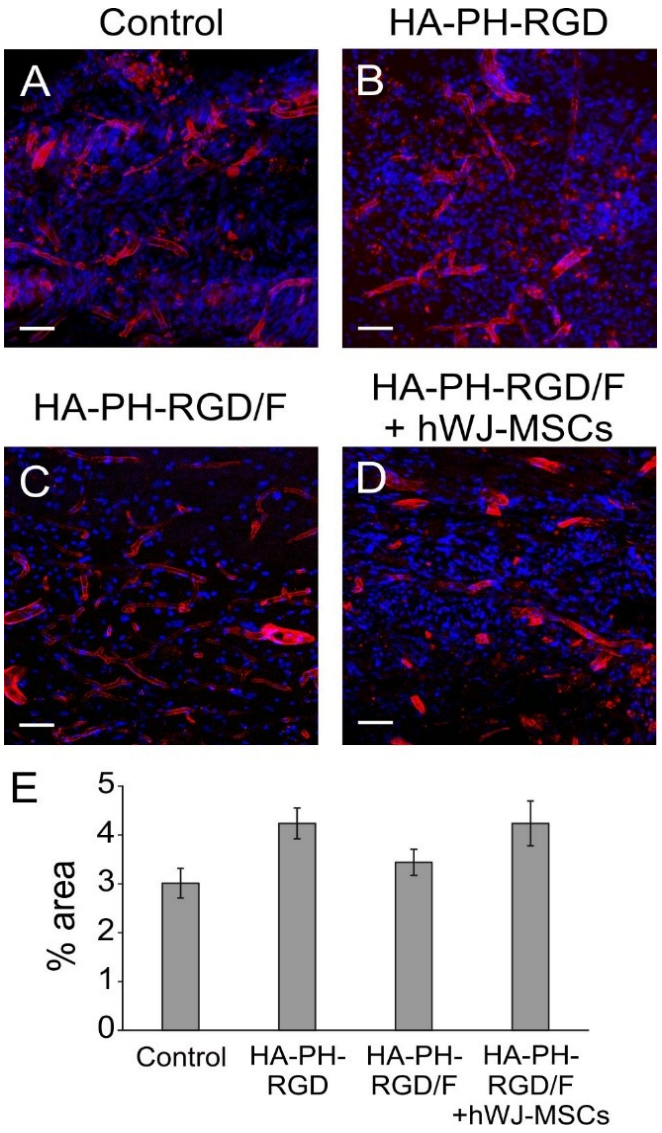


**Figure 21:** Representative images of the longitudinal sections of the spinal cord lesion in (A) control and at 8 weeks after subacute injection of (B) HA-PH-RGD, (C) HA-PH-RGD/F and (D) HA-PH-RGD/F combined with hWJ-MSCs stained for blood vessels (RECA, red) and DAPI (blue). (E) Quantitative analysis of blood vessel ingrowth is expressed as the percentage of RECA positive area of the total lesion area (n = 6). Scale bar: 50 µm.

ED1 staining, specific for microglia/macrophages, combined with CD206 staining specific for M2 macrophages confirmed the migration of both M1 and M2 macrophages into the hydrogel treated lesion. However, no quantification was performed to detect the M1/M2 ratio (Figure 22 A-D). Oligodendrocytes were detected in the area of hydrogel treated lesions, but not in the control lesion (Figure 22 E-H).

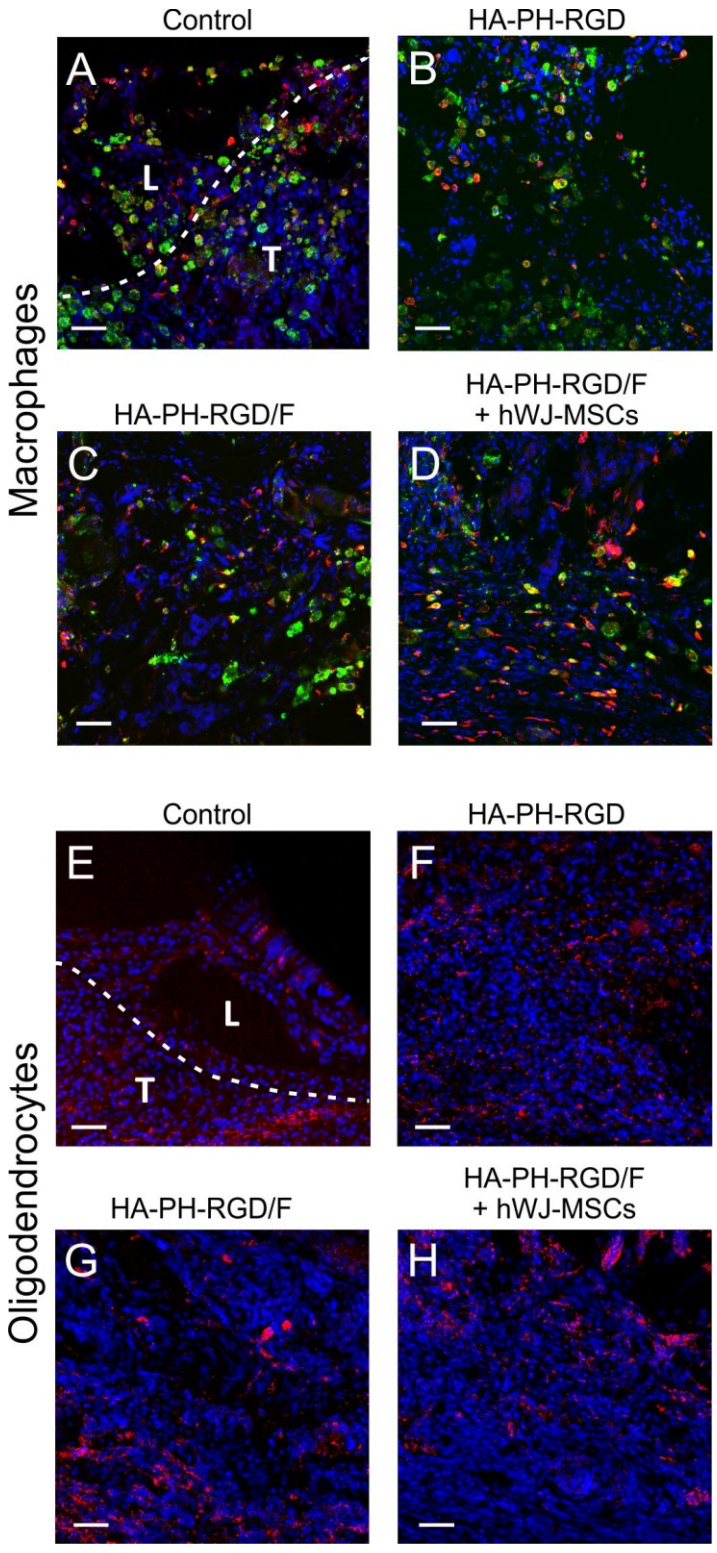


**Figure 22:** Representative images of the longitudinal sections of the spinal cord lesion in (A, E) control and at 8 weeks after subacute injection of (B, F) HA-PH-RGD, (C, G) HA-PH-RGD/F and (D, H) HA-PH-RGD/F hydrogel combined with hWJ-MSCs. Staining for (A-D) macrophages (ED1, green) and M2 macrophages (CD206, red), (E-H) oligodendrocytes (OSP, red) and (A-H) DAPI (blue). The dotted lines in (A, E) outline the border of the tissue (T) and the lesion area (L). Other images are taken from the centre of the lesion. Scale bar: 50 µm.

It is of note that we did not observe any hWJ-MSCs in the spinal cord tissue 8 weeks after cell application, which we attempted to visualize using the staining of the human mitochondria marker (MTCO2) used for the detection of human MSCs in the host tissue.

### *5.2.4 Gene expression analysis in subacute SCI lesions*

Changes in the mRNA expression of selected genes were determined 8 weeks after the injection of HA-PH-RGD, HA-PH-RGD/F and HA-PH-RGD/F combined with hWJ-MSCs (Figure 23).

Both the HA-PH-RGD and HA-PH-RGD/F hydrogel injections resulted in a decrease in mRNA expression of genes related to inflammation (*Irf5, Cd86, Ccl3*) or glial scar formation (*Gfap, Ptprz1*), but these changes were not significant. Significant downregulation was then found in the expression of *Gap43* when compared to the untreated control lesion. On the contrary, the expression of *Gap43* was significantly increased when the HA-PH-RGD/F was combined with hWJ-MSCs. Similarly, a combination with hWJ-MSCs led to significant upregulation of both M1 (*Irf5, Cd86*) and M2 macrophages markers (*Mrc1*).

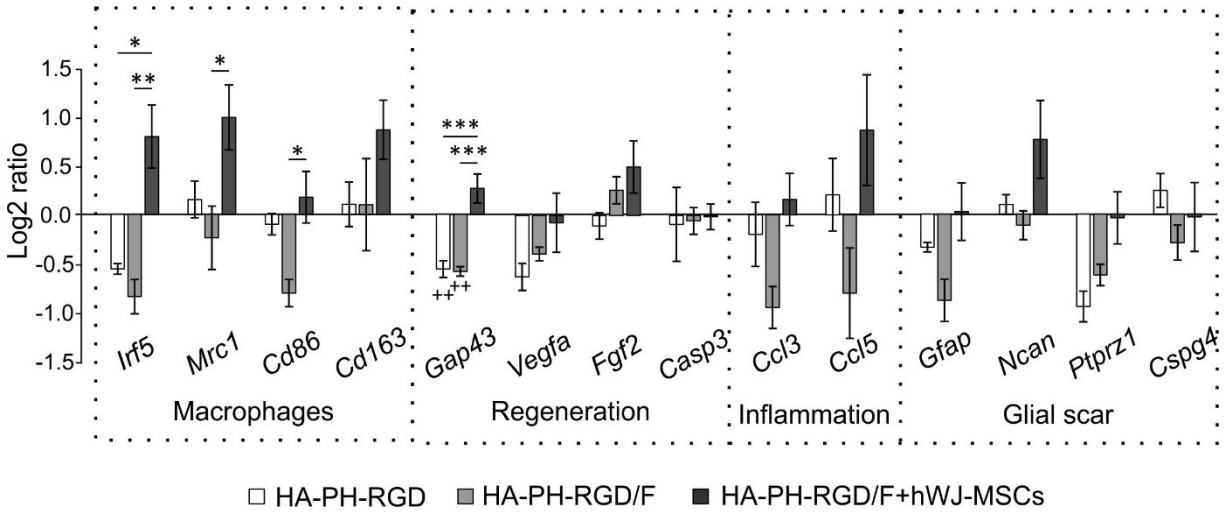


**Figure 23:** Analysis of mRNA gene expression of selected genes involved in the reparative processes following spinal cord injury treated with HA-PH-RGD, HA-PH-RGD/F and HA-PH-RGD/F hydrogel combined with hWJ-MSCs. The graph shows the log2-fold changes in gene expression over the control lesion with saline. Significance is calculated using ΔCt values (n = 5). ++p < 0.01: versus control lesion, *p < 0.05, **p < 0.01, ***p < 0.001.

### *5.2.5 Analysis of locomotor functions in subacute SCI lesions*

The effect of the hydrogel treatment on the locomotor functions of the experimental animals was quantitatively analysed using the TSE Motion 8.5.11. We evaluated those parameters which revealed differences between the gait of healthy and injured animals, such as knee and ankle angles and hind limb retraction and protraction (distance on x axis of metatarsophalangeal joint in relation to iliac crest) (Figure 24). The most substantial differences were found in the parameter of hind limb protraction, which reflected the ability of the hind limb to move forward during walking, and which significantly decreased in all injured groups and all observed time intervals when compared to the healthy animals. Significant improvement in protraction was found only after 2 weeks in animals treated with HA-PH-RGD/F when compared to control untreated lesion. A significantly higher maximal ankle angle in the HA-PH-RGD/F + hWJ-MSCs group vs. the HA-PH-RGD/F group at 2 weeks. No statistical differences between the control and hydrogel injected animals were found at 5 and 8 weeks.

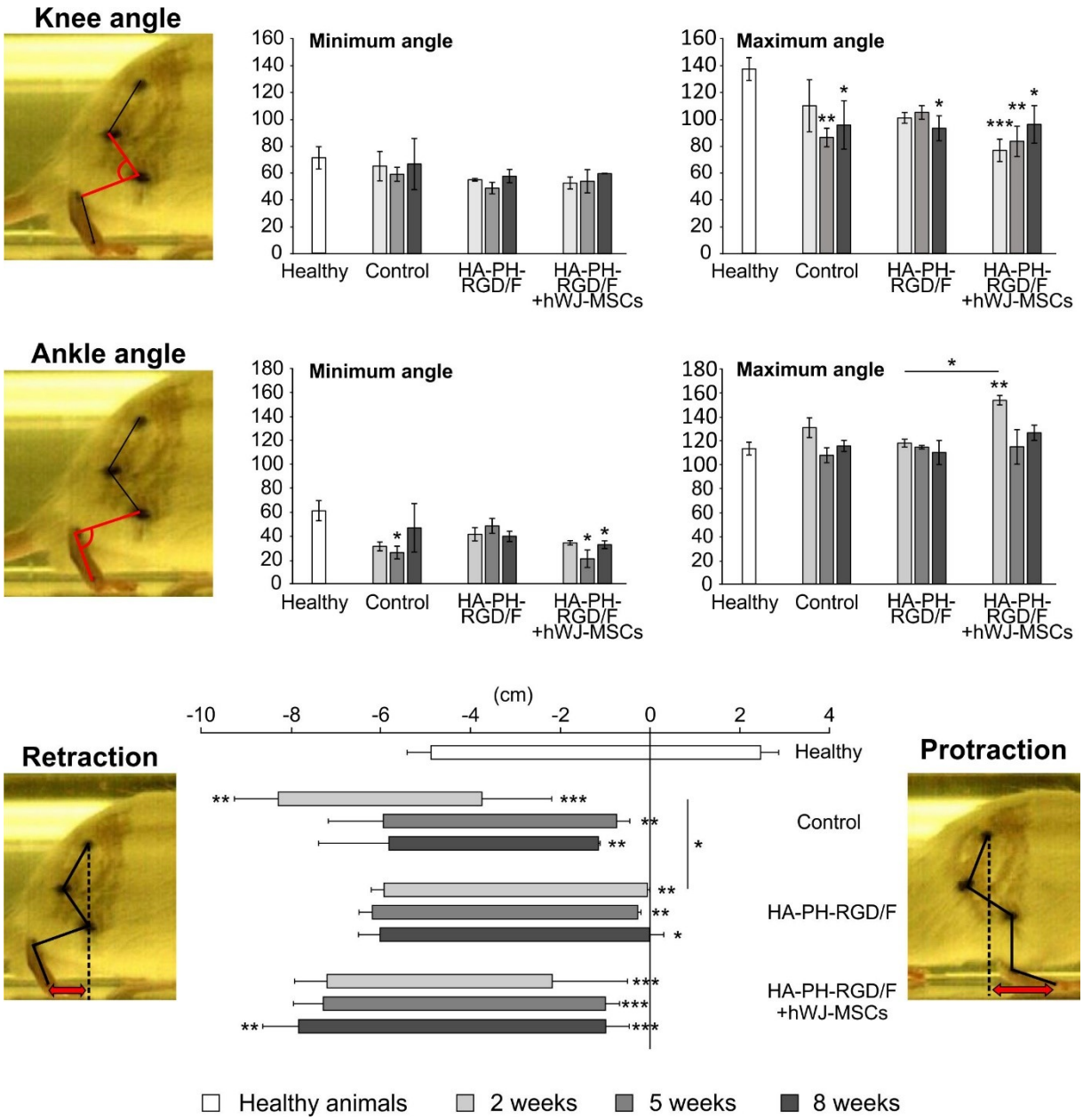


**Figure 24:** Analysis of locomotor functions of the right (affected) leg 2, 5 and 8 weeks after the subacute injection of HA-PH-RGD/F hydrogel, and HA-PH-RGD/F hydrogel combined with hWJ-MSCs compared to the control (lesioned) (n = 4 in all groups) and healthy animals (n = 7). *p < 0.05, **p < 0.01, ***p < 0.001 versus healthy animal when is not indicated by a line.

### *5.2.6 Summary II*

- Both injected and implanted HA-PH-RGD hydrogels filled the lesion cavity and promoted tissue bridging.
- Transplanted hydrogels alone increased axonal growth into the lesion.
- Combination of HA-PH-RGD/F hydrogel with hWJ-MSCs further improved axonal ingrowth and enhanced infiltration of macrophages.

Limitations:

- Transplanted HA-PH-RGD hydrogels either alone or in combination with hWJ-MSCs had no significant effect on glial scarring or ingrowth of blood vessels.
- HA-PD-RGD neither alone nor combined with hWJ-MSCs did not improve motor function when compared to the control group.

## 5.3 Effect of different hWJ-MSCs doses on spinal cord regeneration (Krupa *et al.*, 2018)

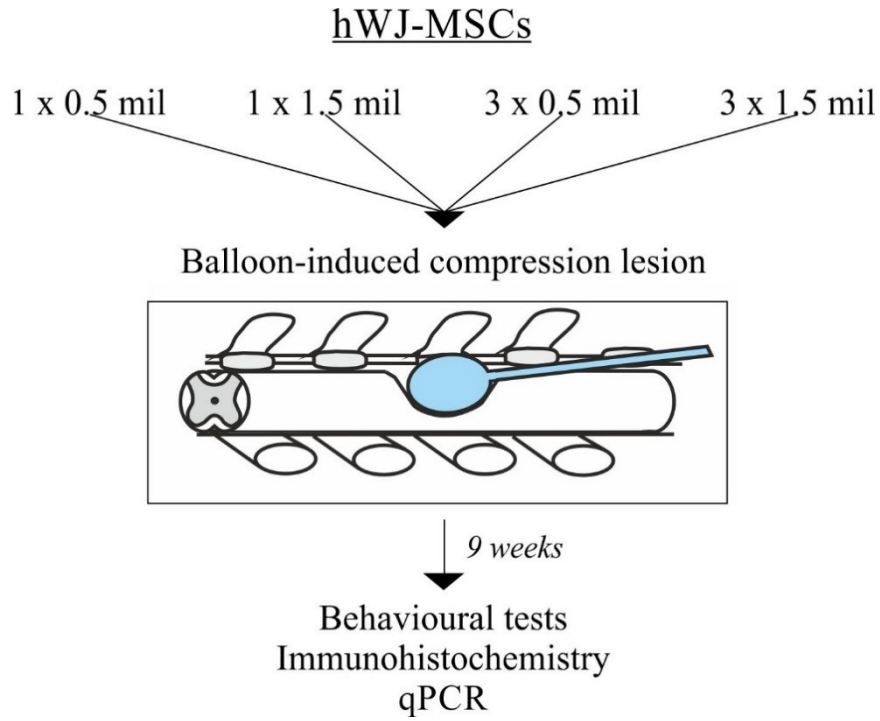


**Figure 25:** Schematic representation of experimental design.

### *5.3.1 hWJ-MSCs characterization*

The mesenchymal phenotype of hWJ-MSCs was confirmed by the presence of CD29, CD73, CD90, CD105 and HLA-ABC and lack of CD14, CD31, CD34, CD45 and HLA-DR (Figure 26).

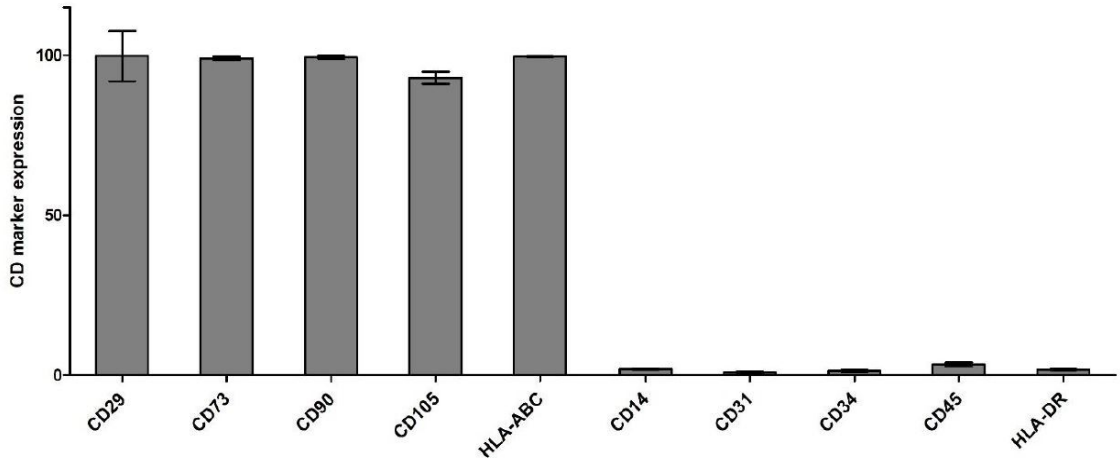


**Figure 26**: Flow cytometry analysis of the surface markers of hWJ-MSCs in the 3rd passage.

Figure 27 shows, that hWJ-MSCs at the 3rd passage were differentiated into all three cell-lineages. Adipocytes were detected by positive Oil-Red-O staining for lipid droplets. Osteoblasts were detected by positive Alizarin Red S staining for calcium-rich deposits. Chondrocytes were detected by Alcian blue staining for acid mucopolysaccharides.

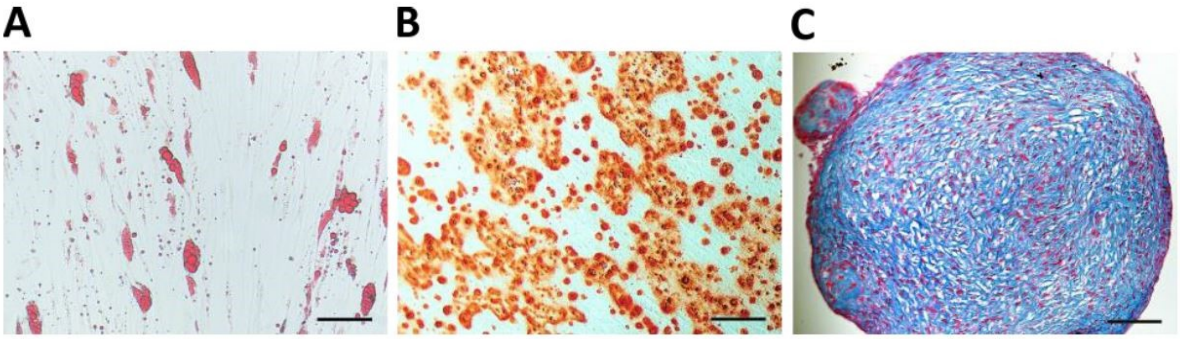


**Figure 27**: Multipotent differentiation of hWJ-MSCs into (A) adipocytes, (B) osteoblasts, and (C) chondrocytes. Scale bar: 100 µm.

### *5.3.2 Behavioural analysis after hWJ-MSCs application*

Recovery of the hind limb locomotor function was evaluated by BBB test every week starting in the first week after SCI. The BBB score was calculated as a mean value from the scores of both legs (Figure 28 A). One week after SCI, all tested animals displayed severe paraparesis or paraplegia. No differences between the groups were observed. The second week after SCI, animals in all groups showed new motions in one or two joints. Among the groups, a significant difference was achieved between the control group and the group treated with a single dose of 1.5M hWJ-MSCs. In the third week after SCI, a rapid improvement of the locomotor functions was observed in the groups treated with a single dose of 1.5M, and the groups with repeated treatment of 0.5M and 1.5M respectively. All three groups recovered significantly better than the control group. Animals treated with only 0.5M showed little improvement compared to control group which was not statistically significant. In the following weeks, improvements of movement and strength of the hind limbs continued but not as rapidly as was seen during the first three weeks. From the fourth week onward until the end of the experiment, rats treated with 1.5M and 3x0.5M and 3x1.5M had comparable results, which were significantly better than the control group and animals treated by 0.5M only. No significant difference between the control group and 0.5M group was observed. Animals in the groups with repetitive treatment were mostly able to achieve effective weight support of their body when standing, or even walking. The gap between score 8 (and lower) and 9 (and higher) is a big step when comparing the strength of the muscles of the hind limbs.

Coordination of the limb movements was tested by a rotarod test (Figure 28 B). Testing was performed every two weeks. Due to the severity of the lesion and limited recovery, no significant differences were observed between the groups.

Advanced locomotor skills and coordination of the hind limbs was measured by beam walk test. Results were evaluated using a 0-7 scale (Figure 28 C). All animals were trained in this task before surgery and then tested every week starting in the second week after SCI. Due to the severity of the lesion, most of the rats showed minimal ability to cross the beam and often just stayed and balanced at the starting point of the beam. The best scores at 7$^{th}$ week after SCI were obtained in animals treated by 3x1.5M, which were significantly better when compared to all of the other groups. For the first three weeks, animals treated with 0.5M achieved significantly better results than the control group, but in subsequent weeks they gradually worsened and the significant difference was lost.

In addition to the beam score, we measured the time needed to cross the beam (maximum of 60 seconds) (Figure 28 D). During the pre-training, healthy rats were able to cross the beam in approximately 3 s. The measurement was performed weekly starting in the second week after SCI. Two weeks after SCI, not all the rats were able to cross the beam and did not move from the starting line. In the following weeks, a significant improvement was observed between the rats treated by 3x1.5M and the other groups. The best score was achieved in the 6$^{th}$ week in the group 3x1.5M.

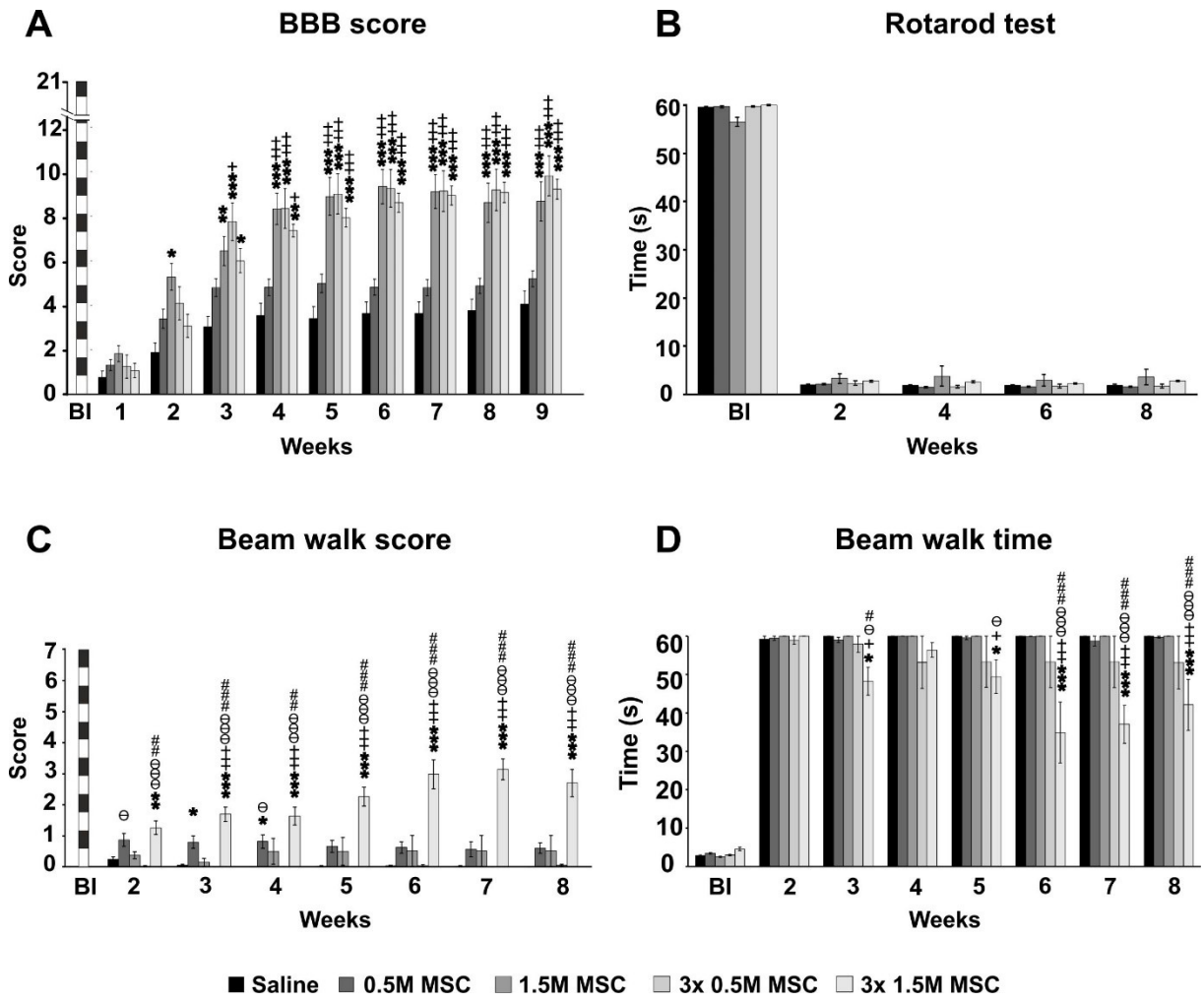


**Figure 28:** Recovery of locomotor functions following hWJ-MSCs transplantation after SCI. The locomotor skills of saline or stem cell-treated rats were measured using (A) Basso, Beattie, and Bresnahan test (BBB), (B) rotarod test, (C) beam walk score and (D) time. BI = before injury. * $p < 0.05$, ** $p < 0.01$, *** $p < 0.001$ versus saline; + $p < 0.05$, +++ $p < 0.001$ versus 0.5M MSC; # $p < 0.05$, ## $p < 0.01$, ###$p < 0.001$ versus 3x0.5M MSC; ɵ $p < 0.05$, ɵɵɵ $p < 0.001$ versus 1.5M MSC.

### *5.3.3 Histology and immunohistochemistry after hWJ-MSCs transplantation*

Concerning the grey matter preservation (Figure 29 A), a significant difference was achieved between the group 3x1.5M and the control group. Comparison of the white matter sparing showed no significant difference between the groups as a whole (Figure 29 B). Similarly to the grey matter, we observed significantly more spared white matter in the center of the lesion an in the surrounding tissue in animals treated with 3x1.5M and 1.5M when compared to the control group and rats treated with 0.5M.

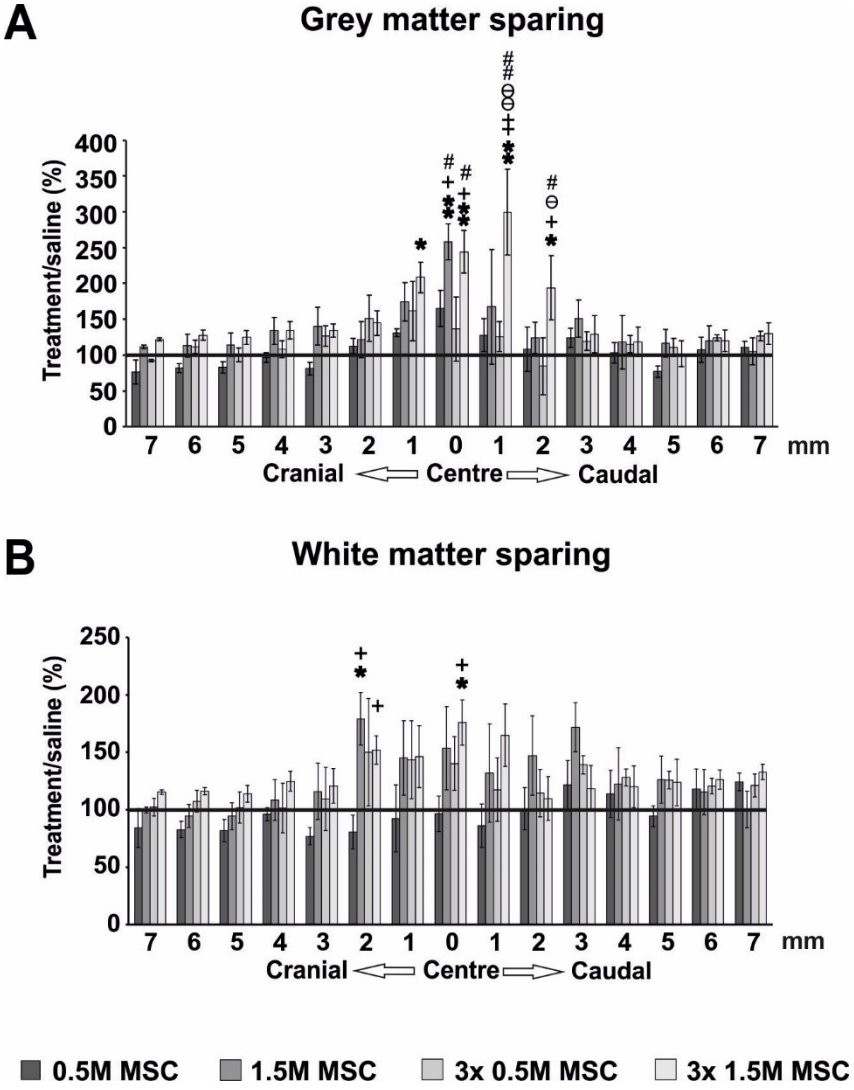


**Figure 29**: Histological analysis 9 weeks after SCI. (A) Analysis of the grey matter and (B) white matter sparing as relative when compared to the control, which was set as 100%. * $p < 0.05$, ** $p < 0.01$ versus saline; + $p < 0.05$, ++ $p < 0.01$ versus 0.5M MSC; # $p < 0.05$, # # $p < 0.01$ versus 3x0.5M MSC; ɵ $p < 0.05$, ɵɵ $p < 0.01$ versus 1.5M MSC.

The total area of the glial scar formed around the central cavity (GFAP staining) was expressed as a ratio of scar tissue to the whole section in percentages (Figure 30 A). Groups treated by 1.5M, 3x0.5M and 3x1.5M had a significantly smaller GFAP positive area around the main cavity compared to the control group. The group treated by 0.5M showed no significant difference compared to saline treated rats. The number of protoplasmic astrocytes was counted in the same samples (Figure 30 B). Rats treated by 1.5M, 3x0.5M and 3x1.5M showed a significantly lower number of protoplasmic astrocytes compared to the control group.

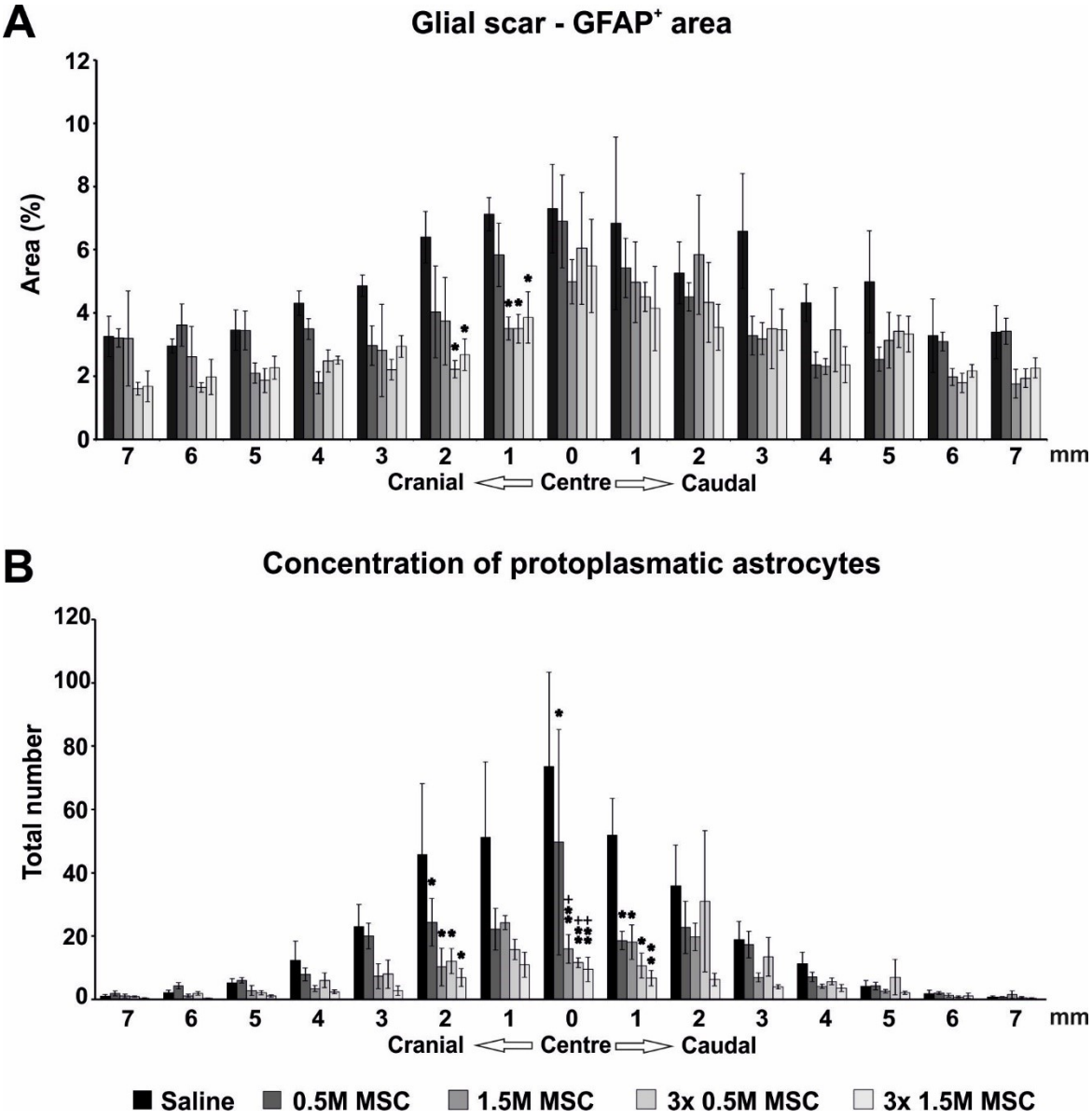


**Figure 30**: Immunohistochemical analysis 9 weeks after SCI. (A) The GFAP positive area showing the glial scar formation around the central cavity. (B) The number of protoplasmic astrocytes near the centre of the lesion. * $p < 0.05$, ** $p < 0.01$ versus saline; + $p < 0.05$ versus 0.5M MSC + $p < 0.05$; # $p < 0.05$, # # $p < 0.01$ versus 3x0.5M MSC.

Axonal sprouting was determined as a number of GAP43 positive fibers and results were compared to the control, which was set as 100%. The significant effect of the cell treatment was not only dose dependent, but further improved after repeated application (Figure 31). Treatment with the lowest dose (0.5M) had no or minimal effect on axonal sprouting. In the other cell-treated groups, the number of positive fibers was gradually increasing with the higher number of grafted cells and a repeated application resulted in a significantly stronger effect than a single dose.

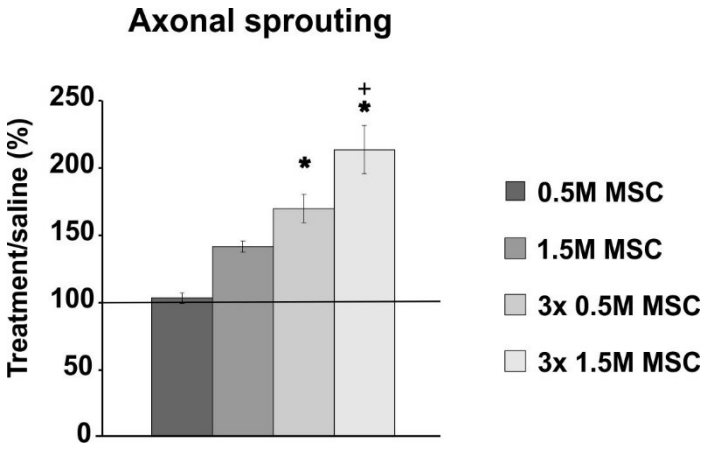


**Figure 31:** The average number of GAP43 positive fibers presented as relative when compared to the control, which was set as 100%. * $p < 0.05$ versus saline; + $p < 0.05$ versus 0.5M MSC.

Survival of the transplanted cells was evaluated by staining with an antibody against human nucleus (HuNu) 2 weeks after the transplantation. Surviving cells were detected as green clusters. Most of the cells remained at the site of the implantation, trapped between the folds of arachnoidea mater in the cauda equina. However, there was a difference in the number of cells present. While after 0.5M application only a few cells were detected, the application of 1.5M resulted in a greater number of trapped cells. No migration into the lesion site was observed.

### *5.3.4 Gene expression induced by hWJ-MSCs application*

Samples from the spinal cord for qPCR analysis were taken 4 and 9 weeks after the cell transplantation. Values were compared to saline treated rats which were set as 0. The expression of genes related to the M1 (*Irf5, Cd86*) and M2 (*Mrc1, Cd163*) macrophage phenotypes, astrogliosis (*Gfap*) and apoptosis (*Casp3*) was analysed (Figure 32).

Pro-inflammatory related genes *Irf5* and *Cd86* were insignificantly up-regulated in the groups treated with 1.5M and 3x0.5M at 4 weeks after the transplantation of cells. On the other hand, 9 weeks after the transplantation, *Irf5* and *Cd86* were downregulated in all groups except for the 3x0.5M. Statistical significance compared to saline group was achieved only in the group 3x1.5M.

The anti-inflammatory related genes *Mrc1* and *Cd163* were downregulated in all treatment groups with significant difference between groups 1x0.5M and 3x1.5M at 9 weeks after the transplantation. However, in groups treated with a total of 1.5M cells (1.5M and 3x0.5M), *Mrc1* and *Cd163* were insignificantly upregulated 4 weeks after transplantation and thus their dynamics changed throughout the experiment.

Four weeks after the cell implantation, *Gfap* was downregulated in all groups except for the group treated with 3x0.5M cells. Nine weeks after the cell implantation, *Gfap* remained significantly downregulated only in the group 3x1.5M, which corresponds with the immunohistochemical analysis of astrogliosis which was lowest in this group. Expression of *Casp3* insignificantly decreased in the groups 0.5M and 3x1.5M and remained stable throughout the entire experiment.

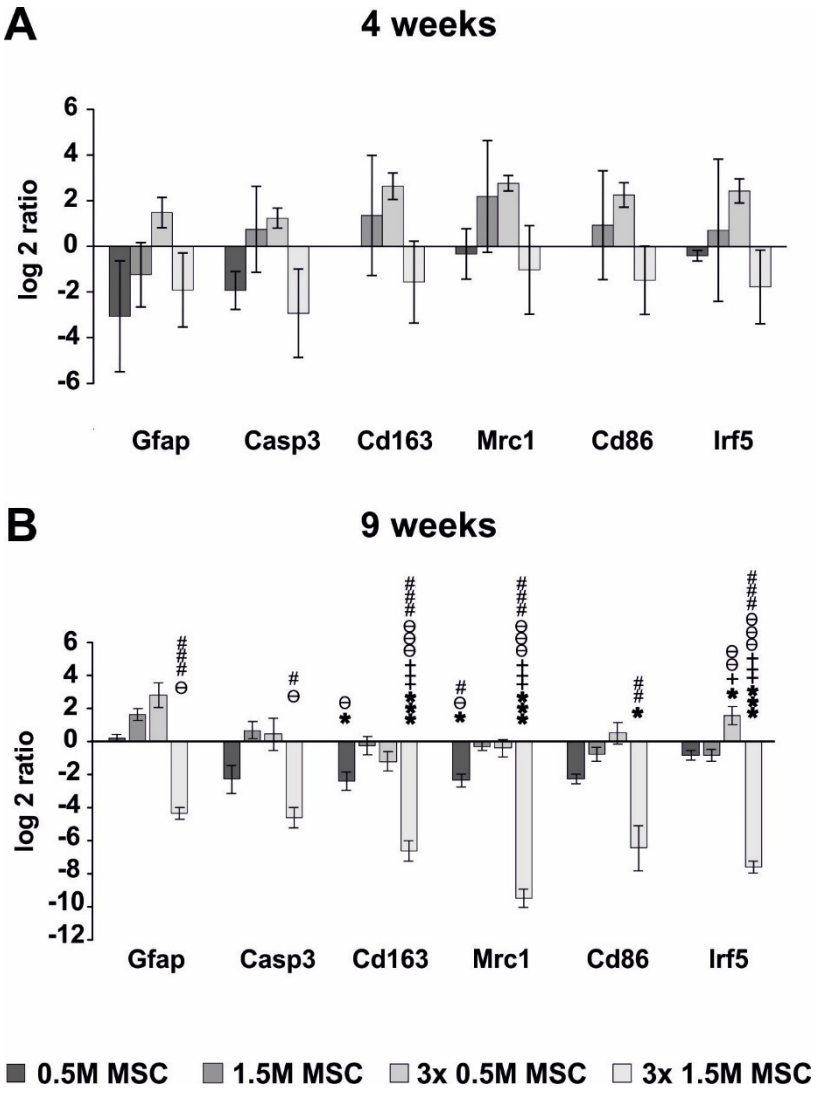


**Figure 32:** The expression of genes related to the M1 (*Irf5, Cd86*) and M2 (*Mrc1, Cd163*) macrophage phenotypes, astrogliosis (*Gfap*) and apoptosis (*Casp3*) shown (A) 4 weeks after the SCI and (B) 9 weeks after the SCI. The graphs show the log2-fold changes of the ΔΔCt values of the indicated genes in comparison to the animals treated with the saline, which were set to 0 and are represented as x axis in the graphs. * $p < 0.05$, *** $p < 0.001$ versus saline; + $p < 0.05$, +++ $p < 0.001$ versus 0.5M MSC; # $p < 0.05$, ## $p < 0.01$, ### $p < 0.001$ versus 3x0.5M MSC; ɵ $p < 0.05$, ɵɵ $p < 0.01$, ɵɵɵ $p < 0.001$ versus 1.5M MSC.

### *5.3.5 Summary III*

- Intrathecal transplantation of hWJ-MSCs had beneficial effect on functional outcome, tissue sparing, glial scar and axonal sprouting and was dose dependent.

Limitations:

- Only repeated transplantation of high dose (1.5M) hWJ-MSCs was sufficient for significant improvement in advanced locomotor test and tissue preservation.

## 5.4 Stimulation of neurite growth by transgenic activation of α9 integrin and kindlin 1 (unpublished results)

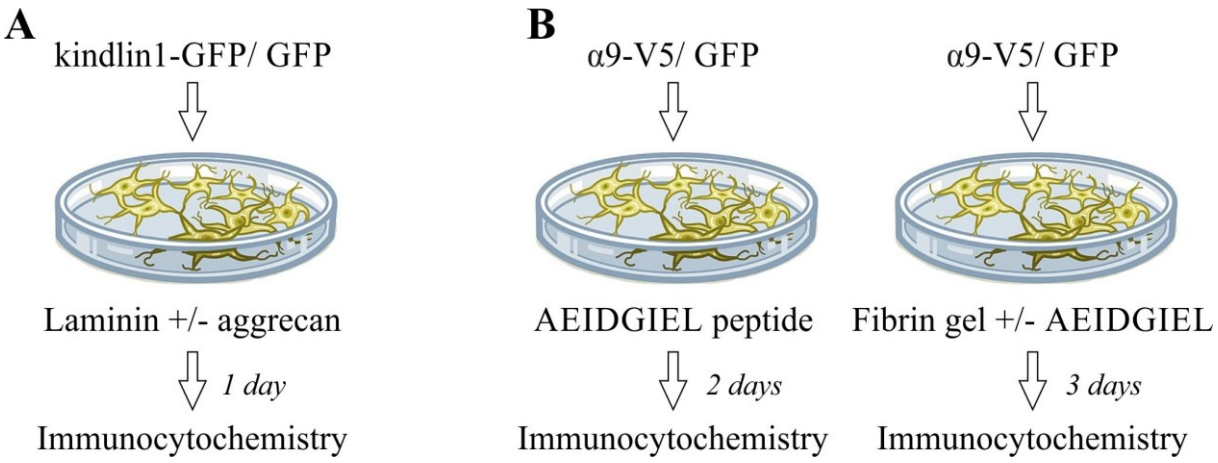


**Figure 33**: Schematic representation of experimental design. (A) Overcoming the effect of aggrecan inhibition on neurite growth by kindlin 1 overexpression. (B) Activation of neurite growth by α9 integrin subunit overexpression on cover slips coated with α9 integrin specific peptide or fibrin gel modified with α9 integrin specific peptide. (https://www.gettyimages.com/detail/illustration/cell-cultures-in-petri-dishes-stock-graphic/155301592)

DRG neurons isolated from adult rats were used as an *in vitro* model of SCI. Transfection with plasmid bearing genes for kindlin 1 or α9 integrin subunits was performed using electroporation. To mimic the inhibitory environment after SCI, aggrecan (25 µg/ml) was used in addition to laminin coating (1 µg/ml). Figure 34 shows that aggrecan significantly reduced neurite length of both DRG neurons transfected either with CAG-GFP or CAG-kindlin1-GFP plasmid. Kindlin 1 overexpression then slightly enhanced the neurite length in comparison with control DRG neurons transfected with green fluorescent protein (GFP), however the difference was not significant.

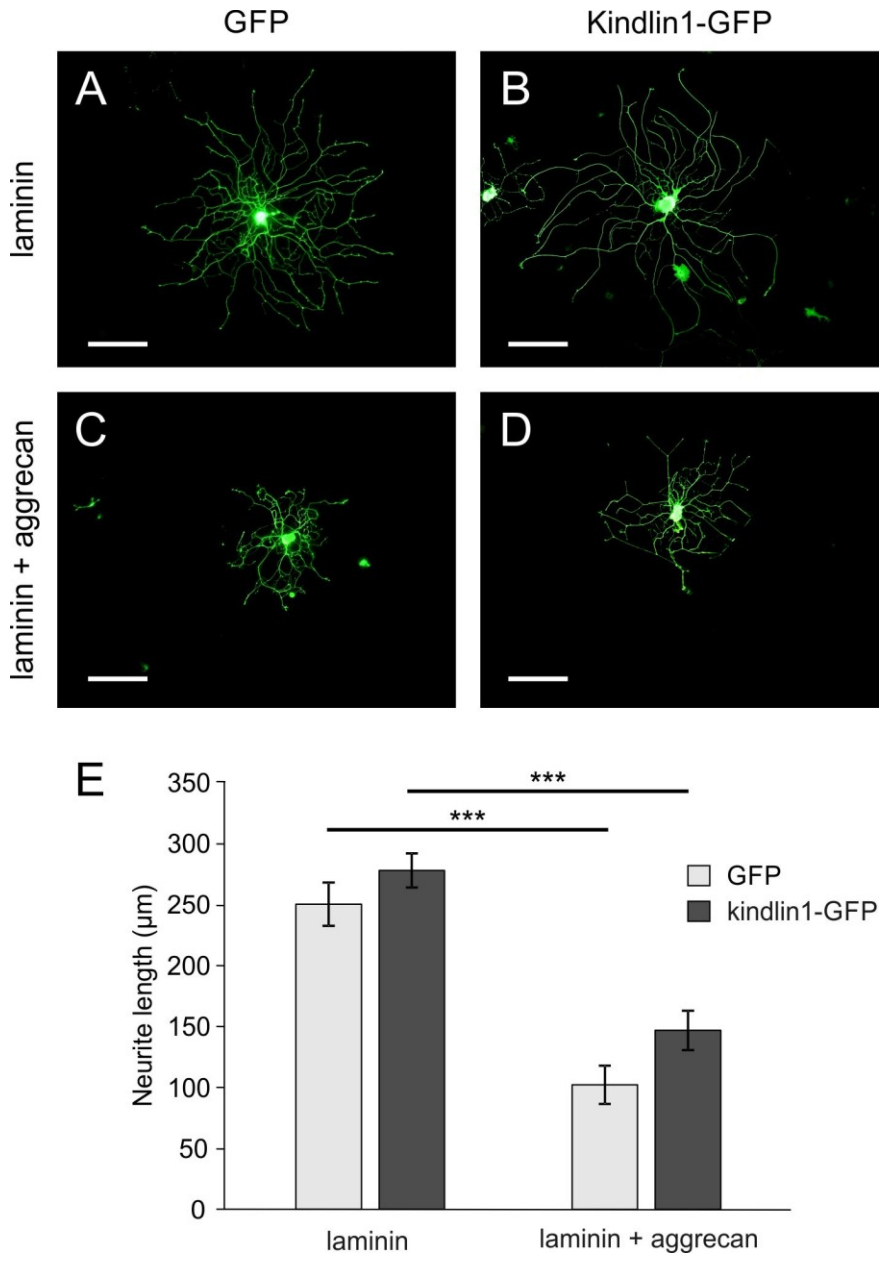


**Figure 34:** Representative images of adult DRG neurons transfected with (A, C) CAG-GFP or (B, D) CAG-kindlin1-GFP plasmid cultivated on cover slips coated with (A, B) laminin or (C, D) laminin and aggrecan stained for GFP. Scale bar: 100 µm. (E) Maximal neurite length of DRG transfected with CAG-GFP or CAG-kindlin1-GFP plasmid after 1 day in culture. *** $p < 0.001$.

The effect of CAG-α9-V5 plasmid was tested on different coating concentrations of AEIDGIEL peptide derived from tenascin-C. AEIDGIEL peptide at concentration at least 10 µg/ml significantly stimulated neurite growth in DRG neurons transfected with α9 integrin, which increased with increasing concentration of AEIDGIEL peptide (Figure 35 C). Similarly, modification of fibrin gel with AEIDGIEL peptide using factor XIIIa as cross-linker enhanced neurite length of α9 transfected DRG compared to control DRG transfected with GFP. Fibrin gel modification with AEIDGIEL peptide at concentration 2 mg/ml stimulated DRG growth

significantly better then fibrin gel alone or fibrin gel with 1 mg/ml AEIDGIEL. Increased growth of α9 transfected DRG on fibrin gel without AEIDGIEL peptide was most likely caused by α9 integrin binding to adhesion domain within fibrin protein different from AEIDGIEL (Figure 35 D).

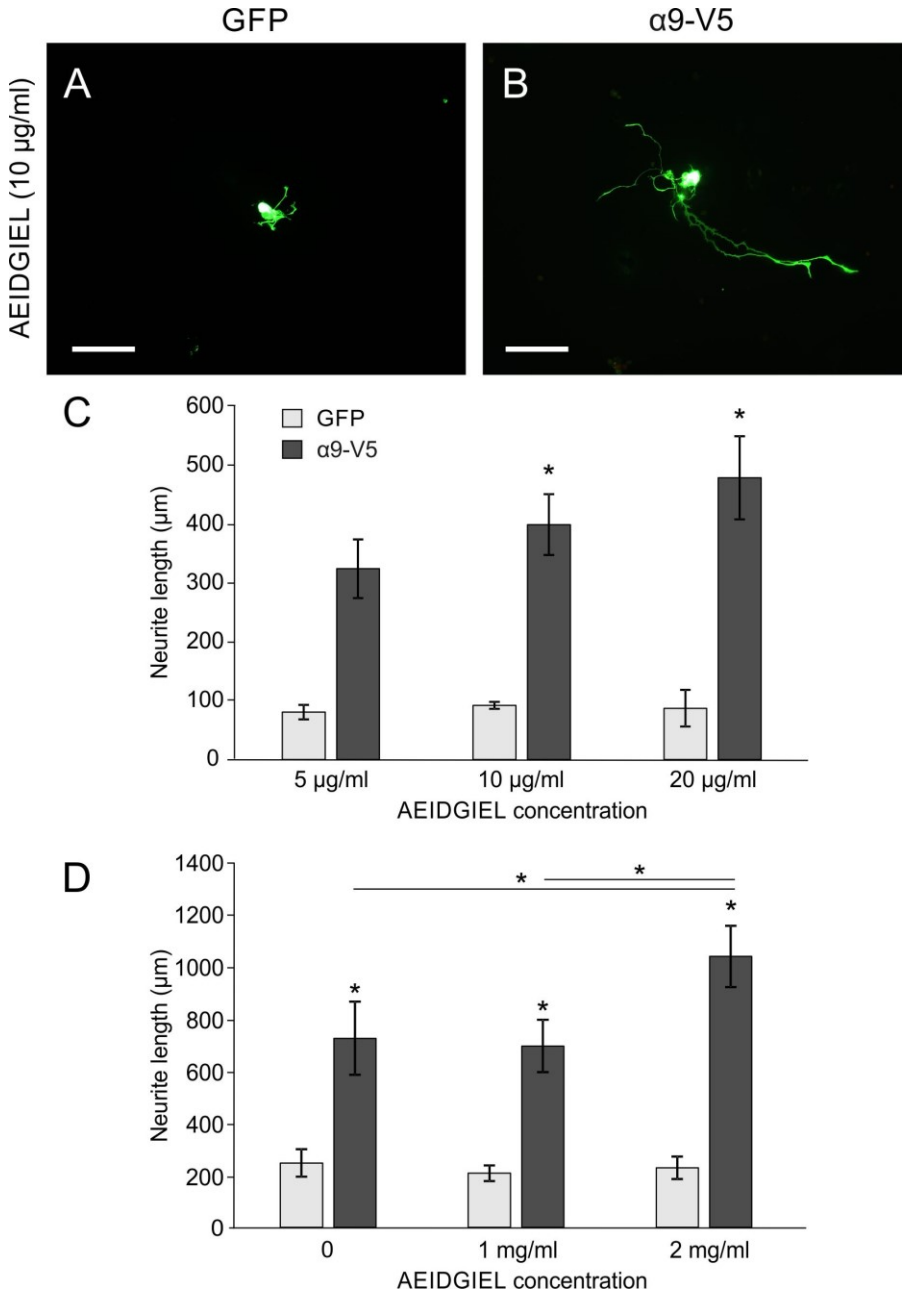


**Figure 35**: Representative images of adult DRG transfected with (A) CAG-GFP or (B) CAG-α9-V5 plasmid cultivated on AEIDGIEL peptide stained for (A) GFP or (B) V5. Scale bar: 100 µm. (C) Maximal neurite length of DRG transfected with CAG-GFP or CAG-α9-V5 plasmid cultivated on cover slips coated with different concentration of AEIDGIEL peptide after 2 days in culture. (D) Maximal neurite length of DRG transfected with CAG-GFP or CAG-α9-V5 plasmid cultivated on fibrin gel alone or fibrin gel modified with different concentration of AEIDGIEL peptide after 3 days in culture. *$p < 0.05$ versus GFP when is not indicated by a line.

### *5.4.1 Summary IV*

- Kindlin 1 overexpression had no significant effect on neurite growth in an aggrecan induced inhibitory environment.
- α9 integrin subunit overexpression enhances neurite growth on AEIDGIEL modified substrates.
- On the basis of these results, the subsequent *in vivo* study is planned in SCI model using α9 integrin and kindlin 1 viral co-transduction combined with implantation of fibrin gel modified with AEIDGIEL.

# 6 Discussion

Despite intensive research of SCI, no effective therapy for patients exists. To study SCI it is necessary to choose the right experimental model, appropriate therapeutic approach and its timing. Based on previous investigations, it seems that biomaterials and stem cells can support recovery after SCI to some extent. Nevertheless, their therapeutic potential is limited and therefore it is required to combine them. In addition, gene therapy could be used for enhancement of intrinsic regenerative capacity of the spinal tissue.

## 6.1 Different animal models of SCI and experimental settings

The majority of experimental studies of SCI use compression, contusion or sharp animal models, with each model having some advantages and limitations (Cheriyan *et al.*, 2014).

The benefit of balloon-induced compression lesion is that it simulates the character of the lesion which occurs in humans by an unreduced dislocation or a fracture dislocation of the spine. It is assumed that both mechanical and vascular factors are involved in the pathogenesis of SCI in this model. Moreover, it is simple and reproducible and requires minimal surgical preparation of the animal (Vanicky *et al.*, 2001).

However, it would be difficult to apply biomaterial into balloon-induced compression lesion in acute or subacute phase when the cavity is not developed. Therefore, a spinal cord hemisection, where part of the spinal tissue is removed, is a more suitable model for the testing the hydrogel effect on the neural tissue repair. It allows filling the lesion cavity with material and clear analysis of the endogenous tissue infiltration into the implant. Additionally, hemisection is also the least invasive and devastating SCI model (Kubinova *et al.*, 2011). On the other hand, this model is a case of partial lesions with a high rate of spontaneous recovery and a high risk of inconsistencies in the injuries between animals, which might lead to misinterpretation of behavioural evaluation (Fouad *et al.*, 2013).

For SCI repair it is also important to choose the right timing of therapeutic intervention. In our study, ECM hydrogels were applied into the model of acute SCI. Therefore, their neuroregenerative potential might be burdened by the hostility of the lesion due to the acute inflammatory response, which in turn may influence the speed of hydrogel degradation and thus the character of tissue replacement. To reveal whether subacute implantation makes some differences in the tissue repair effect, we applied HA-PH-RGD hydrogels acutely and subacutely one week after the SCI in the following study. Nevertheless, both acute and subacute

hydrogel application had similar effects on tissue repair regarding the tissue bridging, material degradation and support of axonal ingrowth.

Another thing that needs to be considered is the delivery method of the biomaterial. We compared two methods of HA-PH-RGD hydrogels application, hydrogel implantation and injection into the hemisection cavity immediately after the injury. However, we did not find any difference neither in the ingrowth of neurofilaments nor blood vessels. Hydrogel injection was then used for the application into the subacute SCI lesion, because of lower invasiveness.

Regarding cell transplantation, hWJ-MSCs were transplanted in the subacute phase ($7^{th}$, $14^{th}$ and $21^{st}$ day after the SCI), which could lead to better cell survival because of the reduced aggressiveness of the host environment. Moreover, the glial scar in the subacute SCI phase has not been fully formed unlike in the chronic phase (Okada *et al.*, 2005; Parr *et al.*, 2007).

Another variable in the SCI treatment using cells is the route of cell transplantation, which can be intraparenchymal directly into the lesion, intrathecal or intravenous. Each approach has its advantages and disadvantages with regard to invasiveness and effectivity.

Direct injection of the cells into the lesion site guaranteed delivery without obstacles but it requires a major surgical opening of the spinal canal and dura mater in the subacute phase of the injury. Intravenous delivery is a less invasive alternative and it offers an easy and safe route for delivery of large number of cells. However, a lower number of cells survived because they were exposed to immune cells in the blood circulation, trapping most of them in the lungs, liver and kidneys (de Haro *et al.*, 2005; Fischer *et al.*, 2009).

Intrathecal delivery is a kind of compromise between the two methods mentioned above. It eliminates the risk of direct surgical implantation without the need for deep analgesia and anaesthesia for the animal, and yet it still guarantees a wide dissemination of cells throughout the subarachnoid space and around the lesion site (Amemori *et al.*, 2015). The procedure can be done either by lumbar puncture or by suboccipital puncture of the cisterna magna. Both methods provide a relatively save approach to the subarachnoid space of the spinal cord. In our study we chose the lumbar puncture, because it is more relevant to clinical medicine. Since cell survival in the vertebral canal is rather low, repeated application substantially increased the trophic and immunomodulatory effects of the cells and could be feasible for use in human patients.

## 6.2 Advantages and limitations of natural biomaterials in spinal cord regeneration

Natural biomaterials have great potential in various tissue engineering applications including SCI. In comparison with synthetic non-degradable materials such as poly(2-hydroxyethyl methacrylate), poly N-(2-hydroxypropyl)-methacrylamide and polyethylene glycol, ECM and HA-PH hydrogels are undoubtedly advantageous in terms of their degradability as well as biologic activity which is able to modulate immune response and stimulate vascularization and axonal ingrowth. On the other hand, *in vivo* hydrogel degradation can be too fast and their variability may also present a problem in their potential clinical use.

We studied ECM hydrogels derived from the CNS (porcine spinal cord) and from non-CNS tissue (porcine urinary bladder). We also tested hydrogels based on HA-PH-RGD specifically developed for neural tissue repair. All studied hydrogels maintained their biologic activity and had the mechanical properties similar to the soft neural tissue with the advantage of injectability and ability of *in situ* polymerization, which allow for minimally invasive delivery techniques and facilitate the possibility of clinical translation.

A potentially important criterion for tissue regeneration may be tissue specificity depending on the ECM hydrogel source. However, no significant differences were found between CNS-derived SC-ECM and non-CNS UB-ECM hydrogels with regards to ingrowth of neurofilaments and blood vessels after injection of these materials into SCI defect. We also did not find significant differences between SC-ECM and UB-ECM hydrogels *in vitro* in terms of the migration of human MSCs, differentiation of NSCs or axonal outgrowth (Koci *et al.*, 2017).

As was shown previously, degradation of a biomaterial is crucial for effective tissue remodelling. The biomaterial should serve as a temporary support that will be gradually replaced by functional tissue and not a scar tissue (Badylak *et al.*, 2009; Valentin *et al.*, 2009). However, hydrogel degradation in our experiments was faster than neural tissue regeneration, which resulted in the formation of small cyst and sparse network of axons, blood vessels as well as other neural tissue elements.

To slow degradation, chemical crosslinking of the ECM hydrogel ensures longer scaffold persistence within the lesion and thus provides more time required for complete tissue remodelling. However, studies suggest that degradation of the ECM scaffold is an essential component of rapid constructive remodelling response and the released matricryptic molecules possess a variety of bioactive properties such as recruitment of endogenous SCs, antimicrobial activity, and pro-angiogenic effects (Valentin *et al.*, 2009). Moreover, crosslinking of the ECM may reduce or eliminate the amount of cellular infiltration into the implant or even cause a

foreign body reaction (Badylak and Gilbert, 2008). Studies also showed that HA degradation products can promote angiogenesis by stimulating proliferation and migration of endothelial cells (Montesano *et al.*, 1996; Peattie *et al.*, 2004).

To form HA-PH hydrogel, we used an enzymatic crosslink reaction initiated by HRP and $H_2O_2$. Concentrations of cross-linking agents were optimized to achieve mechanical properties comparable to native spinal cord tissue and to get the optimal gelation time of the material during application into the site of the defect. Moreover, the used crosslink reaction was non-cytotoxic and enabled the formation of a cell-laden hydrogel under physiological conditions. The big advantage of this material over other ones is that it can be manufactured in a reproducible manner under good manufacture practice conditions, which are required to allow the transfer of its production from bench-to-bedside in clinical practice.

One possibility of how to enhance regenerative potential of a biomaterial is its modification with a specific integrin ligand. HA-PH was functionalized with RGD peptide derived from fibronectin, which has been previously shown to support effective cell spreading and cytoskeletal organization as well as cell proliferation (Mackova *et al.*, 2016). However, the most abundant integrin ligand in the damaged CNS is tenascin-C and one of the reasons for poor axon regeneration is the lack of integrin α9 receptor specific for tenascin-C (Andrews *et al.*, 2009). We confirmed that AEIDGIEL peptide derived from tenascin-C serves as a ligand for α9 integrin subunit and transgenic activation of α9 can promote *in vitro* neurite outgrowth on the biomaterial modified with this peptide. We also showed that transgenic activation of kindlin 1, an integrin activator, is able to partially improve neurite outgrowth in an inhibitory environment. Therefore, we plan a subsequent *in vivo* study in the model of SCI using an integrin α9 viral DRG transduction and an implantation of biomaterial with AEIDGIEL peptide, which should promote specific axon growth into the scaffold. As integrins are inhibited by the presence of CSPGs at the injury site, the viral vector mediated expression of integrin activator kindlin 1 could further improve regeneration even in an inhibitory environment (Cheah *et al.*, 2016).

### 6.3 Therapeutic potential of hWJ-MSCs for SCI repair

The hWJ-MSCs currently represent a promising cell type in regenerative medicine and are already being evaluated in many clinical trials including ones focusing on SCI. Advantages for the potential clinical use include the facts that they are allogenic, their production can be

easily scaled up and they can be prepared in advance, cryopreserved and be ready for use as an off-the-shelf product in a relatively short time (Cheng *et al.*, 2014).

In our SCI study, we compared effects of single and triple repeated intrathecal delivery of hWJ-MSCs with different numbers of cells (0.5M or 1.5M) in each application. Triple delivery and cell number was chosen based on previous studies with bone marrow MSCs. Cizkova *et al.* found, that rats treated with three injections of bone marrow MSCs at days 7, 8, and 9, but not on days 3, 4, and 5 after SCI, showed significantly higher motor function recovery (Cizkova *et al.*, 2011). Our experimental setting was also comparable to our previous study with single application of 0.5M human bone marrow derived MSCs (Machova Urdzikova *et al.*, 2014), but repeated application of hWJ-MSCs leaded to higher axonal sprouting and better results in beam walk test.

In terms of cell survival, many of the intrathecally transplanted hWJ-MSCs were detected at the site of the implantation after 2 weeks. We therefore assumed that a combination of cells with hydrogels, which could create a supporting niche, would promote hWJ-MSCs survival. However, despite immunosuppression, few cells were detected within the lesion after 4 weeks when WJ-MSCs were combined with the ECM hydrogel, and no hWJ-MSCs survived within HA-PH-RGD/F 8 weeks after implantation. This is in agreement with our unpublished observation that the human MSCs are able to survive for a maximum of 4 weeks even in case of spinal cords of heathy rats with immunosuppression. Nevertheless, we showed the effect of cells using immunohistochemical and qPCR analyses, which support the commonly proposed hypothesis that transplanted cells release trophic factors providing long lasting neurotrophic, neovascularization, and immunomodulatory effects (Assinck *et al.*, 2017; Petrenko *et al.*, 2017; Urdzikova *et al.*, 2014).

## 6.4 Tissue regeneration after SCI using histology and qPCR

It this thesis we used histological analysis and qPCR mainly for the evaluation of axonal and blood vessel ingrowth, glial scarring and macrophage phenotype. Two different markers of axonal ingrowth and sprouting were used. Spinal cord tissue after implantation or injection of SC-ECM, UB-ECM and HA-PH-RGD hydrogels was stained against NF-160. GAP43 was used for staining after hWJ-MSCs transplantation and for qPCR in studies with ECM or HA-PH-RGD hydrogels.

Histology results showed that both implantation approaches with any of the tested biomaterials and different doses of hWJ-MSCs supported axonal growth into the lesion site.

Moreover, our study with hWJ-MSCs demonstrated that the axonal growth into the lesion gradually increased along with the cell dose. Surprisingly, some results from histology did not correspond with results from qPCR. Decreased mRNA expression of *Gap43* in both ECM scaffolds after 2 weeks and in HA-PH-RGD hydrogel groups after 8 weeks did not correlate with robust axonal growth into the lesion revealed by the histological staining of NF-160. An explanation can be the fact, that NF-160 stained the already mature sprouting axons, whereas *Gap43* is expressed at high levels mainly in neuronal growth cones during axonal regeneration. It is likely that axonal sprouting might finish during earlier period after the injury (Hsu and Xu, 2005). In contrary, significant increase in mRNA expression of *Gap43* was found in all hydrogels combined with hWJ-MSCs, together with an elevated axonal growth into the lesion seen in histological slides. It suggests that hWJ-MSCs prolong axonal regeneration process.

In addition to axonal ingrowth, the blood vessel ingrowth is also necessary for proper regeneration of the spinal cord. Our experiments showed enhanced ingrowth of blood vessels after acute transplantation of ECM or HA-PH-RGD hydrogels only. We also observed an increased mRNA expression of angiogenesis marker *Vegfa* in SC-ECM combined with hWJ-MSCs compared to SC-ECM alone. While histological analysis of blood vessels stained with RECA showed similar results for all groups with SC-ECM.

Another indicator of proregenerative environment after SCI is the reduced glial scarring. For measurement of the glial scarring, an enhanced expression of GFAP is the most broadly used marker of the reactive astrocytic response in the injury site (Macaya and Spector, 2012). Implantation of our hydrogels resulted in partially decreased expression of *Gfap*, but notable glial scar reduction was achieved after repeated application of hWJ-MSCs.

Inflammation is also an important factor in tissue regeneration. Macrophages are one of the crucial immune cell types involved in SCI. They migrate into the lesion, and their polarization into the anti-inflammatory M2 type has been reported to be beneficial (Slivka *et al.*, 2014). In our experiments, the expression of genes related to both pro-inflammatory M1 and M2 macrophages/microglia decreased at 2 weeks after SC-ECM and UB-ECM injection and a similar trend was observed also at 8 weeks after application of HA-PH-RGD and HA-PH-RGD/F. It might reflect that both inflammatory as well as anti-inflammatory responses were inhibited after hydrogel treatment. In contrast, expression of M1 and M2 markers was increased when HA-PH-RGD/F was combined with hWJ-MSCs 8 weeks after implantation. Surprisingly, a downregulation of all M1 and M2 markers was observed after 3x1.5M hWJ-MSCs transplantation at 9 weeks after SCI. It suggests that the macrophage polarization might be

variable after different stem cells dosage and in different SCI models (hemisection and balloon-induced compression lesion).

## 6.5 Behavioural outcome after SCI

Analysis of behavioural tests in the study using intrathecal application of WJ-MSCs revealed that the functional recovery of hind limb motion was dose-dependent. Significantly higher scores in BBB test were observed in all groups which received at least 1.5 million of hWJ-MSCs, when compared to the control and 0.5 million cells. In the beam walk test, which requires more advanced motor function to keep the balance, the effect was visible only in animals that received repeated injections of 1.5 million of hWJ-MSCs. In addition, no effect was detected in the rotarod test, which is greatly demanding due to a higher level of motor coordination and stepping required.

As our cell transplantation study revealed, the minimal amount of cells needed for locomotor recovery is 1.5 million, thus it is not surprising that we did not find any behavioural improvement after transplantation hWJ-MSCs combined with HA-PH-RGD/F because the total number of implanted cells within the hydrogel was relatively small (~ $3 \times 10^4$) due to the limited volume of the implanted scaffold (~ 5 µl). A higher dose of transplanted cells would probably increase the number of surviving cells as well as the behavioural outcome. To overcome the limitation of the number of cells that can be implanted along with the hydrogel, we propose a combination of hydrogel with additional cell application via intrathecal application or direct cell injection into the lesion site.

# 7 Evaluation of study aims

**Hypothesis 1:** Injectable natural biomaterials are suitable for SCI repair and help create permissive environment for tissue regeneration. Combination of biomaterials with hWJ-MSCs enhances effects of the treatment.

*Aim 1:* We demonstrated that both SC-ECM and UB-ECM hydrogels support tissue regeneration, such as growth of axons and blood vessels into the SCI lesion. A combination of hWJ-MSCs and SC-ECM did not further improve histological results, but it had a positive effect on gene expression.

*Aim 2:* We showed that all tested biomaterials derived from HA-PH-RGD support axonal regeneration after SCI. A combination of HA-PH-RGD/F with hWJ-MSCs further enhances neural growth into the lesion.

**Hypothesis 2:** Repeated intrathecal transplantation of hWJ-MSCs into SCI have beneficial and dose dependent effects on tissue repair and functional recovery after SCI.

*Aim 3:* We proved that repeated application of 0.5 million of hWJ-MSCs, but not a single 0.5 million dose, leads to tissue repair and functional recovery after SCI. The best improvement in both behavioural outcome and tissue regeneration was observed after repeated transplantation of 1.5 million of hWJ-MSCs.

**Hypothesis 3:** Transfection of adult DRG neurons with α9 integrin subunit and/or integrin activator kindlin 1 stimulates neurite outgrowth and has the potential to overcome the effect of the inhibitory environment which occurs after SCI.

*Aim 4:* We observed that overexpression of integrin activator kindlin 1 stimulated neurite outgrowth in an inhibitory environment simulated by aggrecan *in vitro*. However, these changes were not significant.

*Aim 5:* We demonstrated that overexpression of α9 integrin subunit supported neurite outgrowth of adult DRG neurons cultured on substrates modified with α9 integrin specific peptide AEIDGIEL *in vitro.*

# 8 Conclusion

This thesis studies new possibilities of how to treat SCI using natural hydrogels and human MSCs derived from Wharton's jelly. Our results show that all studied biomaterials and hWJ-MSCs alone or in combination supported tissue regeneration after SCI. Scaffolds are able to increase axonal growth and sprouting, which can be further enhanced by combination with hWJ-MSCs. However, to achieve functional improvement of locomotor functions, it is necessary to transplant repeatedly high doses of hWJ-MSCs. Therefore, a combination of ECM or HA derived hydrogels with transplantation of high dose of hWJ-MSCs has great potential to restore lost function after SCI. Preliminary data also suggest that transgenic integrin activation together with implantation of fibrin gel modified with specific adhesion peptide can be another method of how to enhance neurite growth in inhibitory environment after SCI.

# 9 Souhrn

Tato práce se zaměřuje na studium nových možností léčby míšního poranění pomocí přírodních hydrogelů a mesenchymálních kmenových buněk izolovaných z lidského pupečníku. Výsledky ukázaly, že testované biomateriály na bázi ECM a HA mají schopnost podpořit regeneraci tkáně po míšním poranění, což může být dále umocněno jejich kombinací s hWJ-MSCs. Avšak k dosažení signifikantního zlepšení motorických funkcí po míšním poranění došlo až po opakované intratekální transplantaci vysoké dávky hWJ-MSCs. Kombinace hydrogelů na bázi ECM nebo HA s transplantací vysokých dávek hWJ-MSCs tak představuje účinnou strategii v léčbě míšního poranění. Předběžné výsledky také ukazují, že transgenní aktivace integrinů společně s implantací fibrinového gelu modifikovaného specifickým adhesivním peptidem by mohla být další metodou, jak podpořit růst axonů v inhibičním prostředí vzniklém po míšním poranění

# 10 Author's publications

**Publications related to the thesis:**

1. **Zaviskova K**, Tukmachev D, Dubisova J, Vackova I, Hejcl A, Bystronova J, Pravda M, Scigalkova I, Sulakova R, Velebny V, Wolfova L, Kubinova S: Injectable hydroxyphenyl derivative of hyaluronic acid hydrogel modified with RGD as scaffold for spinal cord injury repair. J Biomed Mater Res A 2018;106:1129-1140. (IF 3.231)
   ***Contribution:*** *in vitro studies, microscopy analysis, gene expression analysis, behavioural tests, data analysis, statistical evaluation and article writing*

2. Tukmachev D, Forostyak S, Koci Z, **Zaviskova K**, Vackova I, Vyborny K, Sandvig I, Sandvig A, Medberry CJ, Badylak SF, Sykova E, Kubinova S: Injectable Extracellular Matrix Hydrogels as Scaffolds for Spinal Cord Injury Repair. Tissue Eng Part A 2016;22:306-317. (IF 3.508)
   ***Contribution:*** *gene expression analysis and statistical evaluation*

3. Krupa P, Vackova I, Ruzicka J, **Zaviskova K,** Dubisova J, Koci Z, Turnovcova K, Urdzikova LM, Kubinova S, Rehak S, Jendelova P: The Effect of Human Mesenchymal Stem Cells Derived from Wharton's Jelly in Spinal Cord Injury Treatment Is Dose-Dependent and Can Be Facilitated by Repeated Application. Int J Mol Sci 2018;19. (IF 3.687)
   ***Contribution:*** *behavioural testing*

**Other author's publications:**

Hejcl A, Ruzicka J, **Kekulova K**, Svobodova B, Proks V, Mackova H, Jirankova K, Karova K, Machova Urdzikova L, Kubinova S, Cihlar J, Horak D, Jendelova P: Modified Methacrylate Hydrogels Improve Tissue Repair after Spinal Cord Injury. Int J Mol Sci 2018;19. 1. (IF 3.687)

Vyborny K, Vallova J, Koci Z, **Kekulova K**, Jirakova K, Jendelova P, Hodan J, Kubinova S: Genipin and EDC crosslinking of extracellular matrix hydrogel derived from human umbilical cord for neural tissue repair. Submitted after revision. Sci Rep. (IF 4.259)

Ruzicka J, Machova-Urdzikova L, Gillick J, Amemori T, Romanyuk N, Karova K, **Zaviskova K**, Dubisova J, Kubinova S, Murali R, Sykova E, Jhanwar-Uniyal M, Jendelova P: A Comparative Study of Three Different Types of Stem Cells for Treatment of Rat Spinal Cord Injury. Cell Transplant 2017;26:585-603. (IF 2.885)

Ruzicka J, Urdzikova LM, Svobodova B, Amin AG, Karova K, Dubisova J, **Zaviskova K**, Kubinova S, Schmidt M, Jhanwar-Uniyal M, Jendelova P: Does combined therapy of curcumin and epigallocatechin gallate have a synergistic neuroprotective effect against spinal cord injury? Neural Regen Res 2018;13:119-127. (IF 2.234)

Kubinova S, **Zaviskova K**, Uherkova L, Zablotskii V, Churpita O, Lunov O, Dejneka A: Non-thermal air plasma promotes the healing of acute skin wounds in rats. Sci Rep 2017;7:45183. (IF 4.259)

**Book chapter:**

**Kekulova K**, Kubinova S: Natural biomaterials for spinal cord injury repair. Nanostructures in biomedicine: Their regenerative and toxic properties 2018.

# 11 References


1. Agrawal V, Brown BN, Beattie AJ, Gilbert TW, Badylak SF: Evidence of innervation following extracellular matrix scaffold-mediated remodelling of muscular tissues. J Tissue Eng Regen Med 2009;3:590-600.
2. Amable PR, Teixeira MV, Carias RB, Granjeiro JM, Borojevic R: Protein synthesis and secretion in human mesenchymal cells derived from bone marrow, adipose tissue and Wharton's jelly. Stem Cell Res Ther 2014;5:53.
3. Amblard M, Fehrentz J-A, Martinez J, Subra G: Methods and protocols of modern solid phase peptide synthesis. Molecular biotechnology 2006;33:239-254.
4. Amemori T, Ruzicka J, Romanyuk N, Jhanwar-Uniyal M, Sykova E, Jendelova P: Comparison of intraspinal and intrathecal implantation of induced pluripotent stem cell-derived neural precursors for the treatment of spinal cord injury in rats. Stem Cell Res Ther 2015;6:257.
5. Andrews MR, Czvitkovich S, Dassie E, Vogelaar CF, Faissner A, Blits B, Gage FH, ffrench-Constant C, Fawcett JW: Alpha9 integrin promotes neurite outgrowth on tenascin-C and enhances sensory axon regeneration. J Neurosci 2009;29:5546-5557.
6. Assinck P, Duncan GJ, Hilton BJ, Plemel JR, Tetzlaff W: Cell transplantation therapy for spinal cord injury. Nat Neurosci 2017;20:637-647.
7. Badylak SF: Decellularized allogeneic and xenogeneic tissue as a bioscaffold for regenerative medicine: factors that influence the host response. Ann Biomed Eng 2014;42:1517-1527.
8. Badylak SF, Freytes DO, Gilbert TW: Extracellular matrix as a biological scaffold material: Structure and function. Acta Biomater 2009;5:1-13.
9. Badylak SF, Gilbert TW: Immune response to biologic scaffold materials. Seminars in immunology 2008;20:109-116.
10. Baptiste DC, Fehlings MG: Update on the treatment of spinal cord injury. Prog Brain Res 2007;161:217-233.
11. Basso DM, Beattie MS, Bresnahan JC: A sensitive and reliable locomotor rating scale for open field testing in rats. J Neurotrauma 1995;12:1-21.
12. Bejjani GK, Zabramski J, Durasis Study G: Safety and efficacy of the porcine small intestinal submucosa dural substitute: results of a prospective multicenter study and literature review. J Neurosurg 2007;106:1028-1033.
13. Borgens RB, Shi R: Immediate recovery from spinal cord injury through molecular repair of nerve membranes with polyethylene glycol. FASEB J 2000;14:27-35.
14. Caicco MJ, Zahir T, Mothe AJ, Ballios BG, Kihm AJ, Tator CH, Shoichet MS: Characterization of hyaluronan-methylcellulose hydrogels for cell delivery to the injured spinal cord. J Biomed Mater Res A 2013;101:1472-1477.
15. Cizkova D, Novotna I, Slovinska L, Vanicky I, Jergova S, Rosocha J, Radonak J: Repetitive intrathecal catheter delivery of bone marrow mesenchymal stromal cells improves functional recovery in a rat model of contusive spinal cord injury. J Neurotrauma 2011;28:1951-1961.
16. Conconi MT, Burra P, Di Liddo R, Calore C, Turetta M, Bellini S, Bo P, Nussdorfer GG, Parnigotto PP: CD105(+) cells from Wharton's jelly show in vitro and in vivo myogenic differentiative potential. Int J Mol Med 2006;18:1089-1096.
17. Condic ML: Adult neuronal regeneration induced by transgenic integrin expression. J Neurosci 2001;21:4782-4788.

18. Crapo PM, Medberry CJ, Reing JE, Tottey S, van der Merwe Y, Jones KE, Badylak SF: Biologic scaffolds composed of central nervous system extracellular matrix. Biomaterials 2012;33:3539-3547.
19. Cui FZ, Tian WM, Hou SP, Xu QY, Lee IS: Hyaluronic acid hydrogel immobilized with RGD peptides for brain tissue engineering. J Mater Sci Mater Med 2006;17:1393-1401.
20. Dahl SLM, Koh J, Prabhakar V, Niklason LE: Decellularized Native and Engineered Arterial Scaffolds for Transplantation. Cell Transplant 2003;12:659-666.
21. Darr A, Calabro A: Synthesis and characterization of tyramine-based hyaluronan hydrogels. J Mater Sci Mater Med 2009;20:33-44.
22. de Haro J, Zurita M, Ayllon L, Vaquero J: Detection of 111In-oxine-labeled bone marrow stromal cells after intravenous or intralesional administration in chronic paraplegic rats. Neurosci Lett 2005;377:7-11.
23. Delgado LM, Bayon Y, Pandit A, Zeugolis DI: To cross-link or not to cross-link? Cross-linking associated foreign body response of collagen-based devices. Tissue Eng Part B Rev 2015;21:298-313.
24. Donnelly DJ, Popovich PG: Inflammation and its role in neuroprotection, axonal regeneration and functional recovery after spinal cord injury. Exp Neurol 2008;209:378-388.
25. Dulak J, Szade K, Szade A, Nowak W, Jozkowicz A: Adult stem cells: hopes and hypes of regenerative medicine. Acta Biochim Pol 2015;62:329-337.
26. Dumont RJ, Okonkwo DO, Verma S, Hurlbert RJ, Boulos PT, Ellegala DB, Dumont AS: Acute spinal cord injury, part I: pathophysiologic mechanisms. Clin Neuropharmacol 2001;24:254-264.
27. El-Sherbiny IM, Yacoub MH: Hydrogel scaffolds for tissue engineering: Progress and challenges. Glob Cardiol Sci Pract 2013;2013:316-342.
28. Eva R, Fawcett J: Integrin signalling and traffic during axon growth and regeneration. Curr Opin Neurobiol 2014;27:179-185.
29. Fischer UM, Harting MT, Jimenez F, Monzon-Posadas WO, Xue H, Savitz SI, Laine GA, Cox CS, Jr.: Pulmonary passage is a major obstacle for intravenous stem cell delivery: the pulmonary first-pass effect. Stem Cells Dev 2009;18:683-692.
30. Fouad K, Hurd C, Magnuson DS: Functional testing in animal models of spinal cord injury: not as straight forward as one would think. Front Integr Neurosci 2013;7:85.
31. Franz S, Weidner N, Blesch A: Gene therapy approaches to enhancing plasticity and regeneration after spinal cord injury. Exp Neurol 2012;235:62-69.
32. Friedman JA, Windebank AJ, Moore MJ, Spinner RJ, Currier BL, Yaszemski MJ: Biodegradable polymer grafts for surgical repair of the injured spinal cord. Neurosurgery 2002;51:742-751; discussion 751-742.
33. Fu YS, Cheng YC, Lin MY, Cheng H, Chu PM, Chou SC, Shih YH, Ko MH, Sung MS: Conversion of human umbilical cord mesenchymal stem cells in Wharton's jelly to dopaminergic neurons in vitro: potential therapeutic application for Parkinsonism. Stem Cells 2006;24:115-124.
34. Fuhrmann T, Obermeyer J, Tator CH, Shoichet MS: Click-crosslinked injectable hyaluronic acid hydrogel is safe and biocompatible in the intrathecal space for ultimate use in regenerative strategies of the injured spinal cord. Methods 2015;84:60-69.

35. Giunti D, Parodi B, Usai C, Vergani L, Casazza S, Bruzzone S, Mancardi G, Uccelli A: Mesenchymal stem cells shape microglia effector functions through the release of CX3CL1. Stem Cells 2012;30:2044-2053.
36. Goldstein LB: Effects of bilateral and unilateral locus coeruleus lesions on beam-walking recovery after subsequent unilateral sensorimotor cortex suction-ablation in the rat. Restor Neurol Neurosci 1997;11:55-63.
37. Guest JD, Moore SW, Aimetti AA, Kutikov AB, Santamaria AJ, Hofstetter CP, Ropper AE, Theodore N, Ulich TR, Layer RT: Internal decompression of the acutely contused spinal cord: Differential effects of irrigation only versus biodegradable scaffold implantation. Biomaterials 2018;185:284-300.
38. Gupta D, Tator CH, Shoichet MS: Fast-gelling injectable blend of hyaluronan and methylcellulose for intrathecal, localized delivery to the injured spinal cord. Biomaterials 2006;27:2370-2379.
39. Hejcl A, Lesny P, Pradny M, Michalek J, Jendelova P, Stulik J, Sykova E: Biocompatible hydrogels in spinal cord injury repair. Physiol Res 2008a;57 Suppl 3:S121-132.
40. Hejcl A, Sedy J, Kapcalova M, Toro DA, Amemori T, Lesny P, Likavcanova-Masinova K, Krumbholcova E, Pradny M, Michalek J, Burian M, Hajek M, Jendelova P, Sykova E: HPMA-RGD hydrogels seeded with mesenchymal stem cells improve functional outcome in chronic spinal cord injury. Stem Cells Dev 2010;19:1535-1546.
41. Hejcl A, Urdzikova L, Sedy J, Lesny P, Pradny M, Michalek J, Burian M, Hajek M, Zamecnik J, Jendelova P, Sykova E: Acute and delayed implantation of positively charged 2-hydroxyethyl methacrylate scaffolds in spinal cord injury in the rat. J Neurosurg Spine 2008b;8:67-73.
42. Hou S, Xu Q, Tian W, Cui F, Cai Q, Ma J, Lee IS: The repair of brain lesion by implantation of hyaluronic acid hydrogels modified with laminin. J Neurosci Methods 2005;148:60-70.
43. Hou Y, Ryu CH, Jun JA, Kim SM, Jeong CH, Jeun SS: IL-8 enhances the angiogenic potential of human bone marrow mesenchymal stem cells by increasing vascular endothelial growth factor. Cell Biol Int 2014;38:1050-1059.
44. Hsu JY, Xu XM: Early profiles of axonal growth and astroglial response after spinal cord hemisection and implantation of Schwann cell-seeded guidance channels in adult rats. Journal of neuroscience research 2005;82:472-483.
45. Huerta-Angeles G, Němcová M, Příkopová E, Šmejkalová D, Pravda M, Kučera L, Velebný V: Reductive alkylation of hyaluronic acid for the synthesis of biocompatible hydrogels by click chemistry. Carbohydr Polym 2012;90:1704-1711.
46. Hulsebosch CE: Recent advances in pathophysiology and treatment of spinal cord injury. Adv Physiol Educ 2002;26:238-255.
47. Hurtado A, Cregg JM, Wang HB, Wendell DF, Oudega M, Gilbert RJ, McDonald JW: Robust CNS regeneration after complete spinal cord transection using aligned poly-L-lactic acid microfibers. Biomaterials 2011;32:6068-6079.
48. Hwang DH, Kim HM, Kang YM, Joo IS, Cho CS, Yoon BW, Kim SU, Kim BG: Combination of multifaceted strategies to maximize the therapeutic benefits of neural stem cell transplantation for spinal cord repair. Cell Transplant 2011;20:1361-1379.
49. Cheah M, Andrews MR, Chew DJ, Moloney EB, Verhaagen J, Fassler R, Fawcett JW: Expression of an Activated Integrin Promotes Long-Distance Sensory Axon Regeneration in the Spinal Cord. J Neurosci 2016;36:7283-7297.

50. Chen BK, Knight AM, Madigan NN, Gross L, Dadsetan M, Nesbitt JJ, Rooney GE, Currier BL, Yaszemski MJ, Spinner RJ, Windebank AJ: Comparison of polymer scaffolds in rat spinal cord: a step toward quantitative assessment of combinatorial approaches to spinal cord repair. Biomaterials 2011;32:8077-8086.
51. Chen J, Joon Lee H, Jakovcevski I, Shah R, Bhagat N, Loers G, Liu HY, Meiners S, Taschenberger G, Kugler S, Irintchev A, Schachner M: The extracellular matrix glycoprotein tenascin-C is beneficial for spinal cord regeneration. Mol Ther 2010;18:1769-1777.
52. Chen RN, Ho HO, Tsai YT, Sheu MT: Process development of an acellular dermal matrix (ADM) for biomedical applications. Biomaterials 2004;25:2679-2686.
53. Cheng H, Liu X, Hua R, Dai G, Wang X, Gao J, An Y: Clinical observation of umbilical cord mesenchymal stem cell transplantation in treatment for sequelae of thoracolumbar spinal cord injury. J Transl Med 2014;12:253.
54. Cheng I, Mayle RE, Cox CA, Park DY, Smith RL, Corcoran-Schwartz I, Ponnusamy KE, Oshtory R, Smuck MW, Mitra R, Kharazi AI, Carragee EJ: Functional assessment of the acute local and distal transplantation of human neural stem cells after spinal cord injury. Spine J 2012;12:1040-1044.
55. Cheriyan T, Ryan DJ, Weinreb JH, Cheriyan J, Paul JC, Lafage V, Kirsch T, Errico TJ: Spinal cord injury models: a review. Spinal Cord 2014;52:588-595.
56. Johnson PJ, Parker SR, Sakiyama-Elbert SE: Fibrin-based tissue engineering scaffolds enhance neural fiber sprouting and delay the accumulation of reactive astrocytes at the lesion in a subacute model of spinal cord injury. J Biomed Mater Res A 2010;92:152-163.
57. Kang KN, Lee JY, Kim DY, Lee BN, Ahn HH, Lee B, Khang G, Park SR, Min BH, Kim JH, Lee HB, Kim MS: Regeneration of completely transected spinal cord using scaffold of poly(D,L-lactide-co-glycolide)/small intestinal submucosa seeded with rat bone marrow stem cells. Tissue Eng Part A 2011;17:2143-2152.
58. Karabekmez FE, Duymaz A, Moran SL: Early clinical outcomes with the use of decellularized nerve allograft for repair of sensory defects within the hand. Hand (N Y) 2009;4:245-249.
59. Karahuseyinoglu S, Cinar O, Kilic E, Kara F, Akay GG, Demiralp DO, Tukun A, Uckan D, Can A: Biology of stem cells in human umbilical cord stroma: in situ and in vitro surveys. Stem Cells 2007;25:319-331.
60. Kasimir MT, Rieder E, Seebacher G, Silberhumer G, Wolner E, Weigel G, Simon P: Comparison of different decellularization procedures of porcine heart valves. Int J Artif Organs 2003;26:421-427.
61. Kim DW, Staples M, Shinozuka K, Pantcheva P, Kang SD, Borlongan CV: Wharton's jelly-derived mesenchymal stem cells: phenotypic characterization and optimizing their therapeutic potential for clinical applications. Int J Mol Sci 2013;14:11692-11712.
62. Knopf-Marques H, Pravda M, Wolfova L, Velebny V, Schaaf P, Vrana NE, Lavalle P: Hyaluronic Acid and Its Derivatives in Coating and Delivery Systems: Applications in Tissue Engineering, Regenerative Medicine and Immunomodulation. Adv Healthc Mater 2016;5:2841-2855.
63. Koci Z, Vyborny K, Dubisova J, Vackova I, Jager A, Lunov O, Jirakova K, Kubinova S: ECM hydrogel derived from human umbilical cord as a scaffold for neural tissue repair and its comparison to ECM from CNS and non-CNS porcine tissues. Tissue Eng Part C Methods 2017.

64. Krupa P, Vackova I, Ruzicka J, Zaviskova K, Dubisova J, Koci Z, Turnovcova K, Urdzikova LM, Kubinova S, Rehak S, Jendelova P: The Effect of Human Mesenchymal Stem Cells Derived from Wharton's Jelly in Spinal Cord Injury Treatment Is Dose-Dependent and Can Be Facilitated by Repeated Application. Int J Mol Sci 2018;19.
65. Kubinova S, Horak D, Hejcl A, Plichta Z, Kotek J, Proks V, Forostyak S, Sykova E: SIKVAV-modified highly superporous PHEMA scaffolds with oriented pores for spinal cord injury repair. J Tissue Eng Regen Med 2013.
66. Kubinova S, Horak D, Hejcl A, Plichta Z, Kotek J, Sykova E: Highly superporous cholesterol-modified poly(2-hydroxyethyl methacrylate) scaffolds for spinal cord injury repair. J Biomed Mater Res A 2011;99:618-629.
67. Kubinova S, Sykova E: Biomaterials combined with cell therapy for treatment of spinal cord injury. Regen Med 2012;7:207-224.
68. Kučera L, Weinfurterová R, Dvořákova J, Kučera J, Pravda M, Foglarová M, Švík K, Klein P, Velebný V, Kubala L: Chondrocyte Cultivation in Hyaluronan-Tyramine Cross-Linked Hydrogel. Int J Polymer Mater PolymerBiomaterials 2015;64:661-674.
69. Kwon BK, Liu J, Lam C, Plunet W, Oschipok LW, Hauswirth W, Di Polo A, Blesch A, Tetzlaff W: Brain-derived neurotrophic factor gene transfer with adeno-associated viral and lentiviral vectors prevents rubrospinal neuronal atrophy and stimulates regeneration-associated gene expression after acute cervical spinal cord injury. Spine (Phila Pa 1976) 2007;32:1164-1173.
70. Kwon BK, Tetzlaff W, Grauer JN, Beiner J, Vaccaro AR: Pathophysiology and pharmacologic treatment of acute spinal cord injury. Spine J 2004;4:451-464.
71. Lee AC, Yu VM, Lowe JB, 3rd, Brenner MJ, Hunter DA, Mackinnon SE, Sakiyama-Elbert SE: Controlled release of nerve growth factor enhances sciatic nerve regeneration. Exp Neurol 2003;184:295-303.
72. Lemons ML, Condic ML: Integrin signaling is integral to regeneration. Exp Neurol 2008;209:343-352.
73. Li LM, Han M, Jiang XC, Yin XZ, Chen F, Zhang TY, Ren H, Zhang JW, Hou TJ, Chen Z, Ou-Yang HW, Tabata Y, Shen YQ, Gao JQ: Peptide-Tethered Hydrogel Scaffold Promotes Recovery from Spinal Cord Transection via Synergism with Mesenchymal Stem Cells. ACS Appl Mater Interfaces 2017a;9:3330-3342.
74. Li X, Tan J, Xiao Z, Zhao Y, Han S, Liu D, Yin W, Li J, Li J, Wanggou S, Chen B, Ren C, Jiang X, Dai J: Transplantation of hUC-MSCs seeded collagen scaffolds reduces scar formation and promotes functional recovery in canines with chronic spinal cord injury. Sci Rep 2017b;7:43559.
75. Liang Y, Walczak P, Bulte JW: The survival of engrafted neural stem cells within hyaluronic acid hydrogels. Biomaterials 2013;34:5521-5529.
76. Lin P, Chan WC, Badylak SF, Bhatia SN: Assessing porcine liver-derived biomatrix for hepatic tissue engineering. Tissue Eng 2004;10:1046-1053.
77. Lindvall O, Kokaia Z: Stem cells in human neurodegenerative disorders--time for clinical translation? J Clin Invest 2010;120:29-40.
78. Litwiniuk M, Krejner A, Speyrer MS, Gauto AR, Grzela T: Hyaluronic Acid in Inflammation and Tissue Regeneration. Wounds 2016;28:78-88.
79. Liu J, Han D, Wang Z, Xue M, Zhu L, Yan H, Zheng X, Guo Z, Wang H: Clinical analysis of the treatment of spinal cord injury with umbilical cord mesenchymal stem cells. Cytotherapy 2013;15:185-191.

80. Macaya D, Spector M: Injectable hydrogel materials for spinal cord regeneration: a review. Biomed Mater 2012;7:012001.
81. Mackova H, Plichta Z, Proks V, Kotelnikov I, Kucka J, Hlidkova H, Horak D, Kubinova S, Jirakova K: RGDS- and SIKVAVS-Modified Superporous Poly(2-hydroxyethyl methacrylate) Scaffolds for Tissue Engineering Applications. Macromolecular bioscience 2016;16:1621-1631.
82. Madigan NN, McMahon S, O'Brien T, Yaszemski MJ, Windebank AJ: Current tissue engineering and novel therapeutic approaches to axonal regeneration following spinal cord injury using polymer scaffolds. Respir Physiol Neurobiol 2009;169:183-199.
83. Machova Urdzikova L, Sedlacek R, Suchy T, Amemori T, Ruzicka J, Lesny P, Havlas V, Sykova E, Jendelova P: Human multipotent mesenchymal stem cells improve healing after collagenase tendon injury in the rat. Biomed Eng Online 2014;13:42.
84. Mantilla CB: Gene therapy and respiratory neuroplasticity. Exp Neurol 2017;287:261-267.
85. McCloy RA, Rogers S, Caldon CE, Lorca T, Castro A, Burgess A: Partial inhibition of Cdk1 in G 2 phase overrides the SAC and decouples mitotic events. Cell Cycle 2014;13:1400-1412.
86. McCreedy DA, Sakiyama-Elbert SE: Combination therapies in the CNS: engineering the environment. Neurosci Lett 2012;519:115-121.
87. McCreedy DA, Wilems TS, Xu H, Butts JC, Brown CR, Smith AW, Sakiyama-Elbert SE: Survival, Differentiation, and Migration of High-Purity Mouse Embryonic Stem Cell-derived Progenitor Motor Neurons in Fibrin Scaffolds after Sub-Acute Spinal Cord Injury. Biomater Sci 2014;2:1672-1682.
88. Medberry CJ, Crapo PM, Siu BF, Carruthers CA, Wolf MT, Nagarkar SP, Agrawal V, Jones KE, Kelly J, Johnson SA, Velankar SS, Watkins SC, Modo M, Badylak SF: Hydrogels derived from central nervous system extracellular matrix. Biomaterials 2013;34:1033-1040.
89. Meng FW, Slivka PF, Dearth CL, Badylak SF: Solubilized extracellular matrix from brain and urinary bladder elicits distinct functional and phenotypic responses in macrophages. Biomaterials 2015;46:131-140.
90. Metz GA, Curt A, van de Meent H, Klusman I, Schwab ME, Dietz V: Validation of the weight-drop contusion model in rats: a comparative study of human spinal cord injury. J Neurotrauma 2000;17:1-17.
91. Mitchell KE, Weiss ML, Mitchell BM, Martin P, Davis D, Morales L, Helwig B, Beerenstrauch M, Abou-Easa K, Hildreth T, Troyer D, Medicetty S: Matrix cells from Wharton's jelly form neurons and glia. Stem Cells 2003;21:50-60.
92. Montesano R, Kumar S, Orci L, Pepper MS: Synergistic effect of hyaluronan oligosaccharides and vascular endothelial growth factor on angiogenesis in vitro. Lab Invest 1996;75:249-262.
93. Mothe AJ, Tam RY, Zahir T, Tator CH, Shoichet MS: Repair of the injured spinal cord by transplantation of neural stem cells in a hyaluronan-based hydrogel. Biomaterials 2013;34:3775-3783.
94. Nistor GI, Totoiu MO, Haque N, Carpenter MK, Keirstead HS: Human embryonic stem cells differentiate into oligodendrocytes in high purity and myelinate after spinal cord transplantation. Glia 2005;49:385-396.
95. Norenberg MD, Smith J, Marcillo A: The pathology of human spinal cord injury: defining the problems. J Neurotrauma 2004;21:429-440.

96. O'Donoghue K, Fisk NM: Fetal stem cells. Best Pract Res Clin Obstet Gynaecol 2004;18:853-875.
97. O'Neill JD, Anfang R, Anandappa A, Costa J, Javidfar J, Wobma HM, Singh G, Freytes DO, Bacchetta MD, Sonett JR, Vunjak-Novakovic G: Decellularization of human and porcine lung tissues for pulmonary tissue engineering. Ann Thorac Surg 2013;96:1046-1055; discussion 1055-1046.
98. Ohta M, Suzuki Y, Noda T, Ejiri Y, Dezawa M, Kataoka K, Chou H, Ishikawa N, Matsumoto N, Iwashita Y, Mizuta E, Kuno S, Ide C: Bone marrow stromal cells infused into the cerebrospinal fluid promote functional recovery of the injured rat spinal cord with reduced cavity formation. Exp Neurol 2004;187:266-278.
99. Okada S, Ishii K, Yamane J, Iwanami A, Ikegami T, Katoh H, Iwamoto Y, Nakamura M, Miyoshi H, Okano HJ, Contag CH, Toyama Y, Okano H: In vivo imaging of engrafted neural stem cells: its application in evaluating the optimal timing of transplantation for spinal cord injury. FASEB J 2005;19:1839-1841.
100. Oliveri RS, Bello S, Biering-Sorensen F: Mesenchymal stem cells improve locomotor recovery in traumatic spinal cord injury: systematic review with meta-analyses of rat models. Neurobiol Dis 2014;62:338-353.
101. Ota T, Gilbert TW, Schwartzman D, McTiernan CF, Kitajima T, Ito Y, Sawa Y, Badylak SF, Zenati MA: A fusion protein of hepatocyte growth factor enhances reconstruction of myocardium in a cardiac patch derived from porcine urinary bladder matrix. J Thorac Cardiovasc Surg 2008;136:1309-1317.
102. Pal R, Venkataramana NK, Bansal A, Balaraju S, Jan M, Chandra R, Dixit A, Rauthan A, Murgod U, Totey S: Ex vivo-expanded autologous bone marrow-derived mesenchymal stromal cells in human spinal cord injury/paraplegia: a pilot clinical study. Cytotherapy 2009;11:897-911.
103. Parr AM, Kulbatski I, Tator CH: Transplantation of adult rat spinal cord stem/progenitor cells for spinal cord injury. J Neurotrauma 2007;24:835-845.
104. Peattie RA, Nayate AP, Firpo MA, Shelby J, Fisher RJ, Prestwich GD: Stimulation of in vivo angiogenesis by cytokine-loaded hyaluronic acid hydrogel implants. Biomaterials 2004;25:2789-2798.
105. Pego AP, Kubinova S, Cizkova D, Vanicky I, Mar FM, Sousa MM, Sykova E: Regenerative medicine for the treatment of spinal cord injury: more than just promises? J Cell Mol Med 2012;16:2564-2582.
106. Petrenko Y, Sykova E, Kubinova S: The therapeutic potential of three-dimensional multipotent mesenchymal stromal cell spheroids. Stem Cell Res Ther 2017;8:94.
107. Raspa A, Pugliese R, Maleki M, Gelain F: Recent therapeutic approaches for spinal cord injury. Biotechnol Bioeng 2015.
108. Reing JE, Zhang L, Myers-Irvin J, Cordero KE, Freytes DO, Heber-Katz E, Bedelbaeva K, McIntosh D, Dewilde A, Braunhut SJ, Badylak SF: Degradation products of extracellular matrix affect cell migration and proliferation. Tissue engineering Part A 2009;15:605-614.
109. Ronsyn MW, Berneman ZN, Van Tendeloo VF, Jorens PG, Ponsaerts P: Can cell therapy heal a spinal cord injury? Spinal Cord 2008;46:532-539.
110. Seidlits SK, Drinnan CT, Petersen RR, Shear JB, Suggs LJ, Schmidt CE: Fibronectin-hyaluronic acid composite hydrogels for three-dimensional endothelial cell culture. Acta Biomater 2011;7:2401-2409.

111. Seidlits SK, Khaing ZZ, Petersen RR, Nickels JD, Vanscoy JE, Shear JB, Schmidt CE: The effects of hyaluronic acid hydrogels with tunable mechanical properties on neural progenitor cell differentiation. Biomaterials 2010;31:3930-3940.
112. Schense JC, Hubbell JA: Cross-linking exogenous bifunctional peptides into fibrin gels with factor XIIIa. Bioconjug Chem 1999;10:75-81.
113. Silva NA, Sousa N, Reis RL, Salgado AJ: From basics to clinical: a comprehensive review on spinal cord injury. Prog Neurobiol 2014;114:25-57.
114. Slivka PF, Dearth CL, Keane TJ, Meng FW, Medberry CJ, Riggio RT, Reing JE, Badylak SF: Fractionation of an ECM hydrogel into structural and soluble components reveals distinctive roles in regulating macrophage behavior. Biomater Sci 2014;2:1521-1534.
115. Snyder TN, Madhavan K, Intrator M, Dregalla RC, Park D: A fibrin/hyaluronic acid hydrogel for the delivery of mesenchymal stem cells and potential for articular cartilage repair. J Biol Eng 2014;8:10.
116. Steffenhagen C, Dechant FX, Oberbauer E, Furtner T, Weidner N, Kury P, Aigner L, Rivera FJ: Mesenchymal stem cells prime proliferating adult neural progenitors toward an oligodendrocyte fate. Stem Cells Dev 2012;21:1838-1851.
117. Sykova E, Homola A, Mazanec R, Lachmann H, Konradova SL, Kobylka P, Padr R, Neuwirth J, Komrska V, Vavra V, Stulik J, Bojar M: Autologous bone marrow transplantation in patients with subacute and chronic spinal cord injury. Cell Transplant 2006;15:675-687.
118. Šedová P, Buffa R, Kettou S, Huerta-Angeles G, Hermannová M, Leierová V, Šmejkalová D, Moravcová M, Velebný V: Preparation of hyaluronan polyaldehyde—a precursor of biopolymer conjugates. Carbohydr Res 2013;371:8-15.
119. Takahashi K, Yamanaka S: Induction of pluripotent stem cells from mouse embryonic and adult fibroblast cultures by defined factors. Cell 2006;126:663-676.
120. Tan CL, Andrews MR, Kwok JC, Heintz TG, Gumy LF, Fassler R, Fawcett JW: Kindlin-1 enhances axon growth on inhibitory chondroitin sulfate proteoglycans and promotes sensory axon regeneration. J Neurosci 2012;32:7325-7335.
121. Taylor SJ, Rosenzweig ES, McDonald JW, 3rd, Sakiyama-Elbert SE: Delivery of neurotrophin-3 from fibrin enhances neuronal fiber sprouting after spinal cord injury. J Control Release 2006;113:226-235.
122. Tukmachev D, Forostyak S, Koci Z, Zaviskova K, Vackova I, Vyborny K, Sandvig I, Sandvig A, Medberry CJ, Badylak SF, Sykova E, Kubinova S: Injectable Extracellular Matrix Hydrogels as Scaffolds for Spinal Cord Injury Repair. Tissue Eng Part A 2016;22:306-317.
123. Uchida K, Nakajima H, Guerrero AR, Johnson WE, Masri WE, Baba H: Gene therapy strategies for the treatment of spinal cord injury. Ther Deliv 2014;5:591-607.
124. Urdzikova L, Jendelova P, Glogarova K, Burian M, Hajek M, Sykova E: Transplantation of bone marrow stem cells as well as mobilization by granulocyte-colony stimulating factor promotes recovery after spinal cord injury in rats. J Neurotrauma 2006;23:1379-1391.
125. Urdzikova LM, Ruzicka J, LaBagnara M, Karova K, Kubinova S, Jirakova K, Murali R, Sykova E, Jhanwar-Uniyal M, Jendelova P: Human mesenchymal stem cells modulate inflammatory cytokines after spinal cord injury in rat. Int J Mol Sci 2014;15:11275-11293.

126. Valentin JE, Stewart-Akers AM, Gilbert TW, Badylak SF: Macrophage participation in the degradation and remodeling of extracellular matrix scaffolds. Tissue Eng Part A 2009;15:1687-1694.
127. Vanicky I, Urdzikova L, Saganova K, Cizkova D, Galik J: A simple and reproducible model of spinal cord injury induced by epidural balloon inflation in the rat. J Neurotrauma 2001;18:1399-1407.
128. Voulgari-Kokota A, Fairless R, Karamita M, Kyrargyri V, Tseveleki V, Evangelidou M, Delorme B, Charbord P, Diem R, Probert L: Mesenchymal stem cells protect CNS neurons against glutamate excitotoxicity by inhibiting glutamate receptor expression and function. Exp Neurol 2012;236:161-170.
129. Wang HS, Hung SC, Peng ST, Huang CC, Wei HM, Guo YJ, Fu YS, Lai MC, Chen CC: Mesenchymal stem cells in the Wharton's jelly of the human umbilical cord. Stem Cells 2004;22:1330-1337.
130. Wei YT, He Y, Xu CL, Wang Y, Liu BF, Wang XM, Sun XD, Cui FZ, Xu QY: Hyaluronic acid hydrogel modified with nogo-66 receptor antibody and poly-L-lysine to promote axon regrowth after spinal cord injury. J Biomed Mater Res B Appl Biomater 2010;95:110-117.
131. Willerth SM, Sakiyama-Elbert SE: Cell therapy for spinal cord regeneration. Adv Drug Deliv Rev 2008;60:263-276.
132. Woerly S, Pinet E, de Robertis L, Van Diep D, Bousmina M: Spinal cord repair with PHPMA hydrogel containing RGD peptides (NeuroGel). Biomaterials 2001;22:1095-1111.
133. Wolfova L, Pravda M, Foglarova M, Memcova M, Niedoba K, Velebny V: Derivates based on hyaluronic acid, capable of forming hydrogels, method of preparation thereof, hydrogels based on said derivatives, method of preparation thereof and use; in., WO2013127374 A1, 2013.
134. Wood JD, Simmons-Byrd A, Spievack AR, Badylak SF: Use of a particulate extracellular matrix bioscaffold for treatment of acquired urinary incontinence in dogs. J Am Vet Med Assoc 2005;226:1095-1097.
135. Woods T, Gratzer PF: Effectiveness of three extraction techniques in the development of a decellularized bone-anterior cruciate ligament-bone graft. Biomaterials 2005;26:7339-7349.
136. Wright KT, El Masri W, Osman A, Chowdhury J, Johnson WE: Concise review: Bone marrow for the treatment of spinal cord injury: mechanisms and clinical applications. Stem Cells 2011;29:169-178.
137. Wright KT, El Masri W, Osman A, Roberts S, Chamberlain G, Ashton BA, Johnson WE: Bone marrow stromal cells stimulate neurite outgrowth over neural proteoglycans (CSPG), myelin associated glycoprotein and Nogo-A. Biochem Biophys Res Commun 2007;354:559-566.
138. Wu DC, Boyd AS, Wood KJ: Embryonic stem cell transplantation: potential applicability in cell replacement therapy and regenerative medicine. Front Biosci 2007a;12:4525-4535.
139. Wu KH, Zhou B, Lu SH, Feng B, Yang SG, Du WT, Gu DS, Han ZC, Liu YL: In vitro and in vivo differentiation of human umbilical cord derived stem cells into endothelial cells. J Cell Biochem 2007b;100:608-616.
140. Yoon SH, Shim YS, Park YH, Chung JK, Nam JH, Kim MO, Park HC, Park SR, Min BH, Kim EY, Choi BH, Park H, Ha Y: Complete spinal cord injury treatment using

autologous bone marrow cell transplantation and bone marrow stimulation with granulocyte macrophage-colony stimulating factor: Phase I/II clinical trial. Stem Cells 2007;25:2066-2073.
141. Young W: Spinal cord regeneration. Cell Transplant 2014;23:573-611.
142. Zantop T, Gilbert TW, Yoder MC, Badylak SF: Extracellular matrix scaffolds are repopulated by bone marrow-derived cells in a mouse model of achilles tendon reconstruction. J Orthop Res 2006;24:1299-1309.
143. Zaviskova K, Tukmachev D, Dubisova J, Vackova I, Hejcl A, Bystronova J, Pravda M, Scigalkova I, Sulakova R, Velebny V, Wolfova L, Kubinova S: Injectable hydroxyphenyl derivative of hyaluronic acid hydrogel modified with RGD as scaffold for spinal cord injury repair. J Biomed Mater Res A 2018;106:1129-1140.
144. Zhang XY, Xue H, Liu JM, Chen D: Chemically extracted acellular muscle: a new potential scaffold for spinal cord injury repair. Journal of biomedical materials research Part A 2011;100:578-587.
145. Zhao Y, Tang F, Xiao Z, Han G, Wang N, Yin N, Chen B, Jiang X, Yun C, Han W, Zhao C, Cheng S, Zhang S, Dai J: Clinical Study of NeuroRegen Scaffold Combined With Human Mesenchymal Stem Cells for the Repair of Chronic Complete Spinal Cord Injury. Cell Transplant 2017;26:891-900.
146. Zhou C, Yang B, Tian Y, Jiao H, Zheng W, Wang J, Guan F: Immunomodulatory effect of human umbilical cord Wharton's jelly-derived mesenchymal stem cells on lymphocytes. Cell Immunol 2011;272:33-38.
147. Zhou C, Zhang C, Chi S, Xu Y, Teng J, Wang H, Song Y, Zhao R: Effects of human marrow stromal cells on activation of microglial cells and production of inflammatory factors induced by lipopolysaccharide. Brain Res 2009;1269:23-30.
148. Zorner B, Filli L, Starkey ML, Gonzenbach R, Kasper H, Rothlisberger M, Bolliger M, Schwab ME: Profiling locomotor recovery: comprehensive quantification of impairments after CNS damage in rodents. Nat Methods 2010;7:701-708.